

DISSERTATION

INNOVATIVE TOOLS FOR MAIZE WATER USE ASSESSMENT

Submitted by

Maria Cristina Capurro

Department of Soil and Crop Sciences

In partial fulfillment of the requirements

For the Degree of Doctor of Philosophy

Colorado State University

Fort Collins, Colorado

Spring 2023

Doctoral Committee:

Advisor: Allan A. Andales

Co-Advisor: Jay M. Ham

Louise Comas

José L. Chávez

Copyright by Maria Cristina Capurro 2023

All Rights Reserved

ABSTRACT

INNOVATIVE TOOLS FOR MAIZE WATER USE ASSESSMENT

Modern agriculture is facing a scenario of decreased water availability and sustainability concerns. Accurate estimation of crop transpiration is crucial to improve agricultural water management. However, transpiration estimation is challenging due to the difficulty in modeling canopy conductance (g_c). There is currently no standardized approach for the calculation of g_c . Additionally, direct measurements of g_c and transpiration at the field scale are difficult. There are few commercially available sensors that measure transpiration, and those available are expensive. For g_c , most of the equipment available use manual or indirect approaches. Meanwhile, during the past years there has been a dramatic development of sensor technology and communications. The expansion of low-cost circuit boards and 3D printing development and the Internet of Things (IoT) has led to a decrease in the cost of sensors and facilitated data acquisition and fabrication of research-grade instruments.

The purpose of this study was to develop low-cost tools to measure actual crop transpiration and g_c and contribute to the improvement of water use estimation in irrigated fields.

We developed two types of IoT plant-based devices using 3D-printing and low-cost electronics and sensors: a sap flow gauge (SFG) and an artificial reference surface (ARS) system.

We developed a new theory for a heat pulse method for calculation of transpiration rate that was coupled with a new type of sap flow gauge. The gauge is easy to build and adaptable to a range of stem sizes. We calibrated and validated the sensors in maize (*Zea mays* L.) plants in the greenhouse and tested them in a well-watered maize field in two locations in northern Colorado, for two years. The sap flow sensors calibration coefficient and standard deviation (SD) was 1.28

g/h \pm 0.2, used to convert heat velocity to transpiration flow. A higher calibration coefficient was found in 2019 when a longer heating time was applied, confirming that the coefficient takes into account wounding effects on the plant. The data collected allowed the calculation of the maize transpiration every 15 minutes and showed that they were in good agreement with estimated transpiration from plants on weighing scales from greenhouse studies, from field measurements with commercially available sap flow gauges and with estimations with the Penman-Monteith (PM) approach in field conditions. Daily transpiration from SFGs compared with measured values in the greenhouse had a root mean squared error (RMSE) of 15.4% and a mean absolute error (MAE) of 12.1% of the mean T value in 2020. In 2019 the RMSE was 12.4% and the MAE was 10.2% from the mean T value. In field conditions, when SFGs were compared to daily transpiration estimates using the PM approach, the RMSE and MAE were 0.70 mm and 0.56 mm, a 13.2% and 11% error, respectively. When compared to commercially available SFGs, the RMSE and MAE were 0.66 mm and 0.54 mm (12.4% and 10.2% from the mean T value), respectively. In 2020, daily transpiration estimation in the field with the developed SFGs had a precision of \pm 1.04 mm SD and when compared to the PM approach had an RMSE and MAE of 0.62 mm and 0.48 mm, respectively (both were within 10% of mean transpiration). Results also showed that error in estimations decrease with additional sensors deployed in the field. More than 4 sensors should be deployed in the field to obtain estimations of corn transpiration with less than 20% error. The required number of gauges varies according to the accuracy desired for transpiration measurements. The ability of the sap flow sensors to measure plant transpiration directly make them powerful tools for multiple applications. They can capture the effects of the environment and characteristics of the plant. Therefore, they are valuable for assessing the partitioning of total crop evapotranspiration (ET_c) into plant transpiration and soil evaporation. They can be used for local basal crop coefficient estimations and for fine-tuning local irrigation applications. They can also provide valuable information for ground-truthing complex multi-layer models and simulations that aim to estimate actual transpiration from the field.

The use of the sap flow sensors for site-specific basal crop coefficients (K_{cb}) derivation was tested. Locally derived K_{cb} values from Trout and DeJonge (2018) for maize was verified using our low-cost sap flow sensors for a period of 22 days in 2020 and for a period of 17 days in 2019. The period was divided into mid-season, beginning of late-season and end late-season. Mean K_{cb} values from SFGs for mid-season and beginning of late season agreed with those from Trout and DeJonge (2018). Locally derived K_{cb} was 1.05 and 0.82, while K_{cb} from SFGs were 1.08 and 1.06 for mid-season during 2019 and 2020 and 0.82 for beginning of late season in 2020. However, end of late-period K_{cb} from sap flow data in 2020 was higher than the tabulated value (0.62 vs 0.4). This was probably due to the fixed end-of-cycle-date for the maize growing season in contrast to variable growing degree days. This approach is especially useful for low budget and rapid evaluations. We described the advantages of using K_{cb} curves for estimation of crop water requirements and highlight the benefits of using sap flow gauges for its derivation.

The second device was an ARS that consisted of a plastic hemispherical surface that allowed monitoring of dry leaf temperature. This temperature was used to estimate actual maize transpiration, g_c and to detect and monitor water stress in field conditions. The hemispherical ARS closely mimicked the temperature of non-transpiring leaves ($R^2=0.99$) in a field study conducted in 2020 at Fort Collins, CO. Actual maize transpiration was adequately estimated for a 14-day period using the thermal approach with the ARS temperature. Comparisons with transpiration calculated from SFGs and the ASCE standardized tall reference ET (ASCE, 2005) with local basal crop coefficient (K_{cb}) values for maize showed a root mean square error (RMSE) of 0.61 mm and margin of error (ME) of 0.53 mm, representing a 12% and a 10% error of the method in relation to the Penman-Monteith approach and a RMSE and ME of 0.78 mm and 0.73 mm in relation to actual maize transpiration from SFGs. Differences from the total transpiration were within 7.5%. Absolute hourly values of g_c were also calculated with this approach during the

daytime, showing a pattern and values similar to the conductance derived from the SFGs for a 6-day period. However, underestimations were observed at the beginning and end of the day. When mean mid-day values of g_c were compared to sap flow measurements, the MAE and RMSE were 0.51 mm/s. and 0.72 mm/s, representing 8.1% and 11.6% error, respectively. The method was also tested in a deficit-irrigated maize field, showing a reduction in transpiration and in g_c due to soil water depletion and demonstrating the sensitivity of the method to detect water stress in the field. However, transpiration values were severely underestimated due to the similarity of the temperatures from the ARS and canopy. Changing the color of the ARS might reduce these errors. Results suggest that a darker color should be used. A simple thermal method for water stress detection was also tested. Its strong correlation with g_c ($R^2=0.7$) demonstrated that it could be a method to detect the onset and development of plant water stress in the field. The use of the dry ARS could be a practical approach for maize transpiration, g_c and water stress estimation since it requires less weather data. Its simplicity of fabrication, implementation, and low requirements for maintenance during the season are also valuable advantages of the method.

We were able to develop versatile low-cost IoT tools for real time monitoring of crop transpiration and g_c . These tools can be used for multiple purposes and have the potential to improve our ability to estimate maize crop water requirements.

ACKNOWLEDGEMENTS

I am thankful for having this great opportunity of doing a PhD at Colorado State University. During this period, I have met truly amazing people and lived experiences that I will carry in my heart forever.

I am deeply thankful for my advisor Allan Andales and co-advisor Jay Ham. For their invaluable help and advice with this PhD. They have supported me in my academic research and daily life, and I have learnt so much from them. I would also like to thank Jose Chavez and Louise Comas for their advice and encourage in critical thinking. This PhD have thought me skills that I never imagined I would, from plant physiology, micrometeorology including electronics, and sensor technology.

I would also like to express my gratitude to my lab friends, AJ Brown, Ian Askland, Dylan Casey, Edson Costa Filho and Garvey Smith. From them I have learnt a lot too and they were present for field and technical support. Finally, I would like to thank to Northern Water and Jon Altenhofen for their support for sap flow field research.

So many things happen during a PhD. I became a mom of two kids during this process, the most wonderful experience. I also endured a pandemic and moving back to Uruguay. Experiences that though me about self-awareness and resilience. Nothing of this would have been possible without Martin, who did not doubt in leaving behind his life in Uruguay to come to this adventure and was always by my side, cheering me up and supporting me. I am grateful for our families and friends in Uruguay, for their strong support from the distance. I would also like to thank to Tom Trout and Vickie Traxler, for being our family in the US, they have been part of this journey too.

TABLE OF CONTENTS

| | |
|---|----|
| ABSTRACT..... | II |
| ACKNOWLEDGEMENTS | VI |
| CHAPTER 1: INTRODUCTION..... | 1 |
| Dissertation Organization..... | 4 |
| References | 6 |
| CHAPTER 2: A NOVEL SAP FLOW SYSTEM TO MEASURE MAIZE TRANSPIRATION USING HEAT PULSE METHODS..... | 8 |
| Summary | 8 |
| Introduction..... | 9 |
| Theory | 12 |
| <i>Our new Theory</i> | 14 |
| Materials and Methods | 17 |
| <i>Gauge design</i> | 17 |
| <i>Components of the system</i> | 20 |
| <i>Calculations and protocol</i> | 22 |
| <i>Greenhouse experiment for gauge calibration and validation</i> | 23 |
| <i>Calibration coefficient: Converting heat velocity to sap flow rate</i> | 25 |
| <i>Field experiment</i> | 29 |
| <i>Evaluation of the performance of the sap flow gauges</i> | 31 |
| Results and discussion..... | 33 |
| <i>Results from season 2020</i> | 33 |
| Greenhouse calibration | 33 |
| Greenhouse validation..... | 37 |
| Field experiment and sap flow gauges performance | 39 |
| Sap flow transpiration accuracy vs number of gauges..... | 45 |
| <i>Results from season 2019</i> | 47 |
| <i>Sap Flow gauges pros and cons for practical uses</i> | 49 |
| Conclusion..... | 51 |
| <i>Future research</i> | 53 |
| References | 54 |
| CHAPTER 3: AN OVERVIEW OF BASAL CROP COEFFICIENTS AND THE POTENTIAL USE OF SAP FLOW GAUGES FOR ITS DERIVATION IN MAIZE..... | 59 |

| | |
|--|-----|
| Summary | 59 |
| Introduction..... | 60 |
| Purpose of this work | 62 |
| <i>Origin of the crop coefficient curves</i> | 63 |
| <i>Use of crop coefficients</i> | 67 |
| <i>Advantages of using basal crop coefficients in a dual Kc approach</i> | 69 |
| <i>Disadvantages of the basal crop coefficients</i> | 77 |
| <i>A potential use of sap flow sensors</i> | 81 |
| The use of low-cost sap flow sensors for basal crop coefficient delineation | 84 |
| <i>New approaches for adjustment of basal crop coefficients</i> | 84 |
| Crop coefficient curves derivation..... | 88 |
| Considerations and drawbacks of VI approaches..... | 88 |
| <i>Use case: Sap flow sensors and surface reflectance data to assess a site-specific Kcb delineation</i> | 90 |
| 4-segment Kcb curve delineation with reflectance data..... | 92 |
| Spectral-based Kcb curve..... | 94 |
| Assessment of the basal crop coefficient curves with sap flow sensors and surface reflectance..... | 99 |
| Conclusion..... | 102 |
| References | 103 |
| CHAPTER 4: A SIMPLE ARTIFICIAL DRY REFERENCE SURFACE FOR REAL-TIME CANOPY CONDUCTANCE AND TRANSPIRATION ESTIMATION IN MAIZE USING INFRARED SENSORS | 112 |
| Summary | 112 |
| Introduction..... | 113 |
| Background | 116 |
| <i>An alternative to measuring weather variables or empirical approaches: reference surface temperatures</i> | 116 |
| <i>Crop water needs estimation using a dry reference and canopy temperatures</i> | 118 |
| <i>Canopy conductance estimation using a dry reference and canopy temperatures</i> | 121 |
| <i>Use of dry ARS in simple approaches for stress detection</i> | 122 |
| Materials and Methods | 123 |
| <i>Weather, plant transpiration and soil monitoring</i> | 124 |
| <i>Temperature sensing</i> | 125 |
| <i>Dry artificial reference surface</i> | 126 |

| | |
|--|-----|
| <i>Calculations</i> | 129 |
| Results and Discussion..... | 130 |
| <i>Reference surface development</i> | 131 |
| <i>Transpiration estimation using dry ARS temperature</i> | 133 |
| <i>Canopy conductance estimation using dry ARS temperature</i> | 139 |
| <i>Potential use for crop water stress detection using a Dry ARS with a simple approach</i> | 147 |
| Conclusions..... | 151 |
| <i>Future research</i> | 153 |
| References..... | 154 |
| CHAPTER 5: GENERAL CONCLUSIONS..... | 159 |
| Future research recommendations | 163 |
| Appendix A..... | 165 |
| Appendix B..... | 171 |
| Appendix C..... | 181 |
| <i>Equations</i> | 187 |

CHAPTER 1

INTRODUCTION

Modern agricultural production faces several challenges. Predictions foreshadow a decrease in water availability for agricultural production due to competition with urban growth and consequences of climate change (Florke et al., 2018; Eekhout et al., 2018). On the other hand, food production must grow to meet the demands of an increasing world population and guarantee food security (Foley et al., 2011). Yet, that needs to be accomplished by producing high yields without degrading natural resources, which would condition the future ability for food production (Brodt, et al., 2011; FAO, 2022). Considering that irrigation is the largest consumer of freshwater in the world, using 70% of global freshwater (Fererres and Soriano, 2007; FAO, 2022), an improvement in water management can have a great impact on the long-term agricultural sustainability. This reinforces the needs for an integrated management of resources and the efficient use of the water (Giovanucci et al., 2012).

Optimal irrigation scheduling is essential for improving water and energy use in irrigated agriculture. An irrigation scheduling plan is usually based on the calculation of the soil water balance, where the main driver for water depletion is the evapotranspiration from the crop. Crop evapotranspiration (ET_c) is defined as the water loss from a surface through the combination of soil evaporation and plant transpiration; leading to water loss from a crop surface (Allen et al., 1998). The transpiration process is the main driver of the crop water requirements and accurate estimations of this variable are essential for proper water management. However, actual plant transpiration is challenging to estimate or model directly because of the difficulty in modelling

canopy resistance (Monteith, 1965; Damour et al., 2010; Sinclair, 2019) (or its inverse, conductance).

There are different approaches to estimate ET_c . The most widely accepted micrometeorological model is the Penman-Monteith approach. Penman developed an equation to estimate evaporation rates from an open water surface from standard meteorological data (Penman, 1948). The model was modified by Monteith (1965), who introduced the stomatal conductance component as a resistance for the water vapor evaporation from the surface to estimate ET_c directly, called the Penman-Monteith approach. Sensitivity studies have shown that the canopy resistance is responsible for 10-20% of the ET_c variation in the case of short grass to 40-50% in the case of tall crops like sweet sorghum, and in situations of water stress, it is the dominant parameter affecting ET_c (Katerji and Rana, 2006). This means that a large error in the resistance term might have a substantial impact on the calculation of ET_c . However, there is no standardized approach to calculate this resistance. Consequently, the practical solution proposed was an empirical approach using a standardized ET from a reference crop and the use of crop coefficients (K_c) (Jensen, 1968).

Modelling stomatal conductance has several challenges because of its complex nature, especially in situations of stress. Stomatal opening has a key role, regulating the water losses from the plant and the intake of CO_2 for photosynthesis. It is controlled by weather parameters, crop characteristics, photosynthesis and interacts with water availability from the soil. This is why simplifications for ET_c modelling lack the ability to capture the actual evaporation from the crop surface and more mechanistic and direct approaches would be an improvement (Lascano, 2000; Katerji and Rana, 2006). New tools can help to quantify and model transpiration.

Measuring the actual canopy conductance or plant transpiration from the field may help to develop modeling and prediction of crop water requirements. However, few sensors are able to measure actual plant transpiration. On the other hand, the measurement of canopy conductance of a crop surface is challenging and most of the methods are manual or use indirect indicators to estimate conductance (Leinonen et al., 2006; Jones, 1999).

Recently there have been significant advances in the development and accessibility of low-cost technologies and the diffusion of wireless communications that have expanded the use of sensors and reduced the cost of research-grade equipment. We used these accessible technologies and new approaches to fabricate practical tools that are able to measure actual transpiration and canopy conductance directly and continuously from the field.

Our aim was to contribute to the improvement of crop water use estimation. Specific objectives of this research were to:

- Develop and test a low-cost research-grade sap flow sensor to measure plant transpiration, using new theory for a heat pulse method and a new design of a sap flow gauge.
- Demonstrate the use of measured transpiration from the sap flow gauges in the development or validation of site-specific basal crop coefficient curves and provide a review of the use of the basal crop coefficients.
- Develop an artificial dry reference surface for continuous estimation of actual canopy conductance, plant transpiration and to monitor crop water status in the field using a thermal approach.

Dissertation Organization

This dissertation is a collection of three manuscripts intended for submission to peer-reviewed journals. In the first manuscript (Chapter 2) we describe the development a Sap-Flow-System to assess plant water consumption and test its performance in the field. The purpose was to develop a research-grade sap flow system using a new theory for a heat pulse method. The method consists of using a heat pulse of a finite length with less power than traditional methods, reducing the thermal wound effect on the plant. The design of the system integrates low cost and open-source sensors and electronics and the use of the Internet of Things (IoT). We tested the performance of a new 3-D printed design containing two temperature probes non equidistant from a heater with a new theory based on the heat ratio method. The gauges were calibrated and validated for maize (*Zea mays* L.) in greenhouse experiments and deployed in fully irrigated corn fields for its evaluation during two years.

The second manuscript (Chapter 3) provides a review of the benefits and constraints of the use of the basal crop coefficient (K_{cb}) in the dual crop coefficient approach of estimating ET_c . We provided a demonstration of the use of the new sap flow sensors for the estimation of maize K_{cb} , since sap flow sensors provide a direct measure of plant transpiration. Field tests during two years showed that the new low-cost sap flow sensors can be used to develop or validate local corn K_{cb} curves under field conditions.

In the third manuscript (Chapter 4) we developed a low-cost hemispherical 3-D printed artificial reference surface (ARS) that imitates the temperature of a maize leaf surface that is not transpiring. The device was integrated in an IoT system with infrared thermometers sensing actual maize canopy temperature and was tested in a well irrigated and in a deficit irrigated maize field. The ARS allowed the continuous estimation of absolute values of maize transpiration and canopy

conductance. The results were compared to the measured transpiration and canopy conductance from the new sap flow gauges. The ARS was also used to test a practical approach to detect and monitor maize water stress in the field.

The dissertation ends with general conclusions and recommendations (Chapter 5) summarized from the three manuscripts.

References

- Allen R, Pereira S, Smith M. 1998. Crop evapotranspiration: Guidelines for computing crop water requirements. FAO, Irrigation and drainage paper, N°56. FAO, Rome. 300p.
- Damour, G.; Simonneau, T.; Cochard, H.; Urban, L. 2010. An overview of models of stomata conductance at leaf level. *Plant, Cell and Environment*. V.33: 1419-1438. doi: 10.1111/j.1365-3040.2010.02181.x .
- Eekhout, J.; Hunink, J.; Terink, W.; de Vente, J. 2018. Why increased extreme precipitation under climate change negatively affects water security. *Hydrology and Earth System Sciences*. V.22: 5935-5946. <https://doi.org/10.5194/hess-22-5935-2018> .
- FAO, IFAD, UNICEF, WFP and WHO. 2022. The State of Food Security and Nutrition in the World 2022. Repurposing food and agricultural policies to make healthy diets more affordable. Rome, FAO. 260p. <https://doi.org/10.4060/cc0639en> .
- Florke, M.; Schneider, C.; McDonald, R. 2018. Water competition between cities and agriculture driven by climate change and urban growth. *Nature Sustainability*. V.1: 51-58. <https://doi.org/10.1038/s41893-017-0006-8> .
- Foley, J.; Ramankutty, N.; Brauman, K.; Cassidy, E.; Gerber, J.; Johnston, M.; Mueller, N.; O'Connell, C.; Ray, D.; West, P.; Balzer, C.; Bennett, E.; Carpenter, S.; Hill, J.; Monfreda, C.; Polasky, S.; Rockstro, J.; Sheehan, J.; Siebert, S.; Tilman, D.; Zaks D. 2011. Solutions for a cultivated planet. *Nature*. V. 478: 337-432. doi:10.1038/nature10452.
- Giovannucci, D.; Scherr, S.; Nierenberg, D.; Hebebrand, C.; Shapiro, J.; Milder, J.; Wheeler, K. 2012. Food and Agriculture: The future of sustainability. New York. pp.80. http://www.un.org/esa/dsd/dsd_sd21st/21_pdf/agriculture_and_food_the_future_of_sustainability_web.pdf .
- Jensen, M. 1968. Water consumption by agricultural plants. In. Water deficit and plant growth. T. Kozlowski, ed. V2, Academic Press, New York. 1-22.
- Jones, H. 1999. Use of infrared thermometry for estimation of stomatal conductance as a possible aid to irrigation scheduling. *Agricultural and Forest Meteorology*. V. 95: 139-149.
- Katerji, N.; Rana, G. 2006. Modelling evapotranspiration of six irrigated crops under Mediterranean climate conditions. *Agricultural and Forest Meteorology*. V. 138: 142-155. doi:10.1016/j.agrformet.2006.04.006 .
- Lascano, R. 2000. A general system to measure and calculate daily crop water use. *Agronomy Journal*. V.92: 821-832.

Leinonen, I.; Grant, O.; Tagliavia, C.; Chaves, M.; Jones, H. 2006. Estimating stomatal conductance with thermal imagery. *Plant, Cell and Environment*. V. 29: 1508-1518. doi: 10.1111/j.1365-3040.2006.01528.x .

Monteith, J. 1965. Evaporation and environment. *Symposia of the Society for Experimental Biology*. V.19: 205-234.

Penman. 1948. Natural evaporation from open water, bare soil and grass. *Proceedings of the Royal Society of London. Series A, Mathematical and Physical Sciences*. V.193(1032):120-145.

Sinclair, T. 2019. "Natural Evaporation from Open Water, Bare Soil and Grass" by Harold L. Penman, *Proceedings of the Royal Society of London (1948) A193:120–146*. *Crop Science*. V.59: 2297-2299. doi: 10.2135/cropsci2019.05.0292 .

CHAPTER 2

A NOVEL SAP FLOW SYSTEM TO MEASURE MAIZE TRANSPIRATION USING HEAT PULSE METHODS

Summary

Finding ways to irrigate more efficiently is crucial for long term agricultural sustainability around the globe. Assessing plant water consumption using sap flow gauges (SFG) can help to quantify irrigation water requirements and different pathways to improve irrigation efficiency. We evaluated a new method for a heat pulse technique and developed a novel type of sensor to measure the flow of water through plant stems. These SFGs were made using a desktop 3D printer, low-cost components, open-source electronics and use cellular-based Internet-of-Things (IoT) technology. Sensors were calibrated and validated in a greenhouse and evaluated in a well-irrigated maize (*Zea mays* L.) field in northern Colorado for two years. The performance of the IoT-SF system was satisfactory. In 2019 SFG greenhouse validation studies showed a strong correlation with gravimetric measurements with a root mean square error (RMSE) of 10% and mean absolute error (MAE) of 9.4% from the mean daily transpiration (T). In the field, comparison with commercially available SFGs showed an RMSE of 12.4% and MAE of 10.2% with an overestimation of 9% for daily T estimation. Comparison with maize T calculated from the ASCE reference evapotranspiration (ET_r) and basal crop coefficients (Kcb) showed similar results. In 2020 greenhouse validation showed an RMSE of 15.4% and MAE of 12.1% of mean T value. At field scale, when multiple SFG measurements were scaled up to estimate T in mature maize, hourly rates of T showed a coefficient of determination of 0.95 with respect to the ASCE $ET_r \times Kcb$. It allowed daily estimates with a difference within 10%. RMSE and MAE was 0.62 mm and

0.48 mm, with a precision of ± 1.04 mm SD. Total difference of T for the period measured with both methods was 4.4%. The accuracy of the measurement varied with the number of gauges deployed. Results demonstrated that these SFGs are an adequate tool for monitoring of crop water use at the field scale.

Introduction

Sap flow gauges (SFGs) are one of the few sensors that can measure the whole plant transpiration. Techniques and gauges are adapted and used in a wide range of plant species and sizes, from herbaceous such as maize, sunflower, soybean or tomato (Miner et al., 2017; Senock and Ham, 1993; Sakuratani, 1984) to woody species such as shrubs or Eucalyptus trees (Wang et al., 2018; Burgess et al., 1998). They are even used in very small structures such as kiwifruit pedicels and ornamental plants leaf petioles (Clearwater et al., 2009).

One of the major advantages of using these devices is that they can be installed in treatment studies and small plots where other micrometeorological sensors are restricted because they need larger areas to work properly (Bethenod et al., 2000; Smith and Allen, 1996). Results from multiple SFG installed in the field can be scaled up in order to calculate a real canopy transpiration (Ham et al., 1990; Bethenod et al., 2000). They provide a valuable advantage by allowing a continuous measurement of the plant transpiration and adaptability for automated recording (Jones, 2004). Plant transpiration reflects the effect of multiple factors, such as soil water depletion, weather changes, pest infestation, physiological characteristics of plants, soil or water salinization or agronomic management practices; therefore, these devices are well suited for a wide range of purposes. They have been used to study effects of CO₂ increase on transpiration (Dugas et al., 1994; Senock et al., 1996; Owensby et al., 1997), soil-plant-water relations (Cohen et al., 1990), plant irrigation with salinity hazard (Cohen et al., 1995), root sap flow studies

(Burgess et al., 1998). SFGs allowed for evaluation of irrigation treatments on plants (Cohen et al. 1995, Jara et al., 1998, Ballester et al., 2013); for irrigation scheduling (Fernandez et al., 2001; Fernandez et al., 2008); evaluation of energy partitioning for evaporation and transpiration in a crop canopy (Ham et al., 1990; Jara et al., 1998; Sauer et al., 2007), water flows in roots under water stress (Burgess et al., 1998), or development of water stress indicators (Ballester et al., 2013) or to study plant hydraulic functioning (Steppe et al., 2015). Gauges have been also used to test the performance of different models, such as Crop water Stress Indices (Ming et al., 2018); water uptake (Chabot et al., 2002), sensitivity of ET models to input parameters (Zhao et al., 2015) and canopy resistance models (Aiken and Klocke, 2012).

Sap flow gauges have also been proven to be a valuable tool for site specific derivation of basal crop coefficient (K_{cb}) curves (Poblete-Echeverria and Ortega-Farias, 2013; Zhao and Zhao, 2014). A dual crop coefficient approach is desired in precision irrigation applications and when a more precise soil water balance is needed (Puig-Sirera et al., 2021). Even though tabulated K_{cb} values are accepted to be transferable for different locations (Allen et al., 1998), some site-specific conditions that modify crop architecture, vigor and canopy management might change the K_{cb} . For example, in maize Trout and DeJonge (2018) found local mean K_{cb} values to be higher than the tabulated, attributed in part to the use of modern maize varieties that have different, more upright architecture than older varieties. However, deriving K_{cb} values is cumbersome. Methods like lysimeters are not usually available and are expensive and other procedures such as soil water balance can be time-consuming and less accurate. SFGs on the other hand, by measuring actual transpiration, are one of the few tools that allow a direct and fast derivation of site-specific K_{cb} values.

By providing the actual measure of plant transpiration or by allowing the adjustment of local K_{cb} values, SFGs have proved to be a useful tool to manage water for plants. In addition, these plant-

based sensors also have a potential use in automated precision irrigation systems (Jones, 2001). Nevertheless, for scientific or non-scientific purposes, the use of several number of commercial SFGs can make the system too expensive and complex to be implemented (Ballester et al., 2013).

During the past years a tendency to develop “Free and open-source hardware” (Pearce, J. 2017) for science and engineering has been growing. This concept focuses on dramatically reducing the cost of research-grade equipment by using low-cost circuit boards and 3D printing (Pierce, J. 2013). This makes the equipment accessible for the general public or allowing the user to build equipment replications for more repetitions (Pearce, J. 2017). In addition, the Internet of Things (IoT) is a key technology enabling continuous monitoring of soil, crops, and microclimate and reduces the total cost of technologies that allow to manage irrigation processes. One of its great advantages is the generation of high spatiotemporal data that can contribute to a better management of farming systems (Chamara et al., 2022).

Numerous low-cost IoT tools are being developed for precision irrigation applications to improve plant water management, such as weather sensing, soil moisture and plant temperature monitoring or tools to aid irrigation automation (Botero-Valencia et al., 2022; Jones et al., 2018; Ham et al., 2021; Payero et al., 2017; Spinelli et al., 2019). Sap flow sensors, by giving an actual measure of plant water needs, are a useful tool to be incorporated into these types of systems. They can be especially useful in situations of incomplete crop canopies or when accurate quantifications of plant water use are needed. Useful information can be obtained from the simultaneous monitoring of soil moisture, plant temperature and transpiration.

Our main goal was to develop a novel IoT-Sap-Flow-System to assess plant water consumption and test its performance in the field. The aim was to develop a research-grade sap flow system using a new theory for a heat pulse method based on the heat ratio method (Marshall, 1958;

Burgess et al., 2001). The method uses a heat pulse of a finite length, with a longer duration and less power than traditional methods, reducing the thermal wound effect on the plant (Kluitenberg and Ham, 2004). Our work improves on the research by Miner et al. (2017), by developing a new heat pulse technique that does not use a side probe and allowing a better adjustment for stem sizes. The SFG consists of two temperature probes at non equidistant distances from a heater. In addition, we incorporated the IoT component to the system, on the assumption that their simple characteristics and electronics would allow it to adapt to IoT, generating the groundwork for creating a sap flow network of wireless sensors nodes covering large areas.

Our objectives were: 1) to develop a new heat pulse method and novel SFG design and system, integrating low cost and open-source sensors and electronics; and 2) to calibrate the sensors in a greenhouse experiment and test their performance in a well irrigated maize field.

Theory

The heat pulse method (HP) of sap flow measurement consists of applying a heat pulse into the plant by a heating probe inserted in the plant stem. The temperature rises at a certain distance from the heater and is measured with temperature probes also inserted in the stem at certain depth. The theory behind the heat pulse method is based on the heat convection-diffusion equation to calculate heat velocity (Marshall, 1958; Cohen et al. 1981; Cohen et al. 1988) and related to the speed of the sap flow through the stem. It is assumed that the sap flow measured from the xylem is equivalent to transpiration (Cohen et al. 1981). The equation describing the temperature elevation combined with the heat wave velocity equation allows the calculation for water flux:

$$V = \frac{\sqrt{x^2 - 4kt_m}}{t_m^2} \quad [1]$$

where x is the distance from the heater to the downstream temperature sensor, k is thermal diffusivity of the stem and t_m is the time to the maximum temperature after the heating pulse. This methodology is called the Tmax method. Tmax method has shown to work well for moderate to high flows.

The HP theory assumes that the heating of the stem is instantaneous, therefore the heating duration should be very small (0.25 seconds) but applying a high amount of heat. This could lead to stem injuries, thus, adjusting the applied heat to lower intensity but with longer durations reduces this risk of damaging the stem, but the theory does not account for non-instantaneous heating time. Kluitenberg and Ham (2004) introduced important corrections to solve for this. Previous methodology assumes that heat is released instantaneously and when heating durations increases this approximation leads to errors in sap flow estimation. This new theory takes into account a finite duration for the heating period.

This improved theory yields:

$$V = \sqrt{\frac{4k}{t_0} \ln\left(1 - \frac{t_0}{t_m}\right) + \frac{x^2}{t_m(t_m - t_0)}} \quad [2]$$

where t_0 is the heat pulse duration. They showed that the use of the previous theory underestimates K and the true value of V , and the magnitude increases as the velocity increases and the error in V increases as t_0 increases. Errors in V are larger when there is a smaller probe spacing and longer heating time (Kluitenberg and Ham, 2004).

The improvements from Kluitenberg and Ham (2004) allows the use of longer heating durations and the use of different probe spacings without introducing errors to the sap flow measurements. This new theory was used with great success for maize and sunflower (Miner et al., 2017).

The water flux is integrated over the stem area to determine the volumetric flow. The heater and temperature sensors were placed in the same longitudinal plane to simplify the solution (Cohen et al. 1988).

Our new Theory

Besides the Tmax method, which is known to be inaccurate for low flows (Cohen et al., 1988) and can be affected by ambient background temperature, there are other various heat pulse techniques. One of them is the heat ratio method (Marshall, 1958; Burgess et al., 2001), which uses the changes in temperature after an instantaneous heat pulse to determine sap flow velocity. To simplify the V approximation, it uses two temperature probes located at the same distance from the heater, upstream and downstream.

$$V = \frac{k}{L} \ln \left[\frac{\Delta T_d}{\Delta T_u} \right] \quad [3]$$

where L is the distance from the heater to the temperature probes and T_d and T_u are the temperature rise at the downstream (T_d) and upstream (T_u) probes. Nevertheless, one of the downsides of the method consists of basing the results on the value for thermal diffusivity (k), likewise Tmax method, that has to be known or determined. The other disadvantage is the need for three probes instead of two, increasing the damage to the plant.

The original heat ratio method (Marshall, 1958; Burgess et al., 2001) involves measuring the ratio of changes in temperature at locations upstream and downstream from an instantaneous heat pulse with probes that are equally distal from the heating source. The heat pulse velocity is determined in terms of the relative temperature rise at known times.

Miner et al. (2017) introduced new theory that showed a theoretical advantage of having measurement of lateral heat flow, this also allowed them to measure the thermal properties of the stem. However, the downside was that it was harder to implement on small diameter stems because it needs enough width to accommodate the lateral temperature probe. To solve for this, the new theory introduced here refers to an upstream probe vertically aligned to the other two probes. In this new approach we are using a new variation of this heat pulse method and likewise Miner et al., (2017) using a non-instantaneous heat pulse. The relative temperature lifts from the probes are found at different elapsed times from the heat pulse, measuring temperature for 160 seconds. The elapsed time of 160 seconds used in this study was based on previous study by Miner et al. (2017) who used 180 seconds. It was seen that the temperature lifts were found in a shorter timeframe, within 160 seconds.

In this new approach probes are not equally spaced from the heater, and we are specifically using an upstream distance (L_u) smaller than the downstream distance (L_d) from the heater. The method assumes isotropic thermal properties of the plant tissue because stem water contents of maize are large. It assumes that sap is moving downstream at a constant rate through a homogeneous plant tissue, with sap and plant tissue in thermal equilibrium. The derivation for the new theory for the heat-pulse velocity from the line source solution (Marshall, 1958) can be found in Appendix A, yielding two approximations for V :

$$V \approx \frac{2k}{L_d + L_u} \ln \left(\frac{L_d^2 \Delta T_{m.d}}{L_u^2 \Delta T_{m.u}} \right) \quad [4]$$

and

$$V \approx \frac{2k}{L_d - L_u} \left[1 - \sqrt{1 - \left(\frac{L_d - L_u}{L_d + L_u} \right) \ln \left(\frac{L_d^2 \Delta T_{m.d}}{L_u^2 \Delta T_{m.u}} \right)} \right] \quad [5]$$

$T_{m,d}$ and $T_{m,u}$ represent the maximum temperature increase or lift after the heat pulse ($T_{\text{maximum}} - T_{\text{initial}}$) of the downstream and upstream probes, respectively.

In this study, we used the first order approximation (equation 1) given that the simplest approximation model with a good fit is best to be used. A drawback of the method is the sensitivity to errors in probe spacing (L_d and L_u).

The method used in this study has low power requirements and the gauge design can allow the use of the gauge in plants with small stem diameters. Likewise heat pulse methods, implies the need of measuring the cross-sectional area of the stem manually and the direct wound to the plant when probe is inserted is lessened by the low heat input.

The new method proposed in this study intends modification in the heat ratio theory to improve the sensitivity to high and low heat pulse velocities simultaneously by implementing two temperature probes at different distances from the heater. We calculated the maximum temperatures for a 160s period after the heating pulse.

Materials and Methods

The study was carried out in two phases. The first phase included perfecting the construction of the gauges, calibrating and testing the prototype gauges and new theory on container-grown maize in the greenhouse. During this phase, sap velocity measured by the gauges was compared to gravimetric measurements of transpiration for calibration and validation studies. The second phase involved testing multiple gauges in a fully irrigated maize field in northern Colorado, USA. The research was carried out at two locations. In 2019 the study was conducted at USDA-ARS Limited Irrigation Research Farm (LIRF), Colorado, USA (40°26'54"N, 104°38'21"W, 1426m). The study period was during August and September 2019 at a large plot of 190 m x 110 m, with a subsurface drip irrigation system. In 2020 it was at the Irrigation Innovation Consortium (IIC) Headquarters, Research Farm, Fort Collins, Colorado, USA (40°33'26"N, 106°59'43"W, 1426m), in a plot of 6 ha with a surface irrigation system. The study was conducted from August to September 2020. Transpiration data from the gauges were compared to the widely accepted model, the ASCE standardized tall reference Penman Monteith equation and a local maize basal coefficient (K_{cb}) curve (Trout and DeJonge, 2018) during both seasons. In 2019 transpiration from the gauges were also compared to data from commercially available SFGs (Daynagage sap flow stem gauges SGB25, Dynamax Inc., Houston, USA) deployed in the field.

Gauge design

The SFG consists of three needles and 3D-printed parts (Figure 1). The hypodermic needles provide the housing for the heater and the thermistors allowing them to be inserted into the stem of the plant. The technique used to fabricate the needle probes was described in Ham and Benson (2004) and Miner et al. (2017). The hypodermic needles used were 18 AWG x 1in veterinary polypropylene hub needles, 25-mm-long and 1.27-mm diameter (Convivial Monoject™

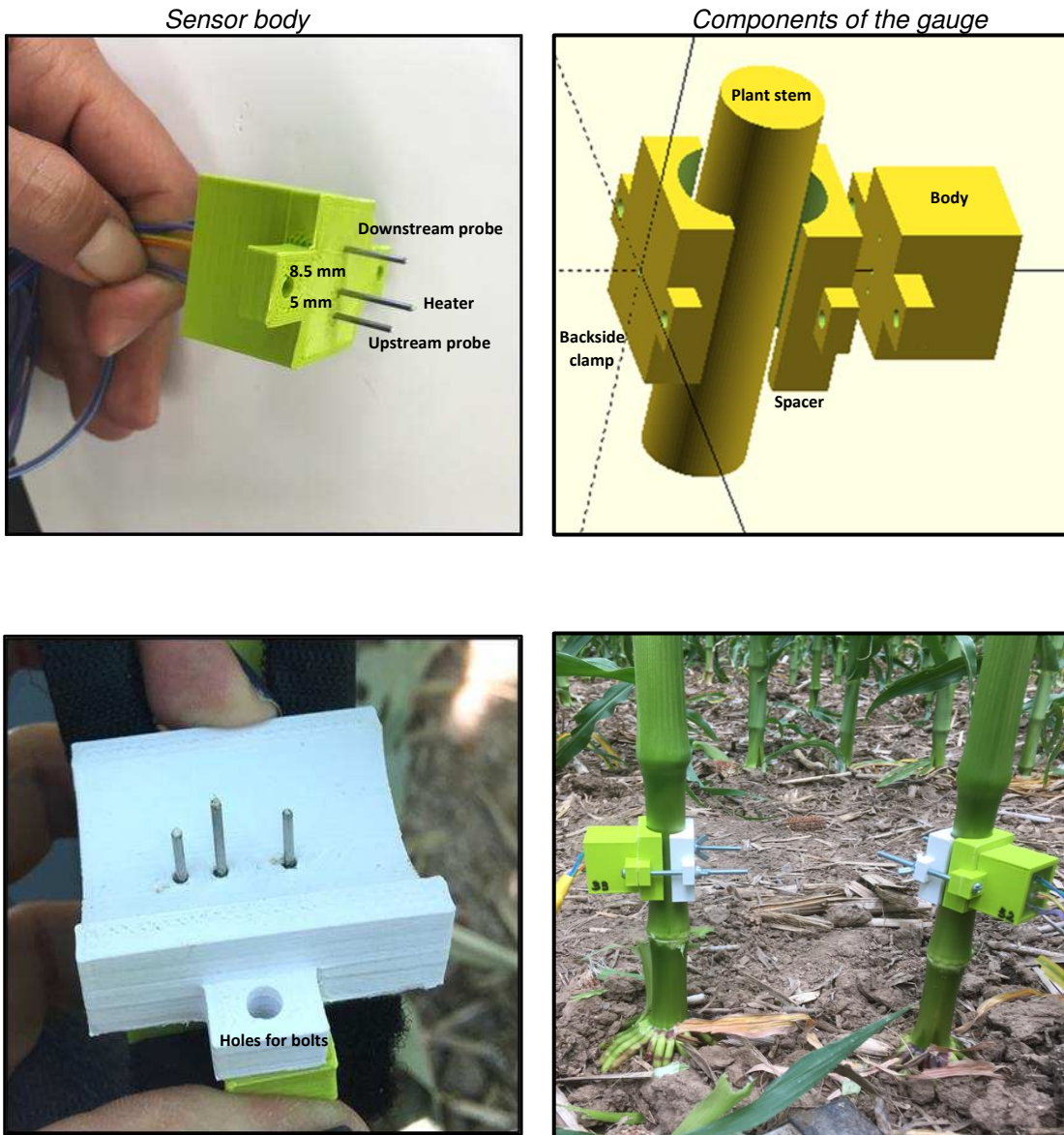
veterinary needles). To make the temperature probes, (Figure 1) the needles were cut to a length of 16.5 mm, and 10K-NTC thermistors (LSMC-700A010KD002, SELCO Products Co, Reno, Nevada, USA) were positioned at the tip. The needles were filled with high-thermal-conductivity epoxy (Omega Bond 101, Omega Engineering, Stamford, Connecticut, USA). Needle lengths were studied by Miner et al. (2017) in order to have an insertion on the plant of 6.5 mm (thermistors) and 9 mm (heater) using the 3D-printed design from the study. Insertion length is similar to the recommended depths by Cohen and Li (1996) and analyzed for maize for a HR heat pulse technique in previous studies (Miner et al., 2017).

To make the heater probes (Figure 1), the needles were first cut to a length of 19 mm. A 115-mm length of enameled heater wire (S2140N80HML, 40 AWG Solid, 0.003mm outside diameter, Nichrome 80, 67.4 ohm/ft; Pelican Wire Company, Naples, Florida, USA) wrapped in two loops was routed back and forth along the length of the tube (four parallel strands total). Heaters were also filled with thermo-conductive epoxy (Omega Bond 101) and typically had a total resistance of 24-27 Ohms.

The probes were connected to the electronics by a ribbon cable protected with a 12.7mm nylon multifilament braided sleeving (Techflex Inc., Sparta, New Jersey, USA).

The 3D printed parts included the body, spacer, and a backside clamp (Figure 1). The assembly was secured to the plant stem using two 3.3 mm, 6 cm long screws with wingnuts. The upstream temperature probe is 5 mm away from the heater and the downstream temperature probe is 8.5 mm from the heater. Similar non-equidistant distances (9mm downstream and 4mm upstream) were used by Cohen et al. (1988) for a compensation heat pulse method, and by Cohen et al. (1995). A distance of 5 mm was the closest that the hypodermic needle cap could be physically positioned next to the heater, inside the 3D printed body. After the needles were positioned, the body was filled up with regular clear epoxy (Loctite® E-30CL hysol). The spacer is a 5 mm module

that can be custom printed with different shapes and sizes to accommodate the needles for different stems. The main function is to control the insertion depth of the sensors in the plant stem (Figure 1). The backside clamp allows the attachment of the gauge to the plant. The 3D printing filament used was a 3mm acrylonitrile butadiene styrene (ABS) using Lulzbot 3D printer (Lulzbot, TAZ-6, Aleph Objects Inc., Loveland, Colorado, USA) with 40% infill.



Spacer

Sap flow gauges on plants

Figure 1. Sap flow gauge and its components.

When using the gauges, first, the stem diameter of the plant is measured along the short and the long radius using a caliper. Then, the plant stems are primed by making holes shorter than the gauge probes using a manual micro-drill or the tip of a hypodermic needle to guide the insertion of the probes. The body with the spacer is inserted into the stem, the backside clamp is positioned at the opposite side of the stem, and the bolts (running through the holes of the three parts) attaches the sensor to the plant (Figure 1).

Components of the system

Four gauges were connected to one circuit board with microprocessor. The gauges along with the microprocessor, electronic components, and power supply worked as a complete sap flow system. The system for the SFGs was fabricated using low-cost-open-source sensors and electronics.

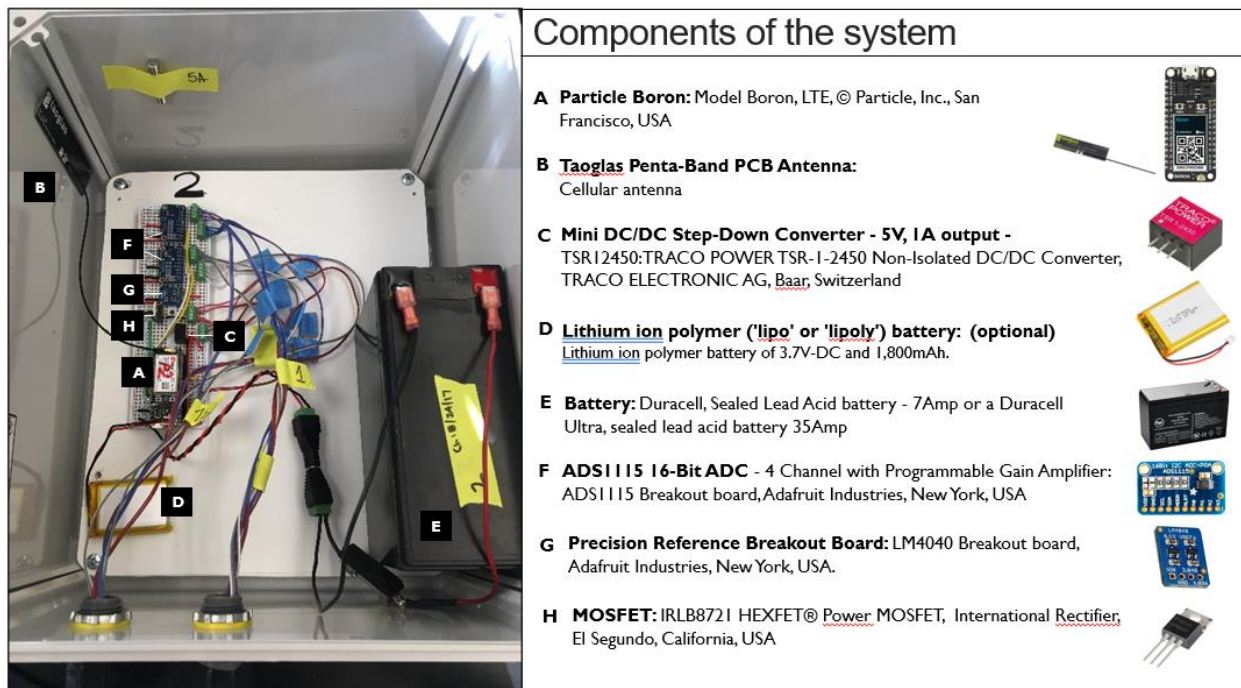


Figure 2. Schematic view for the sap flow gauge microcontroller.

The SFG heaters produce a 3s-heat pulse using 12V supplied by a battery (Figure 2E). The pulse is controlled with a MOSFET (Figure 2H), a type of transistor that switches the power on and off to the heater. A mini DC/DC step-down switching regulator with 3V, 1A output (Figure 2C) was used to convert the 12V battery to 3V in order to power the boron. A voltage divider using a 1KOhm and a 10KOhm resistor was used to monitor the voltage from the battery.

The power supply for the sap flow system was a 12V battery (Figure 2E) and a 10W solar panel.

A precision voltage reference breakout Board (Figure 2G) was used to ensure a stable input voltage of 2.048V to the thermistors. A 10 KOhm circuit bridge was used to measure the analog signal from the thermistors that was converted to digital using a 16-Bit ADC (Figure 2F), (Analog to 16-bit digital conversion from the thermistor to the microprocessor) to be read by the microprocessor. The thermistors resistance readings were converted to temperature using the Steinhart-Hart equation provided by the Selco thermistor Products. The resolution for temperature was 0.002 °C.

A circuit board with microprocessor from Particle was installed, using the model Boron (Figure 2A) which has a LTE-cellular modem, using an electronic SIM card. A lipo battery (Figure 2D) was connected to the Boron (Figure 2A) for power backup. For the greenhouse experiment a Taoglas Penta band antenna (Figure 2B) was connected to the boron, for the field experiment an external wideband directional antenna was used (700-2700 MHz, 75 Ohm; Wilson Electronics LLC). This board enabled the use of the IoT technology, using Ubidots as the IoT provider (Ubidots, Medellin, Colombia). The cloud platform was used for real-time data visualization and storage.

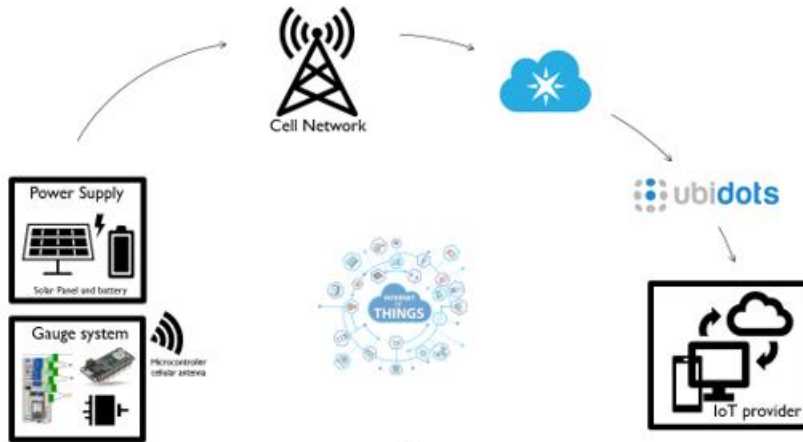


Figure 3. Schematic for the Internet of Things Sap Flow system in the field.

The complete system consists of sensors (SFGs) deployed in the field, connected to a logger with IoT connectivity and to the power supply. Cellular network was used to send data to the cloud. Data collected from the four gauges was sent to the Particle cloud primarily and then the data was sent to the IoT provider, Ubidots for the user interface. Data was stored in the Ubidots cloud and was also available for real time visualization from any device and from any place in the world (Figure 3).

Calculations and protocol

The system was able to read 4 gauges simultaneously and was programmed to take measurements every 15 minutes daytime and nighttime.

The reading protocol is illustrated in Figure 4. The sap flow system first took the initial temperature readings of all stems, followed by a heat pulse of a duration of 3 seconds. It read the temperature of the upstream and downstream probes at 4hz during 160 seconds after the heat pulse was sent. The maximum temperature lift (T_{md} and T_{ms}) was determined from a 3-point moving average filter to smooth out short-term fluctuations and help identify the maximum. Next, it sent the data

to the cloud for storage and visualization. The system was designed to conserve the energy of the battery by sending the microprocessor to a power-saving state for 15 minutes (between readings).

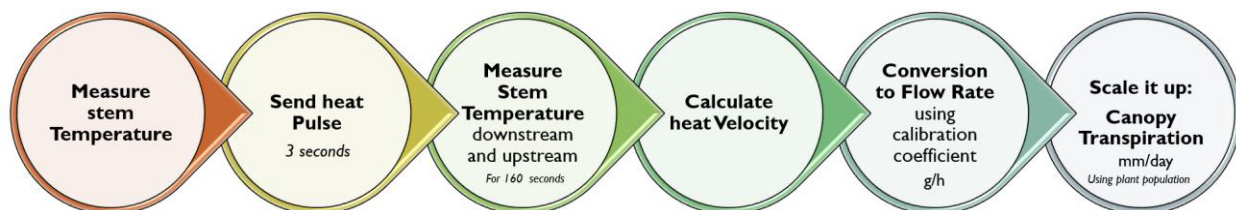


Figure 4. Schematic of the methodology used for maize transpiration calculation.

With the temperature collected the heat velocity was calculated using equation 4. The heat velocity was converted to flow rate by using a calibrated coefficient from greenhouse studies. The calibration procedure is described in section 3.3. The results for individual plant transpiration in g/h can be ultimately scaled up into canopy transpiration by using the plant population field.

For the calculations for heat velocity the thermal diffusivity value used was $2.4 \times 10^{-7} \text{ m}^2.\text{s}^{-1}$, similar to the value used by Cohen et al. (1993a) for mature soybean plants and maize. This value was also used for maize (Miner et al., 2017).

Greenhouse experiment for gauge calibration and validation

Calibration and validation of the SFGs was executed in 2019, 2020 and 2021 in greenhouse studies. Maize hybrid used was a Dekalb DKC51-20RIB, planted at the Colorado State University, Fort Collins, Colorado, Horticulture Center greenhouse facilities.

Plants were grown in 23.6L pots following suggestions by Miner et al. (2017) and Eddy and Hahn (2010). The growth medium was calcinated clay granules, also known as porous ceramic (Profile

®, Greensgrade TM). Plants were fertilized at each irrigation event with a concentration of 200 ppm N, using a 15-5-15 fertilizer with Ca 5% and Mg 2%, (Peters Excel Cal-Mag®).

Temperature at the greenhouse was maintained within 27-32°C during the day and 18-22°C at night. Supplemental lighting used was 1000W High Pressure Sodium (HPS) lights during a photoperiod of 16 hr. (6:00AM-10PM) for all stages of growth.

For calibration and validation of the SFGs the pots were sealed using a glued plastic wrap to avoid water evaporation. Plants were placed on a digital scale (ADAM® PGL 20001, Adam Equipment Inc., Fox Hollow Road, Oxford, CT) $\pm 0.1\text{g}$, connected to a laptop for data acquisition using ADAM DU Data Capture Utility software (Adam Equipment, Maidstone Road, Kingston, Milton Keynes, U.K.). The rates of water loss from the plants were determined by automatically weighing the pot to the nearest 0.1g at one-minute intervals, similar to Miner et al. (2017), during day and night hours. Plants were surrounded by a three-wall plastic sheath to reduce air flow effects on the scale readings and stabilize scale samples.

Leaves were peeled off from the stem section where SFGs were installed and the stem diameter at the point of the gauge insertion was measured with a caliper ($\pm 0.1\text{mm}$).

Two SFGs per plant were used for the experiments. The gauges were inserted in the internodes #2 and #3, staged in opposite sides of the stem. Probes were removed from each plant after 6 days and installed in a new plant. Three plants were used for the calibration at R3-R4 growth stage.

For calibration, the estimated flow velocity using the SFGs was compared against the gravimetric water loss measured by the automatic weights from the scale to determine the calibration factor,

a common procedure with heat pulse gauges (Cohen et al., 1993a, Miner et al., 2017). The transpiration estimated by the SFGs was calculated as the sap flow velocity multiplied to the stem cross sectional area using Equation 6.

Precision of the calibration factor was evaluated using the coefficient of determination (R^2) between observed and estimated sap flow. The amount of bias expressed in percentage was derived from the slope of the regression line between the different plants used for calibration.

For validation, the gravimetric transpiration was compared to the transpiration estimated with the SFGs. Agreement between both measurements would validate the calibrated factor and the new developed theory for heat velocity. Hourly transpiration rates were integrated over 24-hrs to estimate daily transpiration from the SFGs and were compared against the same 24-hour integration for gravimetric measures for maize.

The statistics used to evaluate performance of the gauges were the coefficient of determination (R^2), the root mean squared error (RMSE), mean absolute error (MAE) and a paired t test. A two-sample student t test (paired t test) was performed to evaluate the overall mean difference of transpiration estimates measured with the SFGs during the validation period.

Calibration coefficient: Converting heat velocity to sap flow rate

When using heat pulse methods, an empirical calibration is needed to relate velocity in the sap to plant transpiration (e.g., Cohen et al. 1981). The effective sap conducting area of the stem is a constant fraction of the sectional area of the stem, thus, increases as the stem area increases (Cohen et al. 1988). Gauge calibration consists of plotting transpiration (T) vs. the product of convective heat velocity (V) and cross-sectional area (A) of the stem at the gauge location. (Cohen

et al. 1988). This should be done for a wide range of stem sizes, measuring different plants (Cohen et al. 1990). A linear relationship between V and $T \cdot A$ is expected. Therefore, a common approach for the calibration coefficient (c) determination is the slope for the relationship:

$$T = c(AV) \quad [6]$$

Cohen and Li (1996) validated the use of a pot plant calibration factor used for field transpiration determination. Later Miner et al. (2017) also validated this procedure using Kluitenberg and Ham (2004) methodology.

The calibration factor has been found to be relatively constant for a particular configuration of the heater and the temperature sensors used (Cohen et al., 1981). It was also found that the calibration coefficient in wet soil conditions was also valid for dry soil conditions (Cohen et al., 1990). The coefficient does not change per plant size, time of day, plant age or environmental conditions (Cohen and Li 1996). Cohen and Li (1996) found that orientation and positioning the gauge in the upper or lower position in the stem did not change the calibration coefficient either. The bundle density did not change with the stem orientation. Nevertheless, there is interaction between the stem anatomical structure and the sensor, therefore the calibration coefficient varies with species and gauge configuration (Cohen and Li, 1996). Thus, the depth of the sensor insertion must be consistent for a given calibration and plant species.

There are anatomical differences in plant species. Dicots for example, have a continuous ring of sap flow tissue around the stem, therefore, there is always a needle section in contact with sap conducting tissue. In monocots like maize, the bundles are dispersed in the stem, hence, it is less probable in comparison to dicot species like sunflower, for the needle to be in direct contact with a conducting element. This decreases with depth (Cohen and Li, 1996). However, according to

Cohen and Li (1996), because of the high density of bundles in maize, most likely there is always a section of the thermocouple needle in contact with sap conducting elements (unless it is too deep). Together with the high thermal conductivity of the stainless steel of the needle, the SFGs temperature probes can easily detect the heat wave carried by the sap (Cohen and Li, 1996). Nevertheless, the calibration coefficient varies with insertion depth of sensors in the stem (either for maize or sunflower), as the number of sap conducting elements varies in depth.

Even though the main purpose of an empirical correction factor is to relate the calculated sap flow to the real transpiration of the plant, this coefficient is also taking into account other sources of error in the estimation of heat pulse velocities such as wound effects, structure of the conducting elements (xylem), physical obstruction of the needle and k .

Wound effects caused by physical damage of insertion of the needles into the plant stem, is an important factor for heat pulse measurements (Cohen et al., 1981; Burgess et al., 2001; Green et al., 2003) and high temperatures applied to plant stems can also damage the tissues (Kluitenberg and Ham, 2004). Thermal wounds cause an underestimation of the heat pulse velocities (Swanson and Whitfield, 1981; Burgess et al., 2001; Vandgehuchte et al., 2014) and the effect is different according to the plant species (Green et al., 2003). There is also an effect for the physical disturbance introduced by the probes per se (Cohen et al., 1981; Burgess et al., 2001) interrupting the normal sap flow and tending to underestimate flow (Cohen et al., 1981). These effects can be corrected using numerical solutions (Swanson and Whitfield, 1981, Burgess et al., 2001; Green et al., 2003) or introducing a correction coefficient like we are presenting and using in this study. On the other hand, some studies on corn borer impact on sap flow (Nicholson, 1999) report that maize is able to overcome small localized vascular disruptions and compensate for impacts on sap flow. This would support that small disruptions of the stem with small needles (i.e. sap flow probes) will likely have no effect on bulk sap flow of maize. However, the injury may still have an

effect on the very close proximity of the needle. Still, any possible affect would be contemplated in the calibration factor.

Thermal diffusivity (k) can be also a source of error in a heat pulse method (Cohen et al., 1988). The k can be determined when no convective transport is happening, that is when velocity is zero, in absence of sap flow. However, thermal diffusivity of the stem is uncertain because the condition of zero flow is hard to certify (Cohen et al., 1988). Predawn measurements have been used to determine thermal diffusivity (Cohen et al. 1981; Green et al., 2003). A different way to estimate k is to use simultaneous measurements for two heat pulse techniques such as T_{max} and Compensation heat pulse (Cohen et al., 1988). The k can also be calculated using empirical methods (Marshall, 1958; Burgess et al., 2001). On the other hand, Miner et al. (2017) found that thermal diffusivity calculations for heat pulse methods should be different. They stated that the calculated thermal diffusivity is not a real thermal property, as it has errors introduced by the model and the measurement errors. Therefore, for the heat pulse method they used a k developed by Cohen et al. (1993) and not the k estimated with predawn data. Similarl to the latter study, in the present work errors with k were also considered in the calibration coefficient.

In addition, errors also vary with the method used to estimate heat pulse velocity. The closer the temperature sensors are to the heater the more sensitive they will be to the measuring the change in temperature (Burgess et al., 2001). Nevertheless, when the spacing is reduced, errors in the position of the sensors have greater impact on the accuracy of the measurements (Burgess et al., 2001). Imperfections in the construction of the gauge or deformations when inserted in the stem, modifies the measurements, and also affects the consistent repetitions (Cohen et al., 1981). Inaccurate probe distances of 1mm can cause an error on the velocity calculations of 20% (Burgess et al., 2001).

Field experiment

Field research was conducted during summer 2020 at the Irrigation Innovation Consortium (IIC) Headquarters, Research Farm in Fort Collins, Colorado, USA (40°33'26"N, 106°59'43"W, 1426 m elevation). The SFGs were tested in a 6.6 ha. well-irrigated field. The field was surface irrigated using siphon tubes and graded furrows. Irrigation amount and timing were scheduled using the Water Irrigation Scheduler for Efficient Application (WISE; <http://wise.colostate.edu/>) that estimates crop evapotranspiration (ET_c) using the ASCE standardized reference ET equation (ASCE-EWRI, 2005) along with alfalfa-based crop coefficients (K_{cr} ; Allen et al., 2007); and estimates the soil water deficit in the crop root zone (Andales et al., 2014). The maize was maintained in a fully irrigated condition, satisfying 100% of the ET demands for the period with each irrigation.

Planting was on May 13th, 2020, with a plant population of 80,000 plants ha⁻¹ and 76 cm of row spacing, using the G02K39-3120 maize variety from Syngenta. Plot management practices, herbicide applications and fertilization were done to avoid weed competition and nutrient deficiencies.

Soil moisture was monitored with a calibrated soil moisture sensor CS655 (Campbell Scientific, Inc.; Logan, USA). Sensors were deployed at 15 cm, 50 cm and 100 cm depths. Data from the field was analyzed to confirm a well-watered condition for the field experiment period.

Eight SFGs were installed from August 9th to September 23rd during mid-season to late maize stages (after VT until R5). The gauges were moved to different plants in a weekly basis to avoid wound effects as much as possible, and stem diameters of each plant were measured. Gauges

were installed in the second internode of the plants (Figure 1) after removing the leaf sheath (Cohen et al., 1993a). Stem diameters were around 20.7mm in both treatments.

Measurements from the gauges were transformed to sap velocity using the new theory for heat pulse velocity (Equation 4). Sap velocities were converted to flow rates using the calibration coefficient estimated from the greenhouse experiment.

Finally, the results for plant transpiration were scaled up into canopy transpiration using plant population to obtain mm/day of water transpired by the crop, similar to the method used by Cohen et al. (1995), Gerdes et al. (1994) and Sauer et al. (2007). These results for maize water use were compared to the “reference transpiration” ($ET_r \times K_{cb}$). In this study the reference transpiration for maize was calculated using the ASCE standardized tall reference (ET_r) equation (ASCE, 2005) multiplied by a maize basal crop coefficient developed locally by Trout and DeJonge (2018). The hourly ET_r values were calculated using weather data from an on-site weather station.

Periods with sporadically missing 15-minutes-data were found in 2020 due to equipment/data-transmission failures or periods when gauges were moved to new plants. Data was gap filled for each of the 8 sensors installed in the field (one sensor per plant). Different gap filling strategies exist. Linear interpolation when 15 minutes data was sporadically missing (similar to Rana et al., 2020) was used. When more than 50% of 15 min data was missing (3 out of the 4 values), the entire hour was removed. The gap filling technique for hourly missing data was a simple regression against weather variables and several variables were tested.

Data for sap flow of eight plants was compared with weather variables such as net radiation measured in the field. Solar radiation is the main weather variable driving plant transpiration directly and indirectly (Gerdes et al., 1994). Energy for ET comes from solar radiation (Sauer et

al., 2007), and there is a close relationship between these variables because stomatal aperture, air temperature and vapor pressure deficit are driven by solar radiation (Gerdes et al., 1994). This is the reason why this weather variable had a strong relationship with sap flow measurements (high mean R^2) and was used for the linear regression in the gap filling strategy in this study. Solar radiation was chosen for regression (mean $R^2 = 0.85$ and 0.86 for the 8 gauges, for the well irrigated and deficit plots respectively). Regressions against other SFGs and/or PM-reference evapotranspiration were omitted because we compared sap flow data against the standardized reference ASCE $ET_r^*K_{cb}$. Independence of the measurements was needed in determining the number of gauges suitable for field maize water use estimation. When more than 50% of daytime hours were missing, the entire day was removed. Gap filling for daily missing data was not performed.

A two-sample student t test was performed to compare the overall mean transpiration estimates measured with the SFGs. Integrations of transpiration rates over 24hrs. to estimate daily transpiration from the SFGs were compared against transpiration from $ET_r^*K_{cb}$ for maize.

Evaluation of the performance of the sap flow gauges

For season 2019, days for transpiration estimated with 8 to 12 gauges was used. A set of 17 days with complete hourly data was used for the assessment.

Transpiration measured with the SFGs was compared to the transpiration calculated with the ASCE standardized tall reference Penman Monteith (PM) equation (ASCE, 2005) and the local K_{cb} (Trout and DeJonge, 2018), referred as “reference transpiration”. For this, the hourly rates were integrated into 24hr to get daily values from each method. This evaluation was carried out in a well irrigated maize field. Transpiration results from the developed SFGs were also compared

to the transpiration from commercially available SFGs also deployed in the field. The following statistics were used to evaluate transpiration: coefficient of determination (R^2), the root mean squared error (RMSE), mean absolute error (MAE) and a paired t test.

Precision of the gauges were evaluated using standard deviation (SD) and R^2 between the reference transpiration and the commercially available SFGs vs the sap flow transpiration from the gauges developed in this study. A similar procedure for 2020 was performed. For season 2020, days for transpiration estimated with 8 gauges was used. A set of 12 days with complete hourly data was used for the assessment.

Precision of the gauge was also evaluated using the SD and R^2 between the reference transpiration and the sap flow transpiration. To evaluate the overall accuracy of transpiration measurements with the 8 sensors in the field, the standard error (SE) and margin of error (ME) were used.

An assessment of the evolution of the statistical parameters (SE and ME) with the number of gauges used for the estimation of the mean transpiration was carried out. For this analysis a number of random gauges were selected for the statistical evaluation using a simulation. We simulated groups of random combinations of the 8 gauges (actual data from the 8 gauges deployed in the field) and created clusters of 2 to 8 gauges. The random groups selected for the SD calculation were iterated 1000 times to ensure an unbiased representation of group sampling. Standard error and ME was calculated for each cluster.

A power analysis was also carried out to evaluate the probability of finding transpiration differences between two treatments of 1 mm/d or above using 8 gauges. The statistical power for the inferential analysis (power.t.test) using the software R was implemented. The reversed

procedure was used to evaluate the number of sensors required to be installed for a probability of 80% or above for finding differences of 1mm/d.

Results and discussion

Results from season 2020

Greenhouse calibration

Calibration for the SFGs was done using potted plants in a controlled environment. The use of a pot plant calibration factor used for field transpiration determination has been validated in previous studies (Cohen and Li, 1996). Later Miner et al. (2017) also validated this procedure using methodology developed by Kluitenberg and Ham (2004). Although calibrations need to be determined for different plant species, coefficients do not vary with different atmospheric conditions (Cohen et al., 1993a).

Transpiration from the potted plants ranged from around 3-4 g/h at night to around 104 g/h and up to a maximum of 150 g/h. The calibration coefficient was derived using the strong linear relationship between the plant transpiration rate and the sap velocity estimated with the new algorithms (Figure A1 in Appendix A and Table 1). A linear relationship was also used by Cohen et al. (1993a) for soybean and Miner et al. (2017) for maize and sunflower.

We found a pooled mean calibration factor of 1.28 with a standard deviation of 0.2 ($1.28 \pm \text{SD } 0.2$, $n = 7$) across sensors and plants, that correlates with Miner et al., 2017, who found the same coefficient for maize, however using a different hybrid. The calibration coefficient varied from 0.94

to 1.49. The variation of the coefficient was likely caused by several factors including gauge construction variations, xylem vessels geometry variations, diameter size, wounding effects, position of the thermistors and vessel. Differences between calibrations can be explained by the location where the thermocouples and heater are inserted. The distribution of the vascular tissues in the cross-sectional area of maize plants is scattered and uneven (Cohen et al., 1993a). The deeper in the stem from the surface, the lower the density of the bundles, therefore, the heat wave measured is slower than the sap moving through the vascular tissue.

Table 1. Greenhouse calibration description for the Sap flow gauges.

| Plant | Calibration factor | R² | Number of days for calibration | Stem diameter (mm) |
|--------------|---------------------------|----------------------|---------------------------------------|---------------------------|
| 1 | 1.12 | 0.95 | 7 | 20.16 |
| 1 | 0.94 | 0.96 | 7 | 21.08 |
| 3 | 1.49 | 0.93 | 10 | 21.52 |
| 3 | 1.19 | 0.95 | 10 | 23.63 |
| 4 | 1.39 | 0.93 | 6 | 24.86 |
| 7 | 1.48 | 0.87 | 1 | 25.28 |
| 7 | 1.38 | 0.95 | 1 | 25.8 |

Calibration coefficients were derived for a range of number of days installed, cross sectional stem areas, sensors, and maize age. A total of 4 plants were used, with stem diameters from 20.16 mm to 25.8 mm (this measurement is the mean of long and short sides of the stem). The maize phenology varied from R3 to R5.

Previous studies have shown a calibration factor SD of 0.101 (Cohen et al., 1993) for a mean calibration coefficient of 1.73 for maize. Cohen and Li (1996) reported less variability in the coefficient, 1.59 ± 0.057 . In our study, the pooled mean calibration coefficient for maize was 1.28 with a margin of error of 0.19, hence, there was a 95% confidence that the coefficient is between 1.47 and 1.09. The maize variety used for this study was different from the one used in Miner et

al. (2017), yet calibration factor estimated were similar in both studies. This agrees with Cohen (1993), who stated that calibration coefficients should not vary between maize varieties. Cohen and Li (1996) also found that calibration coefficient should not vary with hybrids or environmental conditions because maize has a constant shape of bundles between plant varieties. On the other hand, a previous study with maize using a 6 second heating time showed a higher factor (results not shown in this chapter). In that work, while the transpiration results from the SFGs agree with the reference transpiration, the stem wound caused by heat was visible. This was probably because the injuring effect on the sap flow estimation was included in the calibration factor. This would explain the differences between calibration factors found for maize in other studies using the heat pulse technique (Cohen et al., 1993).

Another factor related to heating injury is the amount of heat applied by the heating probe. Heat is created because of the current flowing through a resistor, the heating wire heats up and by conduction is transferred to the stem. Two factors define the amount of heat: time of heating pulse and resistance. If the resistance of the wire changes, then using the same heating time would result in different heat exposure of the plant. Care should be taken when constructing the gauge, to maintain the same characteristics of the heating probe (length of the heating wire and loops along the steel needle) and measure its resistance. Manufacturing differences can produce differences in the amount of heat using a certain heating time.

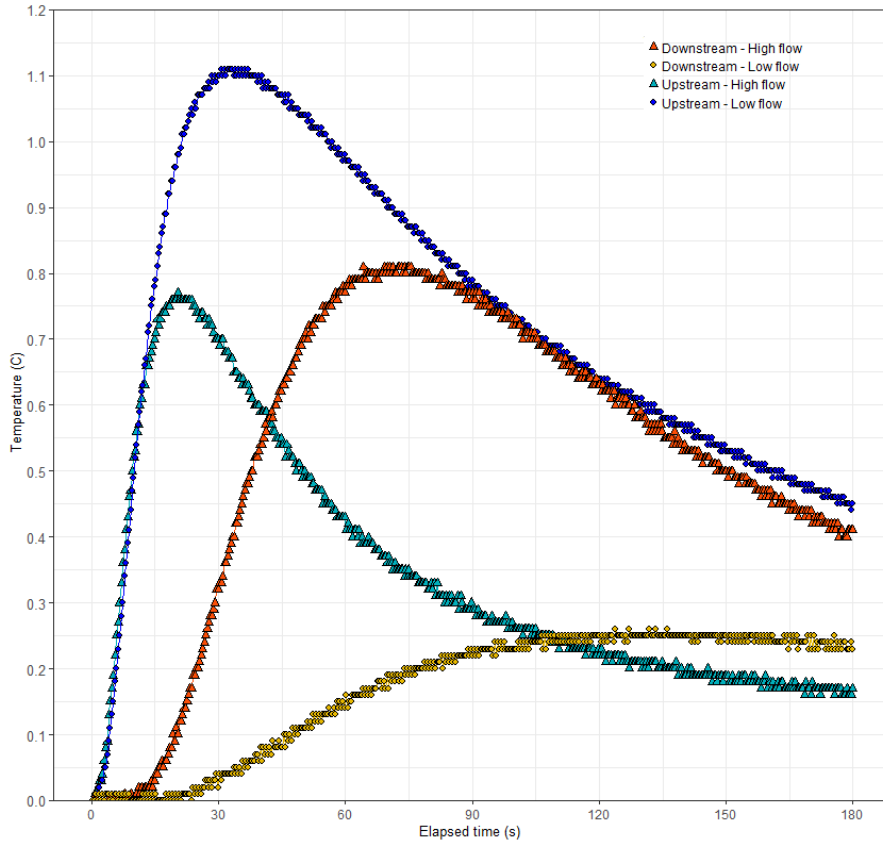
Day and night transpiration measures were taken into account for the calibration estimation in this experiment. Studies have excluded low flows for calibration given the noisy results (Green et al., 2003; Miner et al., 2017). Miner et al. (2017) took into account measurements over 25 g/h, attributing the noisy results to the method used to calculate sap velocity. They stated that the method relies on the thermal diffusivity (k), which is found when sap flow is zero, but this condition is hard to obtain in some species that have large nocturnal sap flows. When there is low flow the

relationship between sap flow and velocity estimated with the Tmax method is not unique, therefore it is not possible to find a unique value for low flows. Miner et al. (2017) stated that thermal diffusivity calculations for Tmax methods should be different. The calculated thermal diffusivity for the Tmax method is not a real thermal property, as it has errors introduced by the model and measurement errors. Therefore, for the heat pulse method they used a k developed by Cohen et al. (1993a) and not the k used in the Tmax method estimated with predawn data.

Limitations in the measurements of low heat velocities were also found by Cohen et al. (1993a) in maize because temperature changes could not be detected. This can be improved by reducing the distance between the heater and the temperature sensor to reduce the time to get a difference in temperature in the stem after the heating event (Cohen et al., 1993a). In a similar way, the gauge design used in this study reduced the distance of the upstream thermocouple to 5 mm to account for this improvement. The accuracy of the heat pulse method is affected by the sap flow rate and not by the plant size or age (Cohen et al., 1993a).

Heat is applied for 3 seconds to the stem and temperature is measured during 160 seconds after the pulse (Figure 5). The thermistor precision and resolution (0.002 °C) allows the detection of temperature lifts between 0.26 °C and little over 1.1 C. The pattern of the two probes were affected by flow rate. The downstream probe shows a high temperature peak with high flows and small and flat peak with low flows. The upstream probe has a smaller peak with respect to the downstream probe with high flows and a pronounced lift at low flows. Figure 5 demonstrates the very small resolution of the thermistors proving that SFGs stem temperature measurements were accurate and reliable. Nevertheless, the flat peak of the downstream probe at low flows can be improved by increasing the heating time a little more. Caution should be taken after the construction of the heater to confirm that with the heating time used the stem temperature lifts are

as small as possible to avoid greater wounding to the plant, but high enough to detect a consistent temperature peak.



| | |
|--|--|
| Temp. lift Downstream = 0.82 C 0.86 C Temp. lift Upstream = 0.77 C 0.52 C Flow = 127.4g/h | Temp. lift Downstream = 0.26 C 0.29 C Temp. lift Upstream = 1.11 C 0.85 C Flow = 9.2g/h |
|--|--|

Figure 5. Temperature lifts of two Sap flow gauges after 3 second-heat pulse – examples for high and low sap flows.

Greenhouse validation

Validation of the calibration factor and the heat pulse theory was performed in a greenhouse experiment, comparing time series of plant transpiration from gravimetric measures and from SFGs (Figure 6 and Figure 7). Results proved a good performance of the gauges in a daily basis.

Daily data results showed an RMSE of 726.9 g/d and a MAE of 576 g/d, representing 15.4% and 12.2% of mean value of transpiration, respectively. Mean daily gravimetric plant transpiration was 4716.4 g.

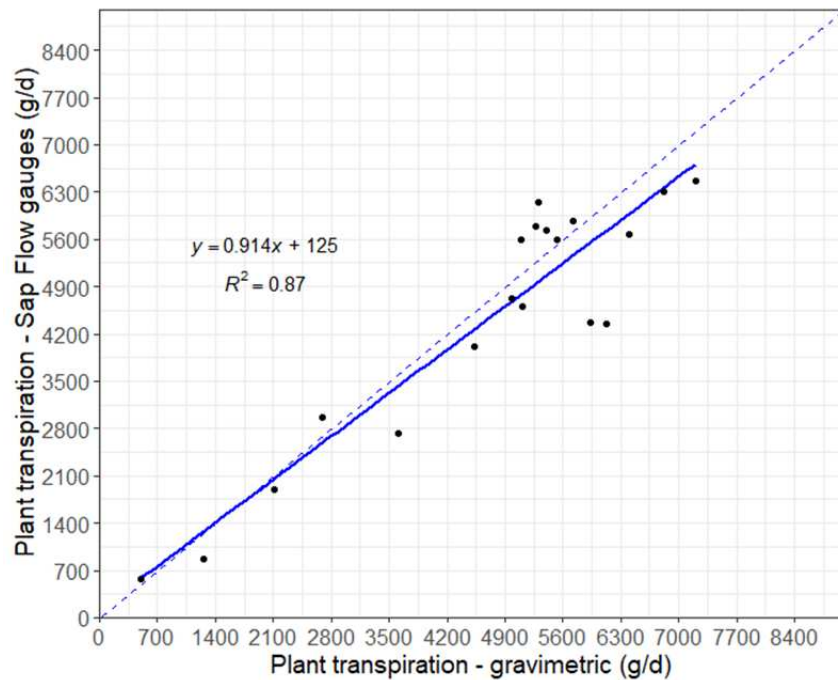


Figure 6. Comparison between daily transpiration estimated from sap flow gauges and maize gravimetric transpiration.

Results from the comparison between transpiration estimation with the sap flow and the gravimetric transpiration for maize showed an R^2 of 0.87, demonstrating a strong linear correlation (Figure 6). A paired t test p-value > 0.05 confirmed no statistical difference between transpiration values from the scale and the SFGs for the validation dataset period. For the 20-day validation period, SFGs underestimated transpiration by 5.9%.

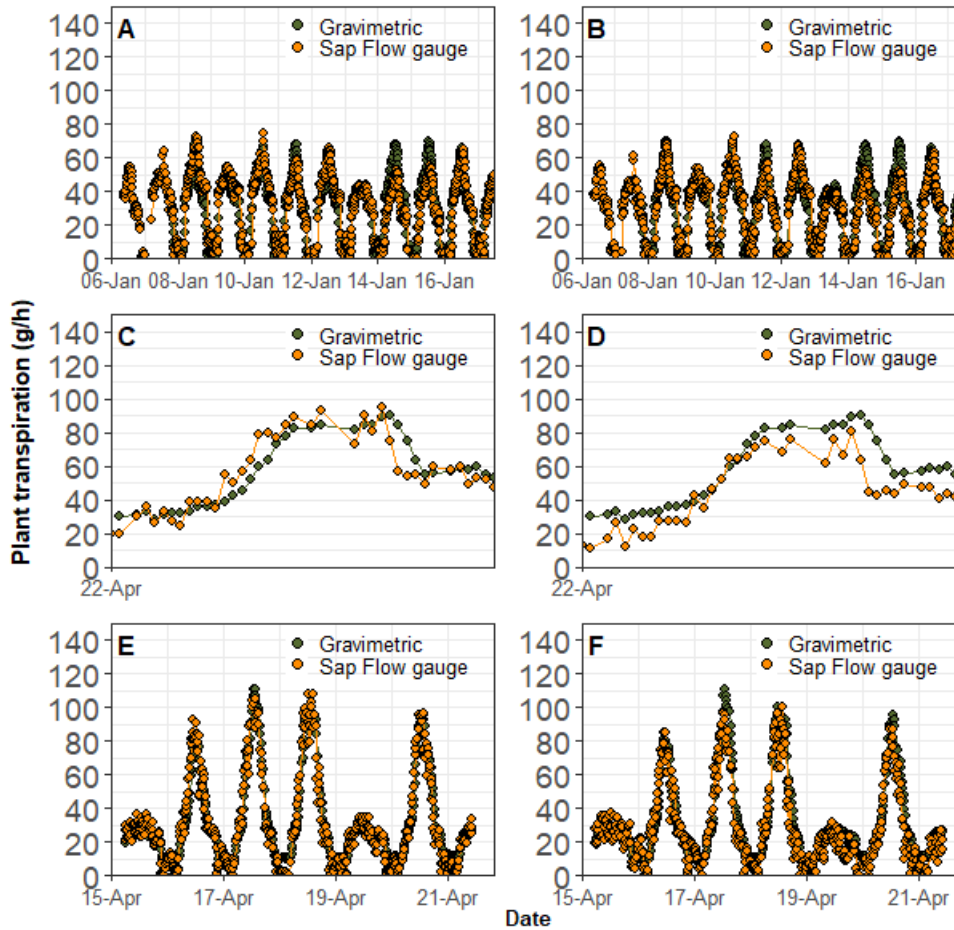


Figure 7. Time series of the validation of the calibration coefficient in greenhouse studies using three plants, with two sensors per plant. Letters A to F correspond to the results of each sensor.

A lag between T and sap flow measurements has been found in previous studies (Bethenod et al., 2000) and explained by the plant capacitance, due to temporal variations in plant water content, mainly found in trees, but also in maize and tomato. In this study, similarly to Jara et al. (1998), this lag was not found (Figure 7).

Field experiment and sap flow gauges performance

Installation of multiple SFGs in the field allow the results to be scaled up in order to calculate canopy transpiration (Ham et al., 1990; Bethenod et al., 2000). Data collected allowed calculation

of crop water use every 15 minutes. Hourly maize water use estimated with the gauges was compared to the reference transpiration (Figure 8 and Figure 9). The gauges in this study were installed in R3-R5 phenology stages, when the maize canopy completely covered the soil, with a leaf area index (LAI) above 3.

An analysis of soil moisture data from the field showed that the maize field maintained a well-watered condition during the period of the sap flow measurements (Figure A2 in Appendix A). Results confirmed that no water stress was induced in the crop, therefore, it was adequate to use the Penman-Monteith approach with no stress coefficient. In addition, a local validated Kcb value for maize was used to estimate maize transpiration. Given that the conditions for the Penman-Monteith method were met (large area, with no water stress and good crop health) the agreement between both transpiration estimation methods would corroborate the performance of the gauges in field conditions.

Sap flow gauges were inserted in plants during around 7-day periods. Some authors have stated that using SFGs for a maximum of one week reduces the negative impact of the plant stem functioning (Aiken and Klocke, 2012). Cohen et al. (1981) stated that there is also an effect of the disturbance introduced by the probes per se, inserted in the stem, that tend to underestimate sap flow. Different time ranges for inserted probes could be tested in future studies to determine the maximum number of days a gauge can be installed without affecting transpiration estimation.

Hourly data from the SFGs compared well with the reference transpiration. An example shown in Figure 8 demonstrates how the gauges tracked transpiration during a 4-day period.

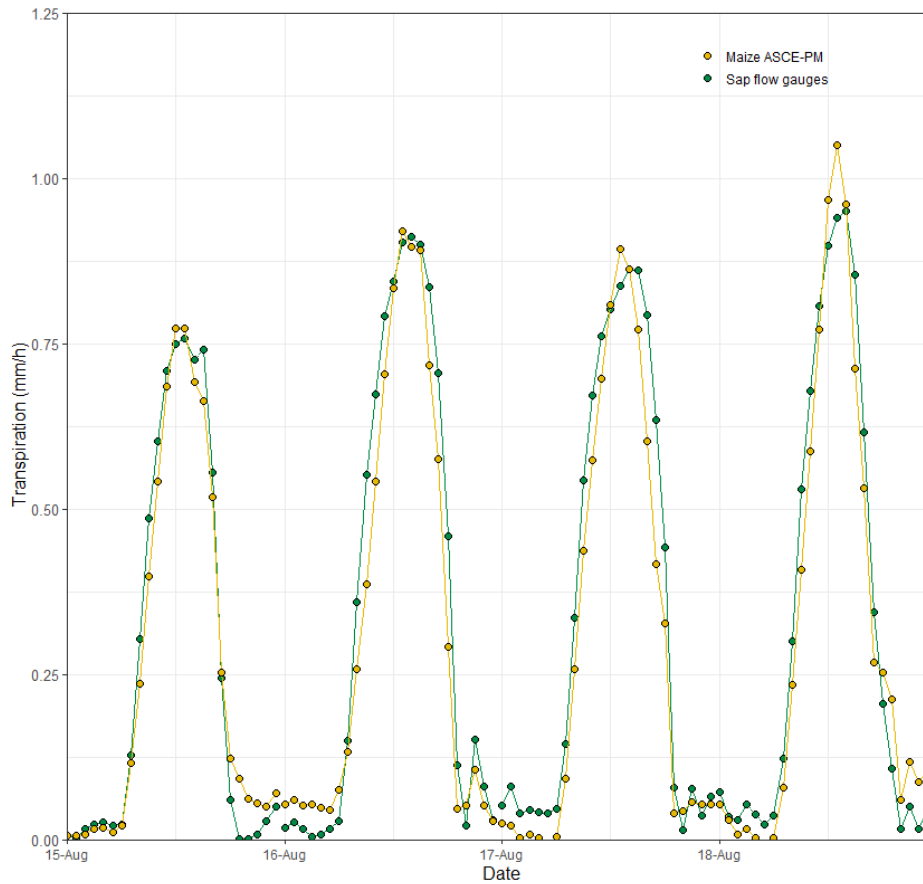


Figure 8. Mean transpiration rate calculated with eight sap flow gauges (one sensor per plant) and estimated with tall reference ASCE-PM equation and a local Kcb for maize in a well irrigated field during a four-day period.

Results from the comparison between transpiration estimation with the sap flow and the reference transpiration for maize show an R^2 of 0.95 on an hourly scale, demonstrating that the maize water use estimated with this methodology and gauge design was consistent with established transpiration theory (Figure 9).

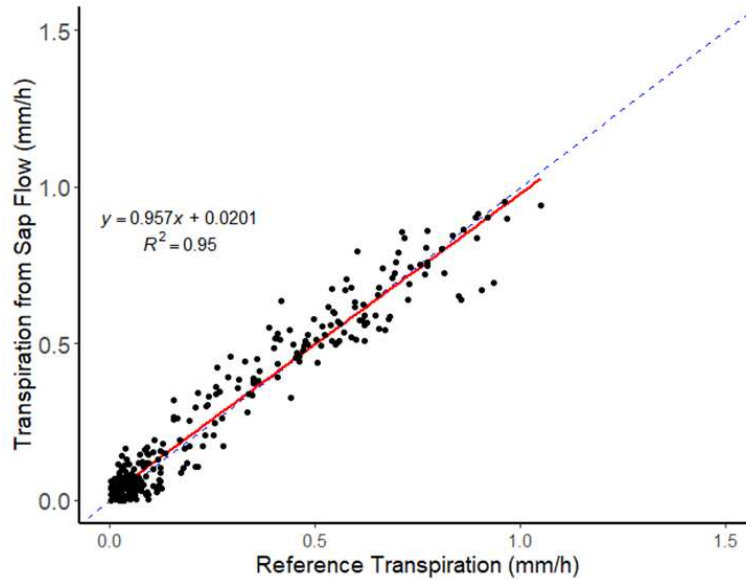


Figure 9. Comparison between hourly transpiration estimated with 8 sap flow gauges and the maize reference transpiration.

The two transpiration estimation methods were also compared on a daily basis. A paired t test was performed to test whether the mean difference between methods is different from zero, showing no difference. Results showed a good overall agreement between the two ($p=0.15$, $R^2=0.8$). Statistical parameters for the evaluation of the methods also reflected an agreement of the methods in the field (Figure 10).

The sum for the 12 days for both methods was 72.3 mm for the reference transpiration and 75.4 mm for the SFGs, with a mean SD of 1.04 mm (Table 2). The SD did not show a strong relation with transpiration amount during the period evaluated. Transpiration was 4.4% higher when measured by the SFGs. The mean absolute error and RMSE was 0.48 mm (8% from mean transpiration value) and 0.62 mm (10% of mean transpiration value) respectively. The SFGs had acceptable performance for daily estimation of maize transpiration. The mean margin of error was 0.87 mm, hence, for a mean transpiration of 6.3 mm in the 12 days, there was a 95% confidence of finding the mean transpiration between 5.4 and 7.15 mm.

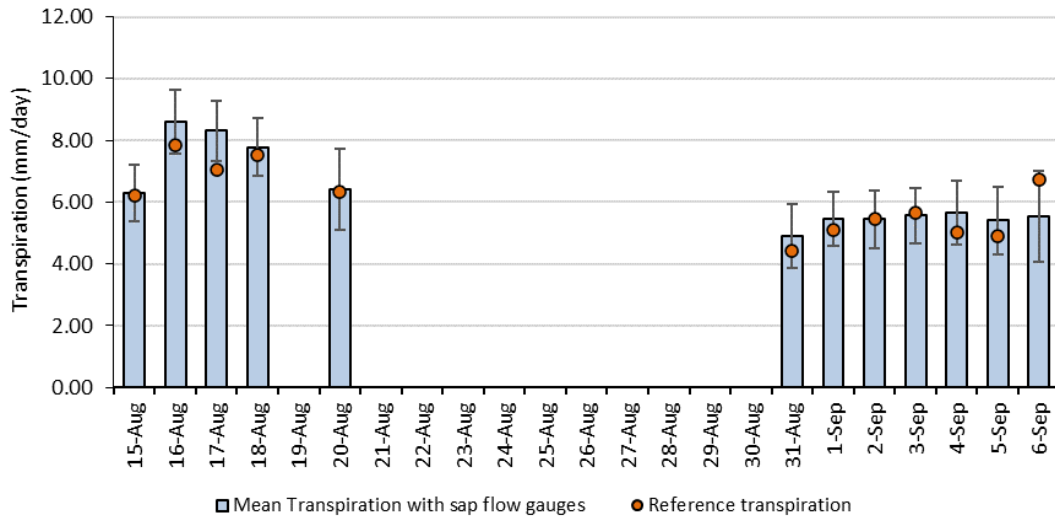


Figure 10. Daily maize water use estimated with 8 SFGs (one sensor per plant) in the field \pm Standard Deviation vs reference transpiration estimated with the ASCE standardized tall reference equation and a local Kcb curve.

Sap flow measurements provide valuable information from the field crop because transpiration constitutes most of the crop ET when measured in a full canopy condition. In sparse crops transpiration can account for 65% of evapotranspiration (ET), and in full canopy condition transpiration accounts for 88% to 92% of the ET (Sauer et al., 2007). This agrees with findings by Jara et al. (1998) who showed a contribution of the soil evaporation of 13.6% in a fully covered maize canopy in wet soils using surface irrigation and at night soil evaporation represented a 5.5% of daytime ET. However, it has been stated that a general drawback for the practical application of the sap flow method is scaling up the measurements (Bethenod et al., 2000). The use of plant population instead of leaf area index can lead to overestimations of plant water use due to the plant-to-plant variability at a field scale (Ham et al., 1990). Nevertheless, similar findings from Bethenod et al. (2000) showed that sap flow measurements for estimation of crop water use is a reliable method in mature crops for transpiration estimation, agreeing with results from this study.

Many effects on sap flow transpiration are corrected by introducing a calibration factor and it can also be corrected using numerical solutions (Swanson and Whitfield, 1981, Green et al., 2003). However, possible sources of error in this study could include the following factors: the resolution of the heat wave peak, the distance between the heater and the temperature sensor deeper in the stem, and imperfections in the construction of the gauge or deformations when inserted into the stem. These factors modify the measurements and also affect the consistency of repetitions (Cohen et al., 1981).

Uncertainty of the transpiration estimation can be assessed with several statistical indicators. SE and ME for a 95% probability were chosen for this study. For the statistical assessment daily data for 8 gauges were taken into account. The daily mean transpiration for the period was 6.28 mm with an accuracy estimated with SE of 0.37 mm, within $\pm 6\%$ of T (Table2).

Table 2. Maize transpiration measured with sap flow gauges, standard deviation (SD), standard error (SE) of the measurement and reference transpiration calculated with the ASCE tall reference standardized equation and local Kcb curve developed by Trout and DeJonge (2018).

| Datetime | Corn reference transpiration | Average transpiration of 8 SF gauges | SD | SE |
|---------------|------------------------------|--------------------------------------|------|------|
| 08/15/2020 | 6.20 | 6.28 | 0.91 | 0.32 |
| 08/16/2020 | 7.83 | 8.61 | 1.03 | 0.36 |
| 08/17/2020 | 7.06 | 8.32 | 0.98 | 0.35 |
| 08/18/2020 | 7.52 | 7.78 | 0.93 | 0.33 |
| 08/20/2020 | 6.32 | 6.42 | 1.33 | 0.47 |
| 08/31/2020 | 4.44 | 4.90 | 1.04 | 0.37 |
| 09/01/2020 | 5.10 | 5.46 | 0.88 | 0.31 |
| 09/02/2020 | 5.45 | 5.46 | 0.93 | 0.33 |
| 09/03/2020 | 5.66 | 5.56 | 0.91 | 0.32 |
| 09/04/2020 | 5.03 | 5.66 | 1.02 | 0.36 |
| 09/05/2020 | 4.92 | 5.41 | 1.10 | 0.39 |
| 09/06/2020 | 6.73 | 5.55 | 1.47 | 0.52 |
| Mean | 6.02 | 6.28 | 1.04 | 0.37 |
| Median | 5.93 | 5.61 | 1.00 | 0.35 |

The mean margin of error of our measurements (using 8 gauges) was 0.87 mm for the period using a 95% confidence interval. This means we have 95% confidence that mean transpiration is between 5.4mm and 7.15mm.

Sap flow transpiration accuracy vs number of gauges

One important question that arises when using SFGs is what is the minimum number of gauges that could be installed in the field to have a good estimation of the maize water use. In practice, it is useful to understand that the number of sensors deployed changes the uncertainty of the measurement. The first question to ask is how much uncertainty of the transpiration measurement we are willing to allow for our specific purpose. The minimum number of gauges must be decided by the user depending on the accuracy needed. Significant effects for treatments could be found depending on the accuracy of the gauges, the experimental design, or a combination of both (Senock, 1996). The cost to run the experiment, the time needed to handle the instrumentation and the availability of sensors are a constrain for the researcher.

For practical purposes it is important to determine the minimum number of sensors (i.e., sample replications) required to find differences between two treatment means with a determined level of confidence. The accuracy of the instrumentation will be used to estimate an adequate sample size. Therefore, we aimed to provide useful information for practical implementation of the SFGs. Three different analyses were made for the assessment of number of gauges vs transpiration accuracy, described in the methodology section.

Results from the analysis showed that the transpiration margin of error for a 95% confidence ranged from 0.87 mm when 8 gauges were deployed and increased drastically to 7.7mm when only 2 gauges were used (Figure 11). Results showed that using two gauges would not be useful for any purpose as the results would be very uncertain; 95% confidence interval for transpiration was ± 7 mm.

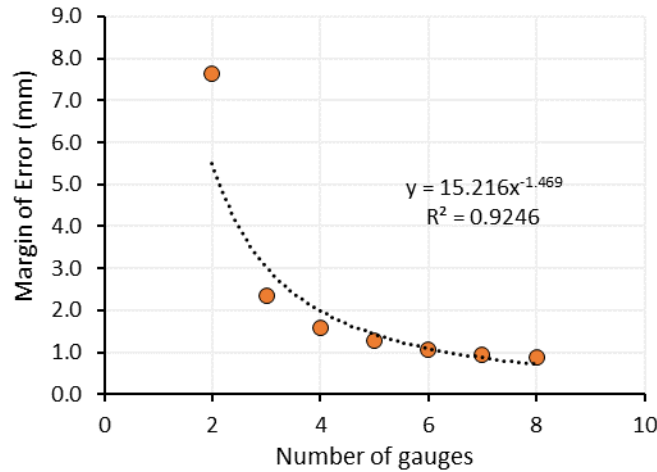


Figure 11. Margin of error of the transpiration measure for a 95% confidence vs number of gauges.

The standard error was also calculated. An exponential increase was found for 2 to 8 gauges, ranging from 0.6 mm to 0.37 mm, respectively.

The probability of detecting an effect, if there is a true effect present, can be analyzed with the statistical power of the test of significance, for a hypothesized a scenario. For the hypothetical scenario where a transpiration difference of 1 mm between two treatments exists and we need our gauges to be sensitive enough to detect it: we can be 65% confident that we would find differences if 8 sensors are deployed in the field. We would need 12 gauges to be 80% confident of finding a difference between treatments and with 16 gauges we can be 95% certain of finding a significant difference between treatments. In the case we need to detect an effect between treatments of 0.5 mm, we would need to install 36 gauges to be 80% confident of our transpiration measurements.

The accuracy of the transpiration estimation using our sap flow sensors is a combined effect of: heat velocity equation (the model accuracy), the calibration factor, differences in the hardware

because is manually manufactured and plant related variations. The latter involves mainly the xylem vessels configuration and the insertion of the probes.

The results reflect the reliability of the model and calibration coefficient for maize in the reproductive phase and for the gauges at different environmental conditions. The precision and accuracy of the sensors showed a great potential use of these gauges for various purposes.

Results from season 2019

A similar study was performed in 2019 in a different location, at northern Colorado. The same SFG design and theory for heat velocity calculation were used. However, a heat pulse of 6-seconds was used. The same approach for calibration and validation in a greenhouse experiment was performed (Results are shown in Figures A3 and A4 in Appendix A). Results from these studies showed that the calibration coefficient was higher than 1.28, being 1.70. Data confirmed that the heat effect on the measurement caused the calibration coefficient to be higher, because the calibration coefficient takes into account wounding effects. Given that not much heat is needed for the method to find the maximum heat peak after the heat pulse, the length of the heating time was reduced to 3 seconds in season 2020 in order to avoid or reduce any wounding on the plant.

Results from the greenhouse validation experiment for daily transpiration from the SFGs and from gravimetric measurements showed a strong coefficient of determination ($R^2= 0.96$), an RMSE of 588.4 g (10% from the mean value) and MAE of 550 g (9.4 % from the mean value). Sap flow gauges showed an underestimation of 9.4%.

The SFGs were also deployed in a well irrigated maize field (Figure A5) and compared to mean transpiration values from commercially available SFGs (Daynagage sap flow stem gauges

SGB25, Dynamax Inc., Houston, USA) and from the reference transpiration estimated as the tall reference ASCE PM approach and the K_{cb} from Trout and DeJonge (2018). Analysis was performed for daily transpiration estimation using 8 or more SFGs (one gauge per plant), up to 12. Seventeen days were used for the comparison. The standard deviation from the measures from each day was estimated, showing a mean value of 1.14 mm for the 17-day period. These methods for daily transpiration estimation were highly correlated.

Sap flow gauges were compared to the commercial version of SFGs for daily transpiration estimation. They were highly correlated ($R^2 = 0.89$). The RMSE and MAE was 0.66 mm (12.4% from the mean value) and 0.54 mm (10.2% from the mean value). Sap flow gauges overestimated transpiration by 8%.

When SFGs were compared to the reference transpiration for daily transpiration estimation, they were highly correlated ($R^2 = 0.74$). The RMSE and MAE was 0.70 mm (13.2% from the mean value) and 0.56 (11% from the mean value). Sap flow gauge transpiration was 2% higher than reference transpiration.

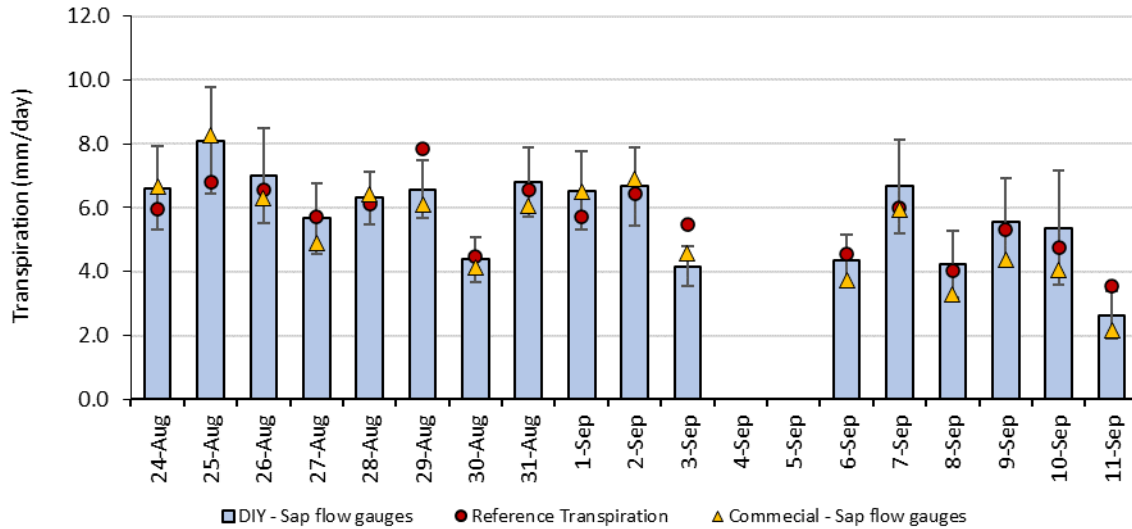


Figure 12. Daily maize water use estimated with 8-12 sap flow gauges (one sensor per plant) in the field \pm Standard Deviation, compared to water use measured with commercially available sap flow gauges and reference transpiration estimated with the ASCE standardized tall reference equation and a local Kcb curve.

The total transpiration from the SFGs was 97.7 mm, 90.4 mm from the commercial SFGs, and 95.8 mm from the reference transpiration.

Results showed a good overall performance of the sap flow gauges for daily transpiration estimation in a maize field. Results from this season regarding the heat length of the pulse was used to improve the method in season 2020.

Sap Flow gauges pros and cons for practical uses

Sap flow gauges can be used for diverse purposes. The error of the estimate according to the number of gauges deployed will define its use because of their ability of detecting changes in plant transpiration. Sap flow gauges can be used for treatment studies. Results of the analysis of the SE and ME for the gauges suggests that our SFGs may not be the best choice to find small

differences between irrigation treatments if a small number of sensors are to be used. Such studies may involve measurement of water used by different crop varieties, irrigation treatments or other treatments that modify sap flow in the plant (i.e., CO₂ exposure, insect/pathogen/fertilizer treatments) or differences in location within a crop field.

Sap flow sensors can be very useful in irrigation management. Its use can be divided in 3 main uses. 1) Transpiration measurements can be used directly as irrigation water requirements. Most of the irrigation systems have application efficiencies around 80% for sprinkler irrigation systems or lower in case of surface irrigation systems and have a resolution larger than 1 mm/day. These SFGs would measure water used by a crop and indicate irrigation amounts for irrigation management. Its continuous measurements combined with IoT make it easily integrated in an automated irrigation system. They can be a useful tool for detecting irrigation amounts in regions with different local weather conditions. 2) They can be used to validate transpiration models. Transpiration can also be used to derive actual canopy conductance values that can be used in simulation models or used to indicate water stress. 3). Sap flow gauges can also be used to develop or verify local K_{cb} curves. The strong agreement between SFG transpiration and reference transpiration demonstrated this. This is a valuable use of the SFGs because it is one of the only methods that can estimate the K_{cb} directly. It can be implemented in any location as a cost-effective tool with accurate results. The use of the K_{cb} to calculate local irrigation needs has been proven to be superior to the single crop coefficients.

Another important aspect of our system is the ability to show the plant transpiration in real time from any device and store data in the cloud. This gives the system a significant value. Similar features can increase the cost substantially in the commercial versions of sap flow devices. When the cost of the gauge plus the cost of the logger, internet service and IoT cloud storage are considered, these lower-cost DIY-IoT-SFGs may have a cost advantage compared to their

commercial counterparts. In addition, any damage of a gauge or other components of the system are easy to repair or replace at low cost.

Conclusion

A new Heat Ratio method for a heat pulse technique was developed in this study. This method was coupled with a new gauge design created with 3D printed parts and low-cost sensors. The combination of the sensor design, model for heat velocity and calibration factor gave an acceptable performance. Implementation of the gauges showed them to be a reliable approach to measure maize transpiration at the individual plant or field scale.

The SFGs were calibrated in the greenhouse and showed a calibration coefficient of 1.28 ± 0.2 , used to convert heat velocity to transpiration flow. This coefficient also accounts for other sources of errors such as the wound effect of the needles. It allowed daily plant transpiration estimation with an RMSE of 15.4% and a MAE of 12.1% of mean transpiration value in greenhouse validation studies and showed a strong coefficient of determination ($R^2 = 0.87$). Sap flow gauges underestimated transpiration by 5.8%. At field conditions the SFGs were compared to the reference transpiration estimated with the P-M approach. It showed a precision of ± 1.04 mm, a MAE of 0.48 mm and a RMSE of 0.62 mm, both were within 10% of mean transpiration. The total transpiration from the reference transpiration was 72 mm and measured from SFGs was 75 mm, estimating a 4.4% higher water use. The method requires the estimate of a calibration coefficient for its use, however, data from this study agrees with Miner et al. (2017), suggesting that the calibration coefficient could be stable for maize varieties. The accuracy of the transpiration measurements varied with the number of sensors deployed in the field. The accuracy measured with ME for a 95% certainty, varied from near 8 mm using 2 gauges to 0.87 mm/d using 8 sensors.

More than 4 sensors should be deployed in the field to obtain estimations of maize transpiration with less than 20% error. The analysis with 3 approaches to assess an adequate number of gauges to be deployed for an accurate measure of maize transpiration showed that 12 gauges would be an optimum number of gauges to have over 80% confidence of detecting a difference of 1 mm between treatments and a SE around 0.3 mm.

Sap flow gauge studies were also performed during 2019. The calibration coefficient accounted for wounding effects due to heat given by a six-second heat pulse and gave a strong coefficient of determination ($R^2 = 0.96$). For these greenhouse studies the RMSE was 10% from the mean transpiration value and MAE was 9.4 % from the mean value. Sap flow gauges showed an underestimation of 9.4%. When gauges were compared in the field to commercially available SFGs, they showed a strong coefficient of determination $R^2 = 0.89$. The RMSE and MAE was 0.66 mm (12.4% from the mean value) and 0.54 (10.2% from the mean value). Sap flow gauges overestimated transpiration by 8%. When compared to the reference transpiration for daily transpiration estimation, they were highly correlated ($R^2 = 0.74$). The RMSE and MAE were 0.70 mm (13.2% from the mean value) and 0.56 (11% from the mean value), respectively. Sap flow gauge transpiration was 2% higher than reference transpiration. The total transpiration from the SFGs was 97.7 mm, 90.4 mm from the commercial SFGs and 95.8 mm from the reference transpiration.

We were able to successfully develop and test the performance of a novel sap flow system. The system is a low-cost option for researchers and technicians to take advantage of real time monitoring for water use, irrigation monitoring or calculation of crop water needs for multiple purposes. Implementation of the gauges can support water use monitoring. The strong agreement between SFG transpiration and reference transpiration demonstrated that this approach can be used to derive local Kcb curves.

Future research

Based on the results of this research, there are several interesting studies that could be carried out in pursuing an improved sap flow system.

- Test the performance of the sap flow system during a complete maize growing season and test its viability for other monocot and dicot plant species.
- Determine the maximum number of days that the gauges are in each plant without affecting transpiration estimation. Allowing for a maximization of resources given that less working hours per week would be needed.
- Different equations to estimate sap flow velocities, one for low to medium flow rates and other for high rates could be tested and analyzed if there is an improvement in precision of the sensor.
- Test for 4 seconds heating time for the heat pulse and analyze the heat waves downstream and upstream and velocity calculations for high and low flows.
- Design and build a custom board for the electronic components of the logger. This will allow for a faster fabrication and reduce possible connection errors when building sap flow systems in a large number.
- Improve the use of the IoT for estimates of plant transpiration in real time. This could be achieved by developing code for user-modifiable variables in real time.

References

- Aiken, R.; Klocke, N. 2012. Inferring transpiration control from sap flow heat gauges and the Penman-Monteith equation. *Transactions of the ASABE (American Society of Agricultural and Biological Engineers)*. V. 55. 543:549.
- Allen, R.; Pereira, L.; Raes, D.; Smith, M. *Crop Evapotranspiration (guidelines for computing crop water requirements)*. 1998. FAO Irrigation and Drainage paper, No.56. FAO, Rome, 300pp.
- Andales, A.A., Bauder, T.A., and Arabi, M. 2014. A Mobile Irrigation Water Management System Using a Collaborative GIS and Weather Station Networks. *Advances in Agricultural Systems Modeling 5*: 53-84. doi:10.2134/advagricsystmodel5.c3
- ASCE. Walter, I.; Allen, R.; Elliot, R.; Itenfisu, D.; Brown, P.; Jensen, M.; Mecham, B.; Howell, T.; Snyder, R.; Eching, S.; Spofford, T.; Hattendorf, M.; Martin, D.; Cuenca, R.; Wright, J. Task Committee on Standarization of Reference Evapotranspiration of the Environmental and Water Resources Institute of the American Society of Civil Engineers. 2005. The ASCE standardized reference evapotranspiration equation. Final Report. 59p.
- ASCE. Committee on Standarization of Reference Evapotranspiration of the Environmental and Water Resources Institute of the American Society of Civil Engineers. 2005. The ASCE standardized reference evapotranspiration equation – Appendices A-F. 115p.
- Ballester, C.; Castel, J.; Testi, L.; Intrigliolo, D. 2013. J. R. CastelCan heat-pulse sap flow measurements be used as continuous water stress indicators of citrus trees?. *Irrigation Science*. V. 31. 1053:1063.
- Bethenod, O.; Katerji, N.; Goujet, R.; Bertolini, J.; Rana, G. 2000. Determination and validation of corn crop transpiration by sap Flow measurement under field conditions. *Theoretical and Applied Climatology*. V. 67. 153:160.
- Brodth, S.; Six, J.; Feenstra, G.; Ingels, C.; Campbell, D. 2011. Sustainable Agriculture. *Nature Education Knowledge*. V.3(10):1.
- Burgess, S.; Adams, M.; Turner, N.; Ong, C. 1998. The redistribution of soil water by tree root systems. *Oecologia*. V. 115. 306-311.
- Burgess, S.; Adams, M.; Turner, N.; Beverly, C.; Ong, C.; Khan, A.; Bleby, T. 2001. An improved heat pulse method to measure low and reverse rates of sap flow in woody plants. *Tree Physiology*. V. 21. 589–598.
- Chabot, R.; Bouarfa, S.; Zimmer, D.; Chaumont, C.; Duprez, C. 2002. Sugarcane transpiration with shallow water-table: sap flow measurements and modelling. *Agricultural Water Management*. V. 54. 17:36.
- Chamara, N.; Didarul Islam, M.; Bai., G.; Shi, Y.; Ge, Y. 2022. Ag-IoT for crop and environment monitoring: past present and future. *Agricultural Systems*. V. 203: 103497. <https://doi.org/10.1016/j.agsy.2022.103497> .

- Clearwater, M.; Luo, Z.; Mazzeo, M.; Dichio, B. 2009. An external heat pulse method for measurement of sap flow through fruit pedicels, leaf petioles and other small-diameter stems. *Plant, Cell and Environment*. V. 32. 1652–1663.
- Cohen, Y.; Fuchs, M.; Green, G. 1981. Improvement of the heat pulse method for determining sap flow in trees. *Plant, Cell and Environment*. V. 4: 391-397.
- Cohen, Y.; Fuchs, M.; Falkenflug, V.; Moreshet, S. 1988. Calibrated Heat Pulse Method for Determining Water Uptake in Cotton. *Agronomy Journal*. V. 80:398-402.
- Cohen, Y.; Huck, M.; Hesketh J.; Frederick, J. 1990. Sap flow in the stem of water stressed soybean and maize plants. *Irrigation Science*. V 11:45-50.
- Cohen, Y.; Takeuchi, S.; Nozaka, J.; Yano, T. 1993a. Accuracy of Sap Flow Measurement Using Heat Balance and Heat Pulse Methods. *Agronomy Journal*. V. 85: 1080-1086.
- Cohen, Y.; Plaut, Z.; Meiri, A.; Hadas, A. 1995. Deficit Irrigation of Cotton for Increasing Groundwater Use in Clay Soils. *Agronomy Journal*. V. 87: 808-814.
- Cohen, Y.; Li, Y. 1996. Validating sap flow measurement in field-grown sunflower and corn. *Journal of Experimental Botany*. V. 47, No. 3014: 1699-1707.
- Dugas, W.; Heuer, M.; Hunsaker, D.; Kimball, B.; Lewin, K.; Nagy, J.; Johnson, M. 1991. Sap flow measurements of transpiration from cotton grown under ambient and enriched CO₂ concentrations. *Agricultural and Forest Meteorology*. V.70: 231-245.
- Eddy, R.; Hahn, D. 2010. Optimizing Greenhouse Corn Production: What Is the Best Lighting and Plant Density? . *Purdue Methods for Corn Growth*. Paper 13. <http://docs.lib.purdue.edu/pmccg/13>.
- Food and Agriculture Organization of the United Nations (FAO). 2017. *Water for Sustainable Food and Agriculture*. Rome, 2017. 27pp. Available at: <http://www.fao.org/3/a-i7959e.pdf>
- Food and Agriculture Organization of the United Nations (FAO). 2008. *Coping with water scarcity. An action framework for agriculture and food security*. Food and Agriculture Organization of the United Nations. Rome. *FAO Water Reports*. No. 38. 78pp.
- Gerdes, G.; Allison, B.; Pereira, L. 1994. Overestimation of soybean crop transpiration by sap flow measurements under field conditions in Central Portugal. *Irrigation Science*. V. 14. 135:139.
- Giovannucci, D; Scherr, S.; Nierenberg, D.; Hebebrand, C.; Shapiro, J.; Milder, J.; Wheeler, K. 2012. *Food and Agriculture: the future of sustainability. Summary of Key points*. United Nations Department of Economic and Social Affairs. Division for Sustainable Development. 11pp.
- Green, S.; Clothier, B.; Jardine, B. 2003. Theory and Practical Application of Heat Pulse to Measure Sap Flow. *Agronomy Journal*. V. 95: 1371-1379.

- Ham, J.; Heilman, J.; Lascano, R. 1990. Determination of soil water evaporation and transpiration from energy balance and stem flow measurements. *Agricultural and Forest Meteorology*. V. 52: 287-301.
- Ham, J.; Heilman, J. 1990. Dynamics of a Heat Balance Stem Flow Gauge during High Flow. *Agronomy Journal*. V. 82: 147-152.
- Ham, J.; Benson, E. 2004. On the construction and calibration of dual-probe heat capacity sensors. *Soil Science Society of America Journal*. V. 68: 1185–1190.
- Ham, J.; Aksland, I.; Casey, D.; Koski, T.; Qian, Y.; McClelland. 2021. Wireless soil moisture measurement in turfgrass with internet of things (IoT) technology and low cost sensors. 6th Decennial National Irrigation Symposium, 6-8, December 2021, San Diego, California 2020-132. doi:10.13031/irrig.2020-132.
- Han, M.; Zhang, H.; DeJonge, K.; Comas, L.; Gleason, S. 2018. Comparison of three crop water stress index models with sap flow measurements in maize. *Agricultural Water Management*. V. 203. 366:375.
- Ishida, T.; Campbell, G.; Cahssendorff, C. 1991. Improved heat balance method for determining sap flow rate. *Agricultural and Forest Meteorology*. V. 56: 35-48.
- Jara, J.; Stockle, C.; Kjelgaard, J. 1998. Measurement of evapotranspiration and its components in a corn (*Zea Mays L.*) field. *Agricultural and Forest Meteorology*. V. 92. 131:145.
- Jones, H. 2004. Irrigation scheduling: advantages and pitfalls of plant-based methods. *Journal of Experimental Botany, Water-Saving Agriculture Special Issue*. V. 55(407). 2427–2436. doi:10.1093/jxb/erh213.
- Jones, H.; Hutchinson, P.; May, T.; Jamali, H.; Deery, D. 2018. A practical method using a network of fixed infrared sensors for estimating crop canopy conductance and evaporation rate. *Biosystems Engineering*. V. 165: 59–69. <https://doi.org/10.1016/j.biosystemseng.2017.09.012> .
- Kluitenberg, G.; Ham, J. 2004. Improved theory for calculating sap flow with the heat pulse method. *Agricultural and Forest Meteorology*. V. 126: 169–173.
- Kluitenberg, G. 2017. TmRatio Method with Upstream and Downstream Probes. White paper. Department of Agronomy. Manhattan, Kansas, USA. 1-19.
- Marshall, D. 1958. Measurements of Sap Flow in Conifers by Heat Transport. *Plant Physiology*. V.33 (6): 385-396.
- Miner, G.; Ham, J.; Kluitenberg, G. 2017. A heat-pulse method for measuring sap flow in corn and sunflower using 3Dprinted sensor bodies and low-cost electronics. *Agricultural and Forest Meteorology*. V. 246: 86-97.
- Nicholson, K. 1999. European corn borer, *Ostrinia nubilalis* (Hubner), and mechanical disruption of sap flow through corn stalks. Kansas State University. 114p.

Owensby, C.; Ham, J.; Knapp, A.; Bremer, D.; Auen, L. 1997. Water vapour fluxes and their impact under elevated CO₂ in a C₄-tallgrass prairie. *Global Change Biology*. V.3(3). 189:195.

Payero, J.; Mirzakhani-Nafchi, A.; Khalilian, A.; Qiao, X.; Davis, R. Development of a low-cost Internet of Things (IoT) system for monitoring soil water potential using Watermark 200SS sensors. *Advances in Internet of things*. V. 7: 71-86. <https://doi.org/10.4236/ait.2017.73005> .

Pearce, J. 2017. Impacts of open source hardware in science and engineering. In.: *The Bridge*. National Academy of Engineering. Vol. 47 (3), pp. 24-29. Founded in: <https://www.nae.edu/File.aspx?id=174936>).

Pearce, J. 2013. Commentary: Open-source hardware for research and education. *Physics Today*. Vol. 66, Issue 11 (8). <https://doi.org/10.1063/PT.3.2160>

Rana, G.; De Lorenzi, F.; Mazza, G.; Martinelli, N.; Muschitiello, C.; Ferrara, R. 2020. Tree transpiration in a multi-species Mediterranean garden. *Agricultural and Forest Meteorology*. Vol. 280- 107767. <https://doi.org/10.1016/j.agrformet.2019.107767>

Sakuratani, T. 1979. Apparent Thermal Conductivity of Rice Stems in Relation to Transpiration Stream. *Journal of Agricultural Meteorology*. V. 34 (4): 177-187.

Sakuratani, T. 1981. A Heat Balance Method for Measuring Water Flux in the Stem of Intact Plants. *Journal of Agricultural Meteorology*. V. 37(1): 9-17.

Sakuratani, T. 1984. Improvement of the Probe for Measuring Vitrater Flow Rate in Intact Plants with the Stem Heat Balance. *Journal of Agricultural Meteorology*. V 40(3): 273-277.

Sauer, T.; Jeremy, Singer, J.; Prueger, J.; DeSutter, T.; Hatfield, J. 2007. Radiation balance and evaporation partitioning in a narrow-row soybean canopy. *Agricultural and forest Meteorology*. V. 145. 206:214.

Senock, R.S.; Ham, J.M., 1993. Heat-balance sap flow gauge for small-diameter stems. *Plant, Cell and Environment*. V. 16 (5). 593:601.

Spinelli, G.; Gottesman, Z.; Deenik, J. 2019. A low-cost Arduino-based datalogger with cellular modem and FTP communication for irrigation water use monitoring to enable access to CropManage. *HardwareX*. V. 6: e00066. <https://doi.org/10.1016/j.ohx.2019.e00066> .

Swanson, R.; Whitfield, W. 1981. A Numerical Analysis of Heat Pulse Velocity Theory and Practice. *Journal of Experimental Botany*. V. 32 (126): 221-239.

Trout, T.; DeJonge, K. 2018. Crop water use and crop coefficients of maize in the Great Plains. *Journal of Irrigation and Drainage Engineering*. V 144(6): 04018009; DOI: 10.1061/(ASCE)IR.1943-4774.0001309.

Wang, S.; Fana, J.; Gec, J.; Wan, Q.; Yongc, C.; You, W. 2018. New design of external heat-ratio method for measuring low and reverse rates of sap flow in thin stems. *Forest Ecology and Management*. V. 419–420. 10-16.

Zhao, P.; Li, S.; Li, F.; Du, T.; Tong, L.; Kang, S. 2015. Comparison of dual crop coefficient method and Shuttleworth–Wallace model in evapotranspiration partitioning in a vineyard of northwest China. *Agricultural Water Management*. V.160. 41:56.

CHAPTER 3

AN OVERVIEW OF BASAL CROP COEFFICIENTS AND THE POTENTIAL USE OF SAP FLOW GAUGES FOR ITS DERIVATION IN MAIZE

Summary

An efficient water management plan is based on accurate estimations of crop water use. The two-step approach estimating a reference evapotranspiration (ET_{ref}) with the use of a crop coefficient (K_c) to calculate potential crop water needs is widely accepted. The calculation of ET_{ref} has been standardized by FAO (Allen et al, 1998) for a short reference crop and the American Society of Civil Engineers (ASCE-EWRI, 2005) for a short and tall reference crop. The purpose was to standardize the calculation of ET_{ref} and improve the transferability of K_c s. Different arguments regarding the transferability of the K_c values exist. However, it is assumed that mid-season basal crop coefficient (K_{cb}) values are transferrable among locations, if local conditions meet FAO56, (1998) and ASCE-EWRI, (2005) criteria: full cover crop, adequate fetch, and climatic adjustment if necessary. Nevertheless, there are different agricultural practices that can change the partition of the water use for transpiration and soil evaporation or situations where delineation or verification of curves are desired. In this work we provide an overview of the origin, the advantages and the disadvantages of the use of K_{cb} in a dual K_c approach compared to a single K_c approach to estimate crop water needs. We also describe modern approaches for adjusting K_{cb} curves according to actual crop growth using spectral reflectance and the advantages and benefits of other tools like sap flow sensors. Data from two field experiments in northern Colorado in 2019 and 2020 provided evidence that sap flow sensors can be a cost-effective tool in developing a K_{cb} curve for maize under field conditions.

Introduction

Irrigation scheduling for efficient water management requires reliable estimates of crop water use. There are numerous ways of estimating crop evapotranspiration (ET), depending on the meteorological data available (Allen et al., 2007). ET is typically estimated using weather data and algorithms describing surface energy and aerodynamics of the vegetation (Allen et al., 2011b). The Penman-Monteith (PM) combination equation is the most widely used equation for estimation of crop evapotranspiration (Jensen et al., 2016). The calculation of reference crop ET (ET_{ref}) has been standardized by FAO (Allen et al., 1998) for a short reference crop and the American Society of Civil Engineers (ASCE-EWRI, 2005) for a short and tall reference crop. This is the basis for the widely used two-step approach for crop water use calculation. The purpose was to standardize the calculation of ET_{ref} and improve the transferability of crop coefficients (ASCE, 2005).

The two-step approach consists firstly in determining the ET_{ref} , representing the weather impact on ET. The method uses weather data to estimate ET for a reference condition and crop; either a short reference using grass as reference (ET_o) or tall reference using alfalfa (ET_r). Numerical constants for surface and aerodynamic resistances and albedo are included in the equation according to the reference crop, grass or alfalfa. (Allen et al., 2005). The reference condition is a 0.12 m clipped, cool season and well-watered grass (short ET_{ref} or ET_o) or a 0.5 m alfalfa crop (tall ET_{ref} or ET_r). Alfalfa reference is up to 1.25 times larger than ET_o from FAO56 (Allen et al., 1998). Reference ET can be estimated in daily or hourly time-steps. Generally, ET_{ref} has a higher potential accuracy when computed in an hourly basis and then summed into a 24 h period since it considers the changes in weather parameters within the day (Allen et al., 2006).

The second step is to multiply the ET_{ref} value by a crop coefficient (K_c) to estimate the crop ET (ET_c). The coefficient represents the relative rate of ET from a specific crop and condition to that of the reference (Allen and Pereira, 2009). This will depend on the amount, type, growth stage, canopy cover and wetness of the soil surface and profile and condition of the vegetation (Jensen et al., 2016; Allen and Pereira, 2009). Hence, the relative roughness, leaf area index (LAI) and albedo of the actual crop surface in relation to the characteristics of the reference surface (grass or alfalfa) are considered.

The crop coefficient curves for different agricultural crops (Allen et al., 1998; Jensen et al., 2016; Allen and Pereira, 2009) represent the ratios of the crop ET to the ET_{ref} during different growth stages. Two families of crop coefficient curves have been developed for agricultural crops, tall or alfalfa reference and short or grass reference, which are used for either the tall or short ET_{ref} . On the other hand, two types of crop coefficient exist. 1) The basal crop coefficients (K_{cb}) and 2) the single (or mean) crop coefficients (K_c).

The basal crop coefficients represent mainly transpiration. It is the crop coefficient for a dry soil condition at the surface, so there is no evaporation from soil or it is minimal, but soil water content does not limit plant growth and transpiration. It can be used along with a soil evaporation coefficient (K_e) to account for soil evaporation losses in the “dual K_c approach” to determine ET_c . The single crop coefficients (K_c) represent the averaged effects of the evaporation from the wet soil due to rainfall or irrigation and crop transpiration. Errors in ET_c calculations using this approach might be caused because of the differences between the frequency of irrigations and rainfall, and soil drying characteristics between the site where it was developed and the location where it is being used (ASCE, 2005).

One difficult aspect when using crop coefficient curves is the timescale, because crop growth rates and senescence rates vary with season, crop type and management practices (Trout and DeJonge, 2018, Hinkle et al., 1984). Hunsaker et al., (2002) states the performance of the dual crop coefficient approach is highly dependent on how accurate the curve is to match the actual conditions and crop stages. A way to better adjust crop coefficient curves and incorporate spatial and temporal variability is relating the crop coefficient curve to remote sensing vegetation indices (VI) (Bausch, 1995; Costa-Filho et al., 2022). They provide real time feedback for estimation of crop water use, including developmental patterns and spatial variability (Campos et al., 2010).

PM standardized equations have been applied in humid to arid conditions with good results. Nevertheless, it is important to define a ET_{ref} with similar aerodynamic properties to the crop in consideration. In this way, the influence of climate, aerodynamic and surface resistances on ET_c are reduced and there are small and recognizable variations on crop coefficient (Pereira et al., 1999). On the other hand, the dual K_c model is recommended since it is able to separate the transpiration component from the soil evaporation (Allen et al, 2011b). Hence, the effect of wetting patterns for specific rainfall events, irrigation methods or the irrigation management are considered separately (Pereira et al., 1999). This approach was found to be 10% to 20% more accurate for estimates of ET_c on a daily basis compared to the use of the mean K_c (Jensen et al., 2016).

Purpose of this work

We divided this chapter in two sections. First is a review section to describe the origin of the K_{cb} curves, the advantages of using basal crop coefficients in a dual K_c approach instead of the mean K_c and the disadvantages of using it. A description of new approaches for adjusting K_{cb} curves according to actual crop growth using surface spectral reflectance and the benefits of using sap

flow data to derive K_{cb} . Then, a second section shows how this was implemented in the field with partial season results for maize for two years. It provides evidence that low-cost sap flow sensors can be used to monitor, determine, or validate, local K_{cb} curves under field conditions.

Origin of the crop coefficient curves

Initiation of water use studies in the US are described in Jensen (1968). His detailed review reveals that water consumption research and early publications were facilitated from around mid-late 1800, nevertheless, previous studies are found before. Extensive experiments of different crops in the field, measurements of water delivered for irrigation, water used by crops in pots, the use of different experimental techniques, and measurements of meteorological data were carried out in western US to determine seasonal consumptive use. Early publications from 1913 and after, observed differences in transpiration depending on the location and conditions of the plants and its relationship with production of dry matter. Investigations also were carried out to study the influence of meteorological factors on evaporation and transpiration. Solar radiation was recognized to be the primary contributor to transpiration and advection energy as a contributor as well.

Many approaches were developed to quantify water use; from using empirical correlations with temperature, or with solar radiation or other weather data to evaporation from a tank. However, none of them were mechanistic approaches (Sinclair, 2019). In 1948, Penman (1948) developed a combined function of the energy balance equation with the aerodynamic equation, which continues to be used around the world. His proposed approach was to analyze the evaporation from open water, to study the relations between evaporation and weather data, and then seek a relation between those losses to the losses from soil and vegetated surfaces using evaporation ratios. Monteith (1965) modified Penman's equation to include a canopy conductance term and

compute the actual crop water use. The modification implicitly assumes that most of the crop water loss is due to transpiration and this transpiration rate is controlled by the canopy conductance (Sinclair, 2019). Monteith et al. (1965) state that when evaporation from the soil is negligible, the conductance term is only a plant parameter. However, when soil evaporation is significant, the resistance term is the combination of the resistance from crop leaves and resistance of vapor flux through soil pores (Monteith, 1965). Nevertheless, there is no straightforward approach proposed for solving for canopy conductance estimates in the field (Sinclair, 2019; Monteith, 1965).

VanWijk and de Vries (1954) proposed a method for using a coefficient of reduction for a potential ET. The ratio between the potential ET and actual crop ET was analyzed for crops in different studies like the one shown by Van Bavel (1967). However, Jensen (1968) explicitly described the use of a crop coefficient for simplification of the estimates of crop evapotranspiration using the potential evapotranspiration from a reference crop (Equation 1). The use of crop coefficients was also implemented for crop irrigation scheduling and forecasts of irrigation needs in the field using computer programs (Jensen, 1969).

$$ET_c = ET_{reference}K_c \quad [1]$$

This is called the two-step approach. He suggested the reference crop ET be estimated with any method already developed for potential ET or measured with a lysimeter. He stated that crop coefficients should be defined experimentally as there is no proposed method for its direct calculation. He also clarified the implications of the conditions in the field in the crop coefficient values, involving the soil and the crop resistances as contributors of total water evaporation from the surface. With partial cover of soil, the wetness condition of the soil affects the value of the resistance to diffusion of water. In wet soils the resistance to diffusion of water decreases and the

albedo decreases increasing net radiation, causing larger evaporation from soil. Plant resistance also changes at different stages of growth and cultural practices also influence water use. For example, biomass cuttings in alfalfa, reduces crop transpiration in alfalfa, however there is some compensation with more evaporation from the soil given less soil cover from the crop.

The interpretation of the potential evapotranspiration (ET_p) as defined by Penman (1948) was ambiguous and led to different interpretations. The use of ET_{ref} , using grass (used by Doornbos and Pruitt, 1977) or alfalfa (suggested by Jensen, 1970) named ET_o or ET_r respectively, cleared up this definition (Burman et al., 1981). It was considered that for irrigation scheduling the estimation of crop water requirements was best calculated on a daily basis and methods based on the combination equation by Penman (1948), were the most suitable (Burman et al., 1981). However, the Penman equation involves the use of coefficients and functions that can be different depending on the user. This is why a standardized equation was later suggested and analyzed. The two standard approaches are widely known as the FAO No.56 standardization for ET_o (Allen et al., 1998) and the ASCE standardization for ET_o and ET_r (ASCE, 2005). Some variables in the Penman-Monteith equation are defined as constants for simplification, such as canopy conductance.

In order to use the two-step approach, the ET_{ref} method has to match the method used to determine the crop coefficients (Wright, 1981). Crop coefficients are experimentally derived, thus, empirical values and tables for different crops were published since general values can be found for each crop type. The use of weighing lysimeters were advised for its determination given the direct estimation and the small errors (Burman et al., 1981, Wright, 1981).

Early crop coefficients (Jensen, 1968; Jensen et al. 1970; Jensen et al., 1971) represented a mean effect of soil and plant on the total surface evaporation. Given the important effects of soil

evaporation after an irrigation or rainfall, adjustments for soil evaporation were suggested (Jensen et al., 1971). The studies performed were based on soil moisture samplings for different locations and for an averaged period of 5 to 15 days including wet and dry soil conditions in the ET estimations (Wright 1981). Therefore, improvements were made later when using lysimeter data for the ETr estimations with the surface of the soil in dry conditions, as found in studies by Wright (1981) to develop basal crop coefficients, Kcb. The first to formalize the use of the Kcb was Jensen et al., (1971), to our knowledge (Equations 2 to 4).

$$K_{cb} = \frac{T_c}{ET_{reference}} \quad [2]$$

$$K_e = \frac{E_{soil}}{ET_{reference}} \quad [3]$$

$$K_c = K_{cb} + K_e \quad [4]$$

where, T_c is crop transpiration and E_{soil} is soil evaporation.

Basal crop coefficients, Kcb, represent a condition of dry soil surface with minimal evaporation, but with soil water availability in the root-zone not limiting plant transpiration and growth (Wright, 1981, Wright 1982). Contributions from the soil evaporation had to be calculated separately. However, it was understood that even though the use of the Kcb allowed more accurate estimates of crop ET, the calculations to estimate the wet soil effects could be impractical (Wright, 1981). Therefore, single crop coefficients were generated for typical crop development stages and management practices, with no water limitation in the root zone (Wright 1981). Tables published described crop development normalized in a percentage basis to fit the curve for different users from planting until full cover and after full cover (Wright, 1981).

An improvement to calculate single crop coefficients was also suggested. A numerical approach for including plant transpiration and soil evaporation, using the basal crop coefficient and the relative proportion of wetted soil (that varies with the irrigation system) and the number of days after the wetting period (that varies with type of soil), (Wright, 1981), similar approach to proposed by Jensen (1971).

The alfalfa basal crop coefficient curves were developed by Wright (1982), using meteorological data and ETr from two weighing lysimeters in Idaho during a period of 11 years. The alfalfa reference was chosen because of its high ET rates in arid locations, where advection can affect water use. Crop coefficient curves were developed for several crops. These Kcb were later converted for using the ASCE standardized reference ETr equation (Jensen et al., 2016). It was developed in a curvilinear form, unlike FAO#56 4-linear-segment style curves. Values are expressed for every 10% of the crop growth time and then they were re-expressed as a function of cumulative or normalized growing degree days (Jensen et al., 2016). Basal crop coefficients should be usable in different locations for which they were developed if procedures for ETr determination are verified and the adjustments of the crop development in the crop curve are implemented (Wright, 1982).

Use of crop coefficients

The use of crop coefficients with the estimation of the ETo or ETr is known as the “two-step” approach for crop evapotranspiration calculation. The basal crop coefficient Kcb) and the soil evaporation coefficient (Ke) are summed up to calculate the single crop coefficient (Kc) and the procedure is known as the “dual Kc” approach (Equations 2 to 4). The use of only one coefficient, using the single crop coefficient, is called “single crop coefficient approach” (Equation 1).

The crop coefficients vary with the crop characteristics and little with climate (Pereira et al., 2021). It considers the characteristics that are different between the reference crop and the actual crop such as: height (related to roughness and aerodynamic resistance), surface resistance (bulk crop-soil or/and crop and relating LAI, leaf condition, stomatal control, soil wetness), albedo (influencing net radiation, R_n) and depends on ground cover and soil wetness. Crop coefficient values refer to optimal (well-watered, no nutrient, pest nor salinity effects), for standard optimal conditions and well-irrigated crops. If there is not enough soil water to maintain the crop transpiration rate, then a stress coefficient (K_s) is introduced to reduce the estimated transpiration (Jensen et al., 1971), called actual K_c in Equation 5.

$$K_{c \text{ actual}} = K_c K_s = K_{cb} K_s + K_e \quad [5]$$

The use of the two-step approach (either with K_c or K_{cb}), has the powerful advantage of being an approach that gives precise results, requiring conventional weather parameters and a relatively low level of expertise from the user (Allen, 2000). The spatial resolution of the method is limited to the extrapolation of the weather data, affected by the heterogeneity and land use of the area (Allen, 2000) and conditions of the crop. Crop coefficient curves have a typical bell-shaped curve (Irmak and Kukal, 2019; Abrisqueta et al., 2016) that has been simplified with polynomial equations (Trout and DeJonge, 2018; Irmak and Kukal, 2019) or in a 4-segment linearization approach (Allen et al., 1998). There is no strong advantage of using polynomial equations over a 4-segment approach shown at the moment. On the other hand, the difficulties of polynomial equations to customize crop coefficient curves for its transferability has been stated by Pereira, (2021) over the advantages of using the 4-segment shape for an appropriate customizable fit (Allen et al., 1998; Trout and DeJonge, 2018).

Crop coefficients are used in several approaches. There are many methods to estimate crop evapotranspiration (ET_c) and many of them use crop coefficients, such as single layer models like the Penman-Monteith or in more complex, multi-layer models. These models are used for irrigation scheduling but also in crop growth models. Other approaches for ET_c calculation are the advanced methods applying energy balance with remote sensing, which have an enormous potential for present and future applications (Gowda et al., 2008). Stability of the crop coefficients in short periods of time is a great advantage and has been used as a gap-filling technique with energy balance (EB) methods (Allen et al., 2007). Remote sensing methods need clear-sky conditions at the time of the sensor overpass to calculate an instantaneous flux for that time (Allen, 2000). To predict ET_c for the time between the sensor overpasses a K_c or an “evaporative fraction” has to be estimated using the instantaneous data and is set constant. The use of crop coefficients (K_{cb} or K_c) curves can aid and improve its prediction by filling the time between overpasses (Neale et al., 2012; Allen, 2000). This also comprises an advantage in the forecasting of crop water needs, extrapolating crop coefficients using curve stability and using meteorological forecasts for ET_{ref} estimation (Calera et al., 2017).

Advantages of using basal crop coefficients in a dual K_c approach

Basal crop coefficients are empirical coefficients developed with dry soil surface conditions; therefore, they represent mostly transpiration. Its interpretation is straight forward, as there is no influence of soil evaporation, unlike with the single crop coefficient.

Since transpiration is governed by weather factors and plant stomata behavior, many approaches for estimating canopy resistance have been developed. Approaches vary from relatively simple descriptive or empirical to mathematical; operating only with weather variables, to complex models considering photosynthesis for its estimation (Damour et al., 2010). However, the complex

nature of stomatal conductance and its relationship with weather in plant communities, made it difficult to find a common function that represents it. Hence, the use of the crop coefficients remains widespread.

Crop coefficients tabulated values are the most common and user-friendly option, however, crop conditions in the field can differ from standard agronomic practices and for these situations the prediction of ET_c using the standard values can be challenging (Pereira et al., 2020). In addition, crop coefficient functions described in literature are time based and lack flexibility to reflect changes in crop development and water-use patterns in the field. Growing degree days (GDD) was found to be a better predictor of the crop coefficients than using days after planting (Irmak and Kukal, 2019).

The additional evaporation from the surface due to wetting of the soil surface caused by irrigation or rainfall events, is represented in the evaporation coefficient, K_e . This evaporation occurs in addition to the evaporation from the crop surface, the K_{cb} (Allen, 2000). The evaporation from the soil depends on the irrigation frequency and irrigation method, soil type, canopy cover and agronomic practices (Doorenbos and Pruitt, 1977; Wright, 1982; Irmak and Kukal, 2019). The range of values for K_c , K_{cb} and K_e depends on which approximation for ET is used (ET_r or ET_o).

Agricultural practices have large impacts on crop growth and soil water evaporation; hence, they affect K_c , K_e and K_{cb} . The dual K_c approach is known for its more accurate estimation of ET_c when compared to the use of a mean K_c (Irmak and Kukal 2019). This is because site-specific surface conditions mainly changing the amount of soil water evaporation due to irrigation or precipitation, have great influence on the K_c values. For this reason, mean K_c values vary greatly with locations and years, reducing their transferability. For example, a study with Bermudagrass by Paredes et al., (2018), observed that the frequency of cuttings changed the mean K_c value. It

was found that single K_c values were specific for each cutting treatment and therefore using a K_{cb} curve was a better strategy to assess water use. With the use of K_{cb} values they were also able to specify cutting treatments where transpiration constituted 90% of the total ET_c , an indicator of a high beneficial consumptive water use and considered as a characteristic of well-managed, sustainable grassland. In another example Zhao et al (2013) studied the basal crop coefficient and the evaporation coefficient for a sequence of maize and wheat, calculating that evaporation from the soil represented 29% of the ET_c in wheat and 41% in maize. They found that mean K_c did not fit well for the local practices and using basal crop coefficients and a dual K_c approach was superior.

Paco et al. (2019) adjusted K_{cb} values for olive trees and advised the use of K_{cb} instead of a mean K_c due to its great variability for different locations, mainly because of the soil evaporation that is especially important in perennial crops like olive orchards. Wei et al. (2015) and Paco et al. (2014b), showed that the transpiration component had a small inter-annual variation in comparison to the soil evaporation that showed a great variation due to the frequency and volume of irrigations and climate.

The basal crop coefficients, in a dual K_c approach, can be used for any type of crop and studies have validated its performance for maize (Allen et al., 2005; Zhao et al., 2013; Irmak and Kukul, 2019); wheat (Zhao et al., 2013); canola (Lopez-Urrea et al., 2020); soybean (Wei et al., 2015); olive trees (Puppo et al., 2019); peach trees (Paco et al., 2014); snap beans (Allen et al., 2005); cotton (Hunsaker, 2003); muskmelon (Lovelli et al., 2005); citrus (Er-Raki et al., 2009); onion (Lopez-Urrea et al., 2009); and for many other species. A review of updated K_{cb} coefficients derived from local experiments was published by Rallo et al., (2021) for numerous species, from deciduous trees, vine and berries, citrus, olive trees to tropical fruit crops. Updated K_{cb} values for vegetable and field crops were published by Pereira et al., (2021a); Pereira et al., (2021b).

Since the dual K_c approach computes transpiration and soil evaporation separately, in addition to being more precise than single K_c approach for irrigation scheduling purposes, it is also useful in studies that aim to reduce soil evaporation and optimize crop production (Allen, 2000). Soil water evaporation is a non-beneficial water use because it is not contributing to carbon uptake and crop growth (Irmak and Kukul (2019). In a dual K_c approach evaporation from the soil can be measured and therefore, managed. For example, Lopez-Urrea et al. (2009) found a large variation in irrigation needs for onions for different locations and irrigation systems, hence, a huge variation in single crop coefficients were reported. To explain these differences, they conducted lysimetric studies finding that the differentiation between K_{cb} and K_e was needed for ET_c determination. They found that the mean K_c was not able to account for the partition between plant transpiration and soil evaporation nor irrigation frequency affecting onion planting surfaces, where the full ground cover is never reached. They found a good correlation between ground cover and the K_{cb} , because values of K_{cb} are directly related to ground cover development. They found differences in mean K_c values compared with the FAO-56 tabulated values because for their conditions, the transpiration and evaporation components were underestimated.

The use of conservation practices that change the ground surface cover and therefore reduce the evaporation of water from the soil, leads to a reduction of the non-beneficial water use of the crop surface and allows to conserve water. Conservation practices can be, reduced tillage, localized and sub-surface drip irrigation, plant spacing, for early canopy closure, cover crops, precise nutrient management, among others (Delgado et al., 2011). Single crop coefficients may not be flexible enough to account for these changes into the calculation of the ET_c .

For example, Irmak and Kukul (2019) studied the effect on crop coefficients in maize of tillage vs no-tillage conditions. They found a great impact of tillage practices in the crop coefficient of maize.

They found higher evaporation rates with tillage that reduced the K_{cb} value by 70% with respect to the mean K_c , specially early and late in the growing season. They also found that the differences were minimal in the mid-season and higher in early and late stages of the crop growth cycle, due to soil evaporation and ground cover. Djaman and Irmak (2013) found an overestimation of the mean K_c for maize at the initial and the end of the crop season and a great variability depending on the moisture condition of the soil. These findings show the great advantage of the use of the K_{cb} , especially when the canopy cover is not complete even in annual row crops such as maize and that agricultural practices have a great impact on the water use estimation.

Nutrient management could also modify ET_c estimations. Ferreira and Carr (2002), in a study with potato using sprinkler irrigation, partitioned the contributions of transpiration and evaporation on the total crop evapotranspiration with different levels of nitrogen fertilization. They found that the contribution of the transpiration to the total ET_c was lower in unfertilized crops and soil evaporation represented 50% of the total ET_c . On the other hand, a well fertilized potato developed rapidly with a large crop canopy and transpiration contributed 75% to 80% of the total ET_c . However, differences compensated and total ET_c for the entire period in both situations was similar. But the difference in water use for non-beneficial purposes was evident. For a study with quinoa, Razzaghi et al. (2012) found that the $K_{cb} + K_e$ calculated in their study was different from the mean K_c derived in different locations, attributed to differences in crop spacing and fertilization (crop growth).

Other agronomic practices that modify the cultivated surface is the use of plastic mulches. These practices, while reducing evaporation from the soil, increase radiative and sensible heat of the surface and could raise crop transpiration. The favorable environment due to the mulch also increases crop growth, hence, mean K_c coefficients change when compared to no-mulch

conditions (Lovelli et al., 2005). For example, studies for melon and pepper in raised mulch beds by Shrestha and Shukla (2014) demonstrated a reduction in irrigation application due to the use of a dual Kc approach for ETc determination that accounted for a 51% of the seasonal rainfall and that could save water and reduce nutrient leaching due to over irrigation. They showed how the water use for a particular local agricultural practice of wetting the soil before plastic mulch deployment brings evaporation from the soil high enough to account for 82% of the ETc in pepper and 92% of the ETc in watermelon during the initial crop growth stage.

The effect of natural mulches (crop residues) was also studied by Martins et al., (2013) in maize, finding that the effect of mulch reduced soil evaporation to less than 9% of the total ETc in drip and sprinkler irrigation systems. They found very low values compared to the no-mulch treatment that had soil water evaporation around 30% of total ETc. The effect of mulch was larger during the initial period and reduced the soil evaporation to minimal values during the development stage and low at the late season stage. However, the magnitude of the effect may vary with type of mulch and amount. They also found that soil evaporation was higher with more frequent irrigation schemes even in presence of crop residues.

The effect of crop varieties and plant density on crop water use and irrigation needs have also been assessed. Trout and DeJonge, (2018) found that the Kcb value from MOP#70 (Jensen and Allen, 2016) was too low for current maize varieties and agronomic practices. The current cultivars with upright leaf architecture planted at higher densities had higher Kcbs compared to the ones used in studies from Wright in the eighties or seventies, values that were used in the MO#70 table (Jensen and Allen, 2016). Jiang et al. (2014) studied the effect of planting densities on the ETc in maize, finding an increase with population that was due to higher crop transpiration and lower soil evaporation. They found the Kcb strongly correlated with LAI, finding higher LAI for higher planting densities.

Ground cover can greatly influence the total ETc, especially in the conservation practice named “active ground cover”. Fandino et al. (2012) studied the Kcb in a vineyard with an inter-row grass cover crop (active ground cover), for 3 years. They calibrated Kcb values for the vineyard and for the active ground cover for local climate, and architecture of a semi-trellised vine since the vineyard architecture modifies the Kcb coefficient. A new Kcb, for the vine and the cover crop together, was generated. They showed how the Kcb in the initial period for the vineyard was dominated by the transpiration from the cover crop and how practices like mowing and herbicide applications reduced Kcb from the cover crop and favored an increase in the Kcb from the vine. They also showed a reduced soil evaporation, constituting 8-17% of the water use for the entire crop season and 83-92% of the total ETc from the vine and pasture. They were able to calculate the partition of the total transpiration, for vine accounting for 37-45% and for the cover crop 43-48%. This approach allowed a better understanding of the water use for this type of setting.

The influence of the irrigation systems on the ETc estimation has also been assessed. The wetting amount and frequency as a result of different irrigation systems and the influence of soil texture was noted and accounted in a manual adjustment approach suggested in the FAO-56 procedure for mean Kc at the initial stages of crops (Allen et al., 1998). The impact of irrigation systems observed in different studies suggest the use of the dual Kc approach for a better adjustment for different situations. For example, Er-Raki et al. (2009) in a citrus orchard adjusted the single crop coefficients for drip irrigation and for flood-irrigation practices, finding that the main source for overestimation in ETc was the soil evaporation. They found that the reduction of the mean Kc for drip irrigation was due to reduced soil evaporation. For the flood irrigation condition, they found a higher soil evaporation than the drip and also a reduced plant transpiration due to a reduction in canopy cover. Therefore, they strongly advise the use of a dual crop coefficient approach, where the transpiration component and the amount of water lost through soil evaporation are partitioned;

and select an irrigation system where water that is not used by the plant is minimized. In this line and studying a highly efficient irrigation system like sub-surface drip (SDI), Phogat et al (2016) studied how the irrigation method and the fraction of soil wetted impacted crop coefficient values. They demonstrated that SDI changes evaporation patterns in the field with respect to surface drip and showed its dependence on texture and particular characteristics of the sub-surface irrigation system. They modeled differences that may possibly cause overestimations in the calculation of ET_c that range from 5% up to 18% due to soil water evaporation in sparse crops like grapevines.

A dual crop coefficient approach is appropriate for precision irrigation and when a more precise soil water balance is desired for irrigation (Puig-Sirera et al., 2021). It is particularly suitable for crops with incomplete ground cover and high frequency irrigations where the surface humidity variations and ground cover have great impact on the estimation of the ET_c (Allen et al, 2005). The partition of the actual ET_c into transpiration and soil evaporation components provide a better understanding of the dynamics of the ET_c specially under conditions of incomplete ground cover (Puig-Sirera et al. 2021). The use of single crop coefficients does not compute for impacts of irrigation or rainfall frequency or irrigation system type on the total ET_c and this accountability becomes important when water is scarce (Rosa et al., 2012).

According to numerous studies, agricultural practices can alter the evaporation and transpiration partition in the total ET_c estimate, mainly due to irrigation frequency (amount of soil water content in the evaporative layer) and crop development (ground cover reducing soil evaporation and higher transpiration, less energy for evaporation and more for transpiration). The effects can be significant. Understanding and measuring the contributions of the available water for crop transpiration or for non-productive uses (soil evaporation) facilitates the development of improved irrigation schedules and water saving practices.

Disadvantages of the basal crop coefficients

Two drawbacks can be found when using a dual Kc approach: the practical implementation because calculations are cumbersome and the difficulty in the derivation of the Kcb.

The dual Kc approach includes the use of the soil evaporation coefficient. Therefore, for its practical implementation, there is the need for estimation of a soil water balance for the evaporation surface layer in addition to the root zone soil water balance (Rosa et al., 2012). In practical applications the surface soil evaporation is modeled using approaches such as the one suggested in FAO-56 (Allen et al., 1998; Allen et al., 2005) or suggested by Pereira et al. (2009) and requires knowing parameters of the soil, wetting events and ground cover. Hence, it implies an additional calculation in contrast to the simpler single Kc approach. However, software like the SIMDUALKc have been developed for irrigation scheduling using the dual Kc approach (Rosa et al., 2012) and automatically calculates soil evaporation using the methodologies suggested by Allen et al., 2005 and Pereira et al. (2009), facilitating the practical implementation. For example, Cancela et al. (2015) successfully used the software for the operation of the dual Kc approach in a real-time automated irrigation system in a vineyard.

A drawback for the use of the Kcb approach remains in the complexity of its derivation.

In general, the dual Kc approach is limited to agricultural crops, since it is hard to apply for natural vegetation because of the great variation in plant density, available water, leaf area (Allen, 2000) and mixed vegetation.

Data supports that, in general, Kcb values are transferrable and can be used in different locations and hybrids without major differences (Fandino et al., 2012; Martins et al., 2012; Paco et al., 2014b; Wei et al., 2015; Puppo et al., 2019; Marek et al., 2020). Tabulated values had been

updated without major differences from tabulated values from FAO-56 and had been tied to a ground cover coefficient facilitating transferability (Rallo et al., 2021). However, some site-specific conditions that modify crop architecture, vigor and canopy management might change the Kcb. For example, Poblete-Echeverria and Ortega Farias (2013) found that the Kcb for a grapevine with a vertical-shoot positioned system changed the values from FAO-56 tabulated values between 11-19% lower. Dragoni et al. (2004) for example, found that the FAO-56 Kcb tabulated values changed for situations of tall but sparse canopies and found lower values in apple trees. They questioned the use of FAO-56 ETo for tall canopies and explained the lower Kcb value due to the dependence of transpiration on net radiation but much more dependent on stomatal conductance and VPD in tall apple trees with respect to that of grass (ETo). The grass reference was too dependent on net radiation and underestimated factors like light interception and stomatal regulation in apple trees. Zhao and Zhao (2014) adjusted the Kcb for maize for a region in China, warning that tabulated values are constant values for all plants all over the world, hence they could be better adjusted. Trout and DeJonge (2018) also found higher mean Kcb values attributed partly to the use of modern maize varieties that have different, more upright architecture than older varieties.

Traditionally crop coefficients have been derived from lysimeters because they were suggested as a very accurate approach for its derivation (Wright, 1981). However different methods were developed with time and can be used for its derivation (Pereira et al., 2021). Many studies have used expensive equipment such as the weighing or drainage lysimeters for local derivations of Kcb (Lovelli et al., 2005; Howell et al., 2006; Lopez-Urrea et a., 2009; Puppo et al., 2019; Abrisqueta et al., 2013). Others have used complex and expensive equipment such as the eddy covariance (Paco et al., 2012; Er-Raki et al., 2009), commercial sap flow sensors (Paco et al., 2012; Paco et al.; 2019) or used approaches for estimating ET using remote sensing (Garcia et al., 2013; Paco et al., 2014). On the other hand, others have used a water balance approach; a

method that does not require any complex and expensive equipment nor a high level of technical knowledge from the user, but it is time consuming, and it might require several years for its derivation. For example, Trout and DeJonge (2018) developed crop coefficient curves using this method, however, 6 years of data was used.

The main drawbacks of the different methods for estimating crop coefficients were reviewed by Pereira et al. (2021), including lysimeters, soil water balance, Bowen ratio, eddy covariance and remote sensing. A review of the crop coefficients in the Mediterranean climate (Lazzara and Rana, 2010) found that most of the actual crop evapotranspiration were measured using eddy covariance technique, followed by the use of lysimeters and soil water balance methods (36%, 33% and 16% of the total, respectively). They found that sap flow techniques were rarely used. From Pereira et al. (2021) updated review for field crop coefficients it can be appreciated that most of the studies for Kc and Kcb derivations come from soil water balance approaches (47%) and following derivations from lysimeters (26%), eddy covariance (11%) and very rarely from sap flow data. The studies reviewed in this chapter mainly used soil water balance and lysimeter techniques (Table 3), studies that used sap flow data for crop coefficient derivations were rare.

Table 3. Compilation of the studies for crop coefficient derivations.

| Technique | Crop coefficient | Crop | Author |
|--|-------------------------|---|--------------------------|
| Lysimeter | Kc and Kcb | - | Allen et al. (1998) |
| Lysimeter | Kc and Kcb | Peach trees | Arbisqueta et al. (2013) |
| Lysimeter | Kc | Maize, wheat, sorghum, soybean, cotton, alfalfa | Howell et al. (2006) |
| Lysimeter | Kc and Kcb | Maize | Marek et al. (2020) |
| Eddy Covariance and soil water balance | Kc and Kcb | Vinyard | Campos et al. (2010) |
| Soil water balance | Kc and Kcb | Vinyard | Cancela et al. (2015) |
| Sap flow | Kcb | Apple orchard | Dragoni et al. (2004) |
| Eddy covariance | Kc and Kcb | Citrus orchard | Er-Raki et al. (2009) |

| | | | |
|------------------------------------|-------------|---|---|
| Soil water balance | Kc and Kcb | Vineyard with/and active ground cover, grass | Fandino et al. (2012) |
| Soil water balance | Kc | Potato | Ferreira and Carr (2002) |
| Sap flow | Kcb | Pear | Goodwin and Green (2012) |
| Sap flow and microlisimeter | Kc and Kcb | Maize | Hou et al. (2014) |
| Soil water balance | NDVI-Kcb | Cotton | Hunsaker et al. (2005) |
| Lysimeter | Kcb | Alfalfa | Hunsaker et al (2002) |
| Soil water balance | NDVI-Kcb | Cotton | Hunsaker et al. (2003) |
| Bowen ratio | Kc and Kcb | Maize | Irmak and Kukal (2019) |
| Eddy covariance and microlisimeter | Kc and Kcb | Maize | Jiang et al. (2014) |
| Sap flow | Kcb | Cherry trees | Juhasz et al. (2013) |
| Lysimeter | Kcb and Kcb | Onion | Lopez-Urrea et a. (2009) |
| Lysimeter | Kc | Muskmelon | Lovelli et al. (2005) |
| Soil water balance | Kc and Kcb | Maize | Martins et al. (2013) |
| Lysimeter and microlisimeters | Kc and Kcb | Olive trees | Puppo et al. (2019) |
| Eddy covariance and Sap Flow | Kc and Kcb | Olive orchard | Paco et al. (2019) |
| Eddy covariance and Sap Flow | Kc and Kcb | Olive trees | Paco et al. (2014) |
| Eddy covariance and Sap Flow | Kc and Kcb | Peach trees | Paco et al. (2012) |
| Soil water balance | Kc and Kcb | Bermuda Grass | Paredes et al. (2018) |
| Sap Flow Soil water balance | Kc and Kcb | Vinyard | Poblete-Echeverria and Ortega-Farias (2019) |
| Sap Flow and Soil water balance | Kc and Kcb | Olive trees | Puig-Sirera et al. (2021) |
| Sap Flow and Soil water balance | Kc and Kcb | Quinoa | Razzaghi et al. (2012) |
| Lysimeter | Kc and Kcb | Canola | Lopez-Urrea et al. (2020) |
| Lysimeter | Kc and Kcb | Bell pepper and watermelon | Shrestha and Shukla (2014) |
| Remote sensing | Kc | Maize, alfalfa, sorghum and soybean | Singh and Irmak (2009) |
| Remote sensing | Kc | Maize | Garcia et al. (2013) |
| Remote sensing | Kc | Alfalfa, sugar beets, maize, potato, spring and winter grains | Tazumi et al. (2006) |
| Soil water balance | Kcb | Maize | Trout and DeJonge (2018) |
| Lysimeter and remote sensing | Kc and Kcb | Sugar beets | Wang et al. (2021) |
| Soil water balance | Kc and Kcb | Soybean | Wei et al. (2015) |
| Lysimeter | Kc and Kcb | - | Wright (1981); Wright, (1982) |

| | | | |
|--------------------|------------|-----------------|----------------------|
| Soil water balance | Kc and Kcb | Maize and wheat | Zhao et al. (2013) |
| Sap Flow | Kcb | Maize | Zhao and Zhao (2014) |

A potential use of sap flow sensors

Another alternative as a cost-effective way to derive Kcb coefficients is the use of sap flow sensors. These sensors have the great advantage of providing a direct and precise measurement of plant transpiration and they have been described as a good alternative for site-specific calculation of Kcb values (Poblete-Echeverria and Ortega-Farias, 2013; Zhao and Zhao, 2014). Sap flow sensors have been used for Kcb derivations in olive trees (Puig-Sirera et al., 2021, Paco et al., 2019), apple orchards (Dragoni et al., 2004), pear orchards (Goodwin and Green, 2012); peach (Paco et al., 2012); vineyards (Poblete echeverria and Ortega-Farias, 2013), Maize (Zhao and Zhao, 2014; Hou et al., 2014), Cherries (Juhasz et al., 2013), or quinoa (Razzaghi et al., 2012), among others.

There are different types of sap flow gauges. They introduce heat into the stem, trunk, or branch of a plant to measure water flowing in the xylem. Transpiration can be calculated using the velocity of the heat carried away from the source or calculated using the dissipation of heat energy due to convection or with the heat balance method where sap flow is calculated from an energy balance of the stem segment (Allen et al., 2011). Either methodology need to be scaled up to extrapolate transpiration for a field. Sap flow gauges are plant-based sensors sensitive to changes in stomata closure and environmental conditions, reflecting the actual crop water status.

Sap flow measurements are valuable for basal crop coefficient determination because they are the most direct estimate of the transpiration component of the ETc during the season, useful for experimental studies and for local derivation or verification of the Kcb. Understanding the partition

of total water use between plant transpiration and soil evaporation is important when looking for an efficient use of the water. In addition, if the dual crop coefficient is not meant to be used, the adjusted mean single K_c for particular locations and agronomical practices can be improved by measuring transpiration and soil evaporation.

Sap flow data can quantify the changes in the crop coefficients that are not related to ground cover but caused by specific environmental modifications that modify plant transpiration. An example of these modifications is the implementation of practices to reduce pesticide applications such as the use of screen structures over vegetables. Moller et al. (2004) measured and modelled the ET_c of pepper under mesh structures. They recommended adjusting crop coefficients for modified crop water requirements in greenhouse environments given that their findings show a significant reduction in crop transpiration that leads to reductions in irrigation.

Factors affecting plant stomatal conductance have a potential significant effect on the K_{cb} value. For example, Rana et al. (2021) studied the effects on transpiration and stomatal resistance in vine of the irrigation with saline water. They found that transpiration of vines was reduced by salinity because the responses of canopy resistance to radiation and VPD changed with high salinity levels in water. Canopy resistance responded differently to high levels of radiation and the stomatal sensitivity to VPD increased.

Stomatal response can also be altered by modifications of the concentration of carbon dioxide in the atmosphere. Several studies similar to Senock et al. (1996) have assessed the effects of elevated carbon dioxide in the atmosphere. The effects are different for different species (Ainsworth and Long, 2020), however studies have proven reductions in stomatal conduction and transpiration and increments in above ground biomass. These are modifications that could also change K_{cb} values.

Other effects on the plant could modify transpiration without modifying its ground cover. An example of these is the effect of insects or diseases that reduce leaf functioning but not leaf area, reducing plant transpiration. For example, Cunningham et al. (2009) in a study of the effects of an insect on Eucalyptus trees, found that the insect reduced the tree transpiration in two ways, reducing the leaf area, but also reducing the functional area of the leaves. They found that affected trees also had a 20% of loss of leaf functional area due to necrosis caused by the insect. This was found in a situation of low insect presence; hence they predict a more substantial effect in circumstances of insect outbreaks and its effects on the plant and ecosystem in the long-term.

Basal crop coefficients can be derived directly by measuring plant transpiration or they can be estimated as the residual of the ET_c measurement and soil evaporation. In these experimental approaches the K_e is measured with micro lysimeters (Paco et al., 2012; Puppo et al., 2019). However, it has been found that the evaporation component using microlysimeters could be overestimated because the effect of the water extraction by the roots (root absorption of water is excluded from the microlysimeter), is not accounted (Zhao et al. 2013; Wei et al., 2015). Therefore, when using combined methods to partition ET_c into soil and plant components it is useful to have sap flow measurements in addition to accounting for soil evaporation.

On the other hand, the trend for future ET_c determination is the use of remote sensing coupled with complex multilayer and multisource ET models (Allen et al., 2020). However, these approaches still need to overcome some challenges for wide-spread use. Crop coefficients and sap flow data can complement these improved modern approaches. The use of crop coefficients and ET_{ref} can be utilized to establish upper limits when remote sensing and complex models for ET_c determination are applied. They can also assist these approaches when used for the interpolation of ET_c between satellite overpasses.

The use of low-cost sap flow sensors for basal crop coefficient delineation

The need for expensive equipment for crop coefficient estimates, hampers studies with low-budget or slows down research because of limited number of sensors per season. The use of sap flow data has proven to be reliable and useful for estimation of K_{cb} values (Pereira et al., 2021; Paco et al., 2012), in this line, low-cost sap flow sensors have a great potential to expand research for locally derived K_{cb}. Low-cost sap flow systems have already been successfully implemented and are able to provide relatively accurate estimation of maize transpiration under field conditions (Miner et al., 2017) and they could be also used for basal crop coefficient development.

New approaches for adjustment of basal crop coefficients

Research during recent decades has shown the strong relationship between crop coefficients and fraction of ground cover (f_c) or canopy cover (CC), leaf area index (LAI), fraction of shaded ground and fraction of intercepted photosynthetic active radiation, and they can explain crop coefficient variability in the field (Pereira et al., 2020). Crop coefficients have been found to increase as LAI increases (Li et al., 2003; Irmak and Kukal, 2019; Jiang et al., 2014) in a curvilinear form (Ritchie and Burnett, 1971; Shih, 1989; Al-Kaisi et al., 1989; Kang et al., 2003, Zhao et al., 2010), or increase in a linear form as f_c increases until full effective canopy cover (Trout and DeJonge, 2018). It is also seen that crop coefficient decreases with senescence, in an apparent linear form as LAI decreases (Steduto and Hsiao, 1998) or as f_c decreases (Trout and DeJonge, 2018). Allen and Pereira (2009), Pereira et al. (2020), for example, showed an upgraded approach to predict

crop coefficient curves applying FAO methodology using f_c or LAI and crop height, called the A&P approach.

A way to incorporate spatial and temporal variability for local adjustments is relating the crop coefficient curve to remote sensing vegetation indices (VI) (Bausch, 1995). They provide real time feedback for estimation of crop water use, including developmental patterns, atmospheric conditions and spatial variability (Campos et al., 2010). Therefore, crop coefficients can be determined using vegetation indices. The basal crop coefficient can be estimated using spectral reflectance, because they show a similar trend, and express the response to weather, management practices and stress in real time (Bausch and Neale, 1987). The advantage of using spectral derived K_{cb} is well understood and recognized because differences in local practices have great impact on its value and VI can capture these variations (Calera et al., 2017). This is useful for situations where climatic conditions and management practices (i.e. cold or wet season, early plant date, plant population) cause a slow growth for example, where ET_c can be overestimated, resulting in overirrigation. The great advantage of using crop coefficients derived from NDVI or other VI is the independence of time parameters, facilitating the estimation of water use since planting dates, and assumptions of effective cover and maturation are not required, and sensitive to slow or fast crop development, therefore, representing a real-time crop coefficient for each specific field (Bausch and Neale, 1987; Bausch and Neale, 1989; Bausch, 1995; Campos et al., 2010). Spectral indices are also sensitive to leaf losses due to stressors, delay or early growth for each location and speed of senescence (Bausch and Neale, 1987).

Pocas et al.(2020) described that the reflectance response from canopies is influenced by several factors: the optical properties of the vegetation, including fruits, leaves, flowers, and their arrangement in the vegetation; the density of the leaves, leaf angle distribution, angle of incident radiation, and optical properties of the soil. Nevertheless, the optical property of the vegetation is

the main factor affecting the canopy spectral response pattern (Pocas et al., 2020). Therefore, the VI derived crop coefficients provide a potential ET estimate for the actual field conditions. ETc modelling based only in VI-approaches can lead to an overestimation of ET since it will not be sensitive to stress until a reduction in biomass or changes in canopy structure (Gonzalez-Dugo et al., 2009; Wang et al., 2021). However, if used along with a water balance or thermal stress crop coefficient such as the traditional crop water stress index (CWSI), that reduces the potential ET in situations of stress, the actual ET could be calculated without the need of highly trained personnel (Kullberg et al. 2017).

The use of VI-based crop coefficients is convenient because they can be analyzed quickly without specialized technicians, covers large areas and the spatial resolution can be high (Allen et al., 2011). Comparable accuracy has been found for irrigated areas between reflectance-based crop coefficient values for estimating ETc and remote sensing EB methods such as SEBAL or METRIC (Tazumi et al., 2006; Rafn et al. 2008; Singh and Irmak, 2009). All models should provide a similar result of ETc in well-irrigated, homogeneous, herbaceous crops (Calera et al., 2017). However, processes of soil wetting are not adequately reflected in the VI (Allen et al., 2011), hence the soil water evaporation component is not captured by this method.

Different VI can be used to estimate crop coefficients (Marcial-Pablo et al., 2021) such as normalized difference VI (NDVI), 2-band enhanced VI (EVI2), wide dynamic range VI (WDRVI), soil adjusted vegetation index (SAVI). The most common VI for estimating Kc or Kcb is the NDVI (Glenn et al., 2011), using the reflectance on the red (~ 0.6 - 0.7 μm) and the near infrared (~ 0.7 - 1.3 μm) bands. The values for NDVI fall between -1 and 1, water has negative values and dense vegetation around 0.95. Red light is absorbed by chlorophyll in leaves and reflected by soil. NIR is very little absorbed and is mostly transmitted, reflected, or scattered in the mesophyll of leaves, penetrating into the canopy. NDVI captures the contrast in the reflection from the canopy of Red

and NIR wavelengths. This VI is correlated with fractional cover, LAI, biomass and chlorophyll content (Bausch and Neale, 1987).

There is a linear relationship between NDVI and crop coefficients. The relationship of NDVI and K_{cb} is more consistent than with K_c and as NDVI is related to the amount of vegetation and transpiration is more closely related to it. It is assumed that the relationship condition is a dry soil surface with low evaporation in relation to transpiration (Pereira et al., 2021). The NDVI is highly correlated to agronomic variables, reaching asymptotic value at LAI of around 3 for maize and canopy cover of around 77% to 80% (Bausch and Neale, 1987; Trout et al., 2008). This VI increases linearly with canopy cover (or f_c) until around 0.8 (full cover), and larger canopy covers do not produce an increase in NDVI (Trout et al., 2008), nor in water use.

Some studies recall using SAVI for crop coefficient derivation as a better VI than NDVI (Huete, 1988), since it is less sensitive to soil reflectance, while others did not find a significant improvement over NDVI (Trout et al., 2008; Campos et al., 2010, Allen et al., 2011), and explained that NDVI was shown to be better than SAVI for estimating crop coefficients as it reaches a maximum at the same time as the coefficients, while SAVI continues to increase with LAI above 3 (Allen et al., 2011). However, care should be taken for days after irrigation or rain events (darkened soils) and the type of irrigation as errors might be introduced because of darker soils (Campos et al., 2010). With intermediate levels of vegetation for example, NIR flux through the canopy produces a soil reflected spectral signal similar to vegetation spectrum (Huete, 1988). Soil induced influences also exist on vegetation indices when there are soil brightness variations, such as moisture differences, shadow, organic matter differences; also, for darker soils vegetation indices are higher.

Crop coefficient curves derivation

Two approaches for estimating Kcb curves using NDVI are observed in literature. Using a unique function for a linear relationship between Kcb and the vegetation index like the NDVI or a two-step approach, where first fc is determined using NDVI and then a linear relationship with fc defines the value of Kcb. Some authors have shown the benefits of the direct estimation of Kcb from the VI (Bausch and Neale, 1989; Bausch, 1995) others have highlighted the benefits of the two-step estimation (Trout and Johnson, 2012). Authors state that prediction accuracy of crop coefficients increases when expressed as a function of two independent variables, fractional cover multiplied by VI (Johnson and Trout, 2012; Marcial-Pablo et al., 2021). The intermediate step of fc and NDVI also allows the extrapolation of fc for periods between or for missing values of NDVI, using any crop growth model with GDD or using visual estimates of fc (Trout and Johnson, 2012).

The smooth shape of the seasonal crop coefficient curve allows extrapolation of the data for up to a week, therefore, this is an advantage since it requires frequent VI measurements, but not daily. The curve can be approximated by a smooth continuous function because its stability in time in comparison with the great variability of ET, opening the possibility of linear interpolation between missing dates (Campos et al., 2010). In addition, the familiarity with the methodology of using crop coefficients for crop water use estimation make it more far-reaching and adaptable for irrigation scheduling (Bausch 1995, Hunsaker et al., 2003).

Considerations and drawbacks of VI approaches

Remote sensing is an exceptional tool for real time spatial ET calculation, however spatial resolution, and availability of timely images from satellite overpasses has been the bottleneck to

capture within-field variability and practical applications (Calera et al., 2017). The effects of irrigation or precipitation between satellite overpasses might also result in an underestimation of ET_c, because the gaps between instantaneous measurements have to be extrapolated and some bias might be introduced. The use of more flexible methods, such as unmanned aerial vehicles (UAVs), or interpolation of the VI data could overcome the drawbacks of cloud interference, resolution, and availability, from satellite imagery that leads to the lack of frequent data (Trout et al., 2008). Proximal remote sensing (ground-based devices or mounted in UAVs) can fill some of the gaps from extra-terrestrial platforms (satellites) or by relations regarding conservation of energy partitioning (Gonzalez-Dugo et al., 2009) or stability of the crop coefficients (Allen et al., 2007).

NDVI values from different satellites show some difference due to difference in bandwidth set for each band, and because of atmospheric corrections, nevertheless, they show close correlation (Allen et al, 2011). There are many platforms available for easy access to reflectance data or processed VI data nowadays. This new technology access makes the use of VI a practical low-cost option to estimate or adjust K_{cb} curves to local conditions. For example, Planet Labs PBC is an earth imaging company owning satellites called CubeSats or Doves that provide open data access images. The company corrected their data using MODIS and atmospheric models' data and normalized their different sensor reflectance, to make it more accurate and comparable to Sentinel-2 surface reflectance.

Studies have found that one equation for reflectance-based crop coefficient is enough to represent several crop species, with a seasonal ET accuracy around 5% for most crops (Tasumi et al., 2006). There is agreement between crop coefficients and f_c for a wide range of crops (Allen and Pereira 2009, Trout 2008) and the relationship of VI and f_c in many cases is linear and similar for different crops (Glenn et al., 2011). However, the NDVI-based crop coefficient is empirically

based, therefore calibration for different locations is necessary (Tasumi et al., 2006). The VI-Kcb relationship can potentially change with crop variety, row orientation, soil background and waveband-used for quantifying NIR and Red. VI range values can change from one season to another and the relationship VI-Kcb could change (Hunsaker et al, 2005). The relationship may vary with vegetation type because stomatal control is different for vegetative species (Allen et al., 2011). Hence, greenness indices or VI vs crop coefficients may vary for species and the crop coefficient derived from the VI requires a field validation (Pereira et a., 2021). Nevertheless, studies by Raft et al. (2008) suggests that NDVI-Kc curves might be spatially and temporally applied without recalibration for regions of similar climate and agricultural type.

In addition, the accuracy of using VI for ETc estimations increases with the accuracy of the ETc ground methods used for its calibration (Glenn et al., 2011). This highlights the importance of having additional and independent measurement of ETc in the field (Wang et al, 2021). This underlines the benefits of low-cost sap flow sensors for transpiration determination in the field. The combined use of sap flow data and surface reflectance can be beneficial for deriving spectral-based Kcb values or to adjust estimated transpiration to actual surface cover.

Use case: Sap flow sensors and surface reflectance data to assess a site-specific Kcb delineation

The description of the sites and the different Kcb curves used in this study are described in Appendix B. The rationale for the determination of each of the 4-segment phases is also described in Appendix B.

For our analysis we used large fields of well irrigated maize, where no nutrient or diseases affected ETc and where Kcb values could be used and estimated with no restrictions.

We used alfalfa reference crop ET and coefficients since maize at full cover has roughness, height and leaf area more similar to an alfalfa than a 12 cm grass surface. Therefore, K_{cr} mid is around 1 and does not need to be adjusted for wind and relative humidity like the grass K_c (Jensen and Allen, 2016). They do not need to be adjusted for climate like grass reference curves because most agricultural crops have an LAI and roughness similar to alfalfa at full cover. Therefore, the maximum alfalfa-based crop coefficients are near 1 for many agricultural crops (Jensen et al., 2016).

We measured maize transpiration using two types of sap flow sensors in 2019. A low-cost sap flow sensor using a heat pulse technique (description in chapter two) and a commercially available sensor that used the heat balance technique. Commercially available sensors were deployed in the field during 2019. The low-cost sap flow gauges were deployed in two different locations and during 2019 and 2020 (description in Appendix B). Using the standardized tall ET_{ref} from ASCE (2005) we were able to estimate a local basal crop coefficient from the two types of sensors.

In addition, we used surface reflectance data from the fields in two different ways. First, to better adjust crop growth stages and define the stages of the 4-segment-type K_{cb} curve, using tabulated local values from Trout and DeJonge (2018). We defined the 4 development stages from the FAO-style, 4-segment type of curve. We calculated NDVI and then with this index we estimated the maize evolution of ground cover. Although the function used for this estimation is empirical (Johnson and Trout, 2012), it has been determined that many different crops behave similarly and the relation is valid for a wide range of crops including maize (Trout and DeJonge, 2018). We took advantage of such relation to delineate the growth stages of maize in an objective way. Specially, for definition of the beginning and end of the mid-season stage, which is a period of very high atmospheric and crop demand, hence, large water consumptions and a critical period for final yield determination in maize.

Second, to estimate K_{cb} values from the functions derived from NDVI or SAVI from Trout and DeJonge (2018), Bausch and Neale (1989) and Bausch (1995). Spectral reflectance can be used to calculate K_{cb} . Two different approaches can be used: a direct calculation of K_{cb} from a vegetation index like NDVI or SAVI or a two-step approach, where first f_c is defined and then K_{cb} is related to f_c .

4-segment K_{cb} curve delineation with reflectance data

It has been stated that a FAO-style 4-segment crop coefficient curve lacks flexibility and other approaches for its delineation are suggested in literature, mainly using functions with surface reflectance, as stated in the introduction section. Two aspects of the 4-segment K_{cb} curve are worthy of discussion: the time scale and the shape.

The most difficult aspect for developing crop coefficient curves is the timescale, because maize growth rates and senescence rates vary with season, variety, and management practices (Trout and DeJonge, 2018, Hinkle et al., 1984). It would not have been adequate to assign a fixed time length for the stages. Trout and DeJonge (2018), suggest practices to reduce this variability: adjustments to the timescale using measured or estimates of crop development; normalization of the time axis, this is best if using thermal time or normalizing time from planting to effective full cover; initiation of the curve after emergence (because variation of air and soil temperature during the early season is the largest seasonal weather effect on plant growth in temperate climates); and relate the crop coefficient directly to f_c . These are all aspects that can reduce interseasonal effects.

We used NDVI to estimate fractional cover and adjust duration of crop growth stages. We drew the 4-segment curve with the aid of reflectance data, shown in Figure B1, in Appendix B, using tabulated values for maize locally derived from Trout and DeJonge (2018). Adjusting growth crop stages using NDVI is a successful method for better adjust Kcb curves to the actual growth in the field. Even though studies have proven that the use of GDD allows a quantitative estimation for shrinking or stretching of the Kc or Kcb curves for interseasonal effects (Jensen and Allen, 2016), and this results in an improvement compared to setting a fixed time-based Kcb curve (Trout and DeJonge, 2018), local observations for plant development are recommended to be used in addition (Jensen and Allen, 2016). This can be addressed using spectral data and adjusting crop growth to actual field conditions as performed in this study.

Regarding the 4-segment shape for a Kcb curve, our results show a good fit to actual Kcb curve for maize in the field based on ground scouting and when compared to the Kcb found with sap flow sensors (Figure 14). This agrees with Hunsaker et al., (2002) who state that basal crop coefficient curve FAO56-style and the performance of the dual crop coefficient approach is highly dependent on how accurate the curve is to match the actual conditions and crop stages. Studies show that even though some error can be introduced by assuming a constant ratio of actual ET vs ETref (Kc or Kcb) from one day to the next one or assumptions with soil evaporation estimation (Jensen and Alen, 2016); a 4-segment-type of line can be adjusted with good fit (Allen et al., 1998; Trout and DeJonge, 2018, Hinkle et al., 1984, Jensen and Allen, 2016). If the values and development lengths are certain, then, ETc estimates would be consistent with the actual crop ET (Hunsaker et al., 2002).

Other studies have examined the use of different shapes of crop coefficient curves. For example, Martinez-Cob (2008) found a better result using a local third-degree polynomial for Kc curves. However, a combination of straight-line equations along the season for the Kcb relationship are

proven to be as effective or better than polynomial functions (Heinkle et al., 1984). Heinkle et al. (1984), found equal or better results when using a 3-segment line function for the K_{cb} relationship when comparing a 4-degree polynomial equation. Pereira et al. (2021) clarifies that non-linear representations of the crop coefficient curves require parameters for curve fitting that vary with locations and year to year, making it almost impossible to transfer for other users.

There is uncertainty in the values of K_c or K_{cb} due to random error in weather data, in ET_{ref} estimation (random error by timescale, fixed aerodynamic, fixed reflectance and surface conductance are implicit in the ET_{ref} equation) and determination of K_c from field or research measurements (Jensen and Allen, 2016). Therefore, the straight-line method from FAO is mostly suitable for general use (Jensen and Allen, 2016).

In addition, the use of the four-segment crop coefficient curve has some advantages. It requires only knowing three values for crop coefficient, the initial, mid-season and late-season. Then the values for the crop development and late-season stage are linearly interpolated with time (Pereira et al., 2021). The transferability is easier than a curvilinear representation of the crop coefficients.

Spectral-based K_{cb} curve

We tested the estimation of K_{cb} directly from a VI, without segment delineation (Figure 13). Figure 13 shows all the datapoints and Figure 14 shows the datapoints for the days there was sap flow data available (with 8 gauges deployed in the field).

Our results showed that spectral based K_{cb} estimates followed the same trend as the 4-segment K_{cb} curve and the actual K_{cb} calculated with sap flow data (Figure 13 and Figure 14). However, there are differences in the model for the K_{cb} delineation and in the source of surface reflectance

data. There were few datapoints for the manual field scouting for surface reflectance because it was a weekly measure, however, they closely follow the 4-segment type curve than the surface reflectance from Planet. Field scouting for surface reflectance showed better results than values from Planet satellites.

We found that even when using data for clear days, normalized and harmonized we found scatter in the values. This indicates that care should be taken when guiding irrigation using only one source of surface reflectance data. We could think that ground scouting was a better option, however, trained personnel had to physically be present in the field to provide data.

Reflectance can be affected by very thin cirrus type clouds that are hard to detect. Planet Labs documentation warns that atmospheric corrections do not consider these. The days 8/24/2020 to 8/28/2020 were cloudier compared to the period 8/31/2020 to 9/06/2020. Figure 13 shows the Kcb estimates using reflectance from Planet had the largest scatter. Daily Kcb estimates from Planet could give the wrong conclusion about the crop Kcb for mid-August. However, manual ground-radiometric reflectance that do not have the cloud interference followed the trend from the 4-segment, theoretical Kcb curve, and sap flow Kcb. However, few datapoints were available because manual measurements were taken only weekly.

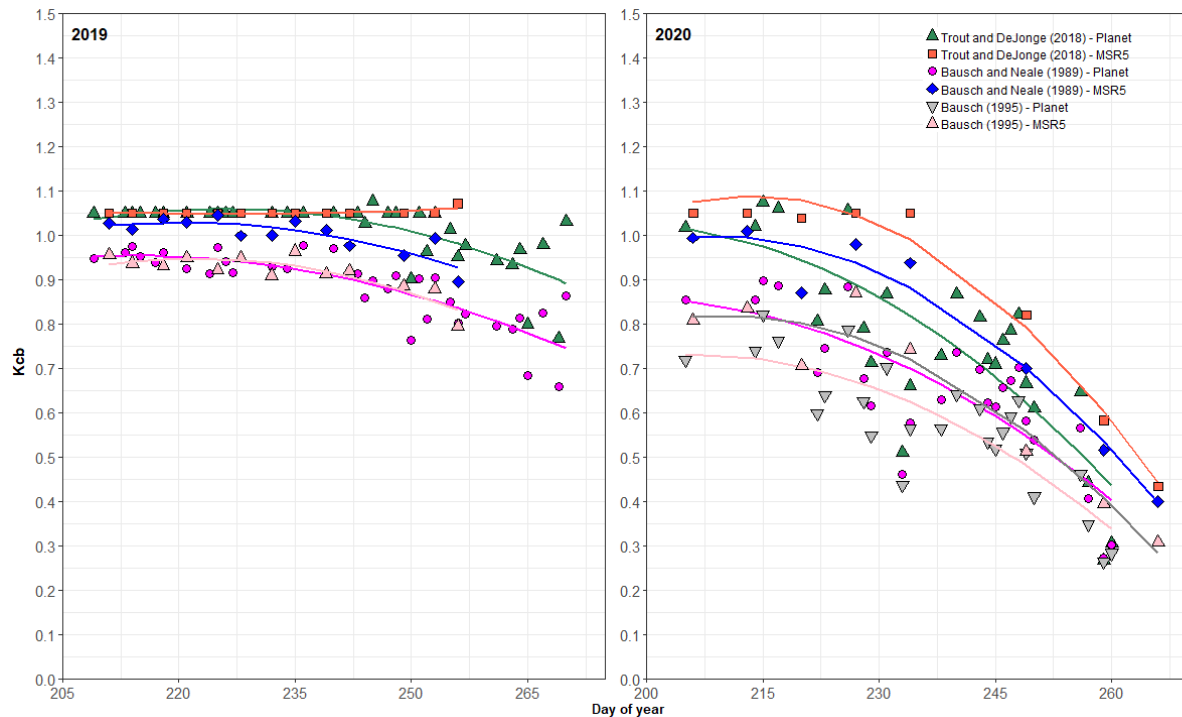


Figure 13. Spectral-based basal crop coefficient from studies located in northern Colorado, USA, during maize seasons 2019 and 2020 estimated with different approaches: Bausch and Neale (1989), Bausch (1995) and Trout and DeJonge (2018) using ground scouting with a handheld spectral radiometer and using Planet satellite data for local surface reflectance.

The two-step approach suggested by Trout and DeJonge (2018) was successful for estimating maize K_{cb} curve in these locations using ground scouting spectral radiometers (Figure 13). The benefit of the two-step approach has been explained by the authors in the flexibility for extrapolation of f_c with different known crop growth models when data is missing or for different analysis. Also, prediction accuracy of crop coefficients was shown to increase when expressed as a function of two independent variables, fractional cover multiplied by VI (Johnson and Trout, 2012; Marcial-Pablo et al., 2021).

In the case of the direct estimation of K_{cb} from the vegetation index, different functions can be found in literature. Bausch (1995) and Bausch and Neale (1989) performed their studies in the same locations as Trout and DeJonge, and nearby our study. Yet, K_{cb} curves are different (Figure 13). They estimated K_{cb} directly from a linear relationship with a VI, NDVI or SAVI, and not a two-

step approach like Trout and DeJonge (2018); and probably the maize varieties are different. Results are clearly different (Figure 13). However, the curve from Bausch and Neale (1989) using MSR5 (ground scouting) was similar to the curve modeled with Trout and DeJonge (2018). The model for Kcb using NDVI adjusted better than the one using SAVI. The reason for the difference between the models is unclear. However, the scatter between different methods generally has either of 3 causes: different models or approaches, difference in the calibration, hence, a location effect; or measurement issues.

The great advantage of using crop coefficients derived from VI is the independence of the time parameters, such as day of planting and effective cover for each specific field and representing a real time crop coefficient (Bausch and Neale, 1987). This is a great advantage because we did not need any previous information of the field. Our results show that NDVI, hence f_c , was sensitive to maize crop growth, maturation, and senescence, as vastly showed in literature (Bausch and Neale, 1987).

We supposed that the scatter found for the satellite data was related to a sensor issue. Care should be taken since VI measured with different sensors may vary because of the spectral and radiometric resolution, atmospheric corrections, sensor degradation, calibrations, and sensor angle (Calera et al., 2017).

Comparison of the trends for late season Kcb values for the 4-segment curve agreed. Surface reflectance or a 4-segment Kcb curve corrected with surface reflectance data agreed with real Kcb from maize measured with sap flow gauges (Figure 14 and Figure 15). These results highlight the benefits of using Kcb estimation methods simultaneously for accurate maize water use estimation and the advantage of user-friendly estimation methods.

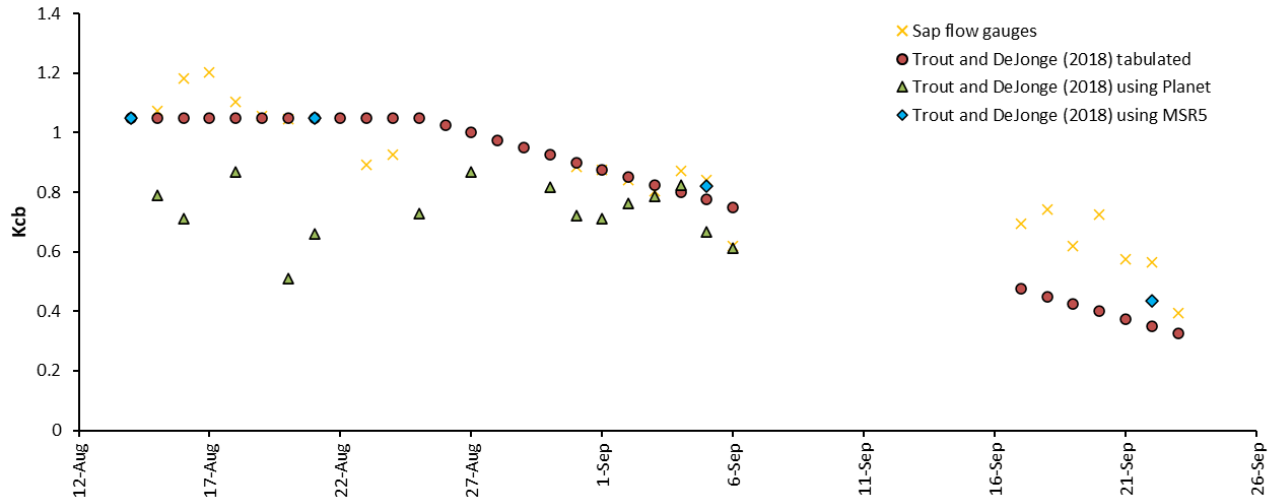


Figure 14. Comparison of basal crop coefficient curves using local crop tabulated coefficients from Trout and DeJonge (2018) with different approaches and with a sap flow derived basal crop coefficient for 2020 season.

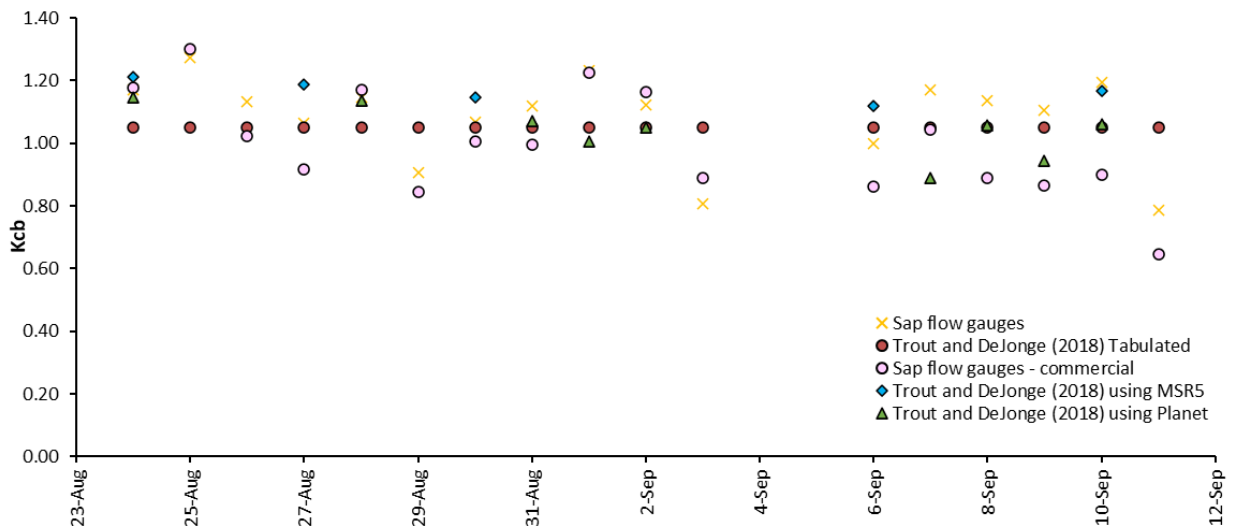


Figure 15. Comparison of basal crop coefficient curves using local crop tabulated coefficients from Trout and DeJonge (2018) with different approaches and with a sap flow derived basal crop coefficient for 2019 season.

The locally derived Kcb values for the initial, mid-season and late-season segments used for Figure 14 and Figure 15, are 0.17, 1.05 and 0.10 respectively (Trout and DeJonge, 2018). Authors developed an updated Kcb curve for maize and stated that the original standard alfalfa-reference

Kcb mid-season value of 0.96 was too low for current maize varieties and practices (table from Jensen et al., 2016). Similar Kcb for these segments were found by Nielsen and Heinke (1996) to work in Akron, Colorado, 0.15, 1.02, for 3 different GDD length maize varieties, based on a GDD timescale Kcb curve; and 0.15, 1.05 and 0.5, for Nebraska, 6 different maize varieties (Hinkle et al., 1984).

Assessment of the basal crop coefficient curves with sap flow sensors and surface reflectance

The mean Kcb values for the mid-season crop growth stage with the datapoints available (Figure 14 and Figure 15) are between the expected values and concurs with Trout and DeJonge (2018). It is reasonable to see ETc values for maize slightly higher or similar to alfalfa ETref because it is taller and aerodynamically rougher (Trout and DeJonge, 2018). However, because of the conservation of mass, there is a maximum upper limit for ET, therefore, Kcr has an upper limit of about 1.1 and Kco of about 1.3 (Allen and Pereira, 2009). For smaller vegetation expanses, these limits should remain unless there is a condition for the “clothesline effect” (vegetation height is higher than of the surrounding) or “oasis effect” (where soil water availability of vegetation is higher than the surrounding), then the crop coefficients could exceed the limits (Allen and Pereira, 2009). The Kcr maximum value of 1.1 is comprised by $K_{cb} + 0.05$; suggesting that wet soil increases the Kcb value by at least 0.05, even if there is a full canopy cover condition (Allen and Pereira, 2009). Crop coefficient reduces when plant density or leaf area is below full ground cover, defined when LAI is less than 3 in some cases (Allen and Pereira, 2009).

Locally derived K_{cb} values from Trout and DeJonge (2018) into a 4-segment FAO-style curve (for maize was verified using our low-cost sap flow sensors for a period of 22 days in 2020 season and for a 17-day period in 2019 season. During 2019 commercially available sap flow sensors were also used. The period was divided into mid-season, beginning of late-season and end late-

season each year. In 2019, the measured period (from 8/24/2019 to 9/11/2019) was during the mid-season period and the mean Kcb derived was 1.08 from the sap flow gauges (sap flow gauges described in chapter two) and 0.99 from the commercial sap flow gauges. For 2020 season, the mid-season Kcb derived from sap flow data (8/16/2020 to 8/24/2020) was 1.06. Locally derived Kcb for mid-season from Trout and DeJonge (2018) was 1.05.

For the beginning of late-season (8/31/2020 to 9/6/2020), both values concurred (0.82) and for the end of late-period (9/17/2020 to 9/23/2020) Kcb was higher than the tabulated value (0.62 vs 0.4). However, this is probably due to the fixed end-of-cycle-date for maize cycle (using GDD), the 4-segment curve was programmed to end at 2500GDD, and this is potentially variable.

We can conclude that sap flow gauges can be used to monitor Kcb throughout the growing season successfully.

Results show that a Kcb curve delineated with low-cost sap flow data can be used to estimate or validate Kcb values for specific locations or agronomic practices. It also highlights the advantage of low-cost sap flow sensors, as they could easily be used as an assessment or as an extra-measurement of plant transpiration in field conditions. The use of more than one method simultaneously ensures the right water needs calculation. The use of low-cost sap flow sensors is especially appropriate for low budget and rapid evaluations.

Surface reflectance can be measured manually with spectral radiometers or data can be downloaded from different satellites platforms. There are pros and cons in every method:

- The advantage of manual plant level data collection is that there is less dependence on atmospheric conditions and corrections, however, the downside is the equipment cost and manipulation. It needs mid-level trained personnel to be present in the field at day and

time, hence, data are not continuous throughout the season; and the areas measured are small.

- The advantage of satellite reflectance are that it covers large areas with no need to be physically present in the field. It allows for a continuous Information available throughout the season with no need for equipment, hence more area can be monitored with one person. However, it depends more on atmospheric conditions and even with corrections, there might be cloud interference. Corrections could be enhanced but with very high skilled technicians. The pixel size could be a constraint.

- The advantages of a 4-segment curve vs reflectance curve are the independence from atmospheric conditions and no interference from irrigation or rain. It can be performed with no special skilled personnel. It mimics a continuous curve through the season and can be used to predict mean K_{cb} values for short periods. However, if not well adjusted in the time scale and the absolute mean values, results can be very different from reality. The best adjustment is using f_c data or LAI, that can be easily obtained with surface reflectance (ground or satellite).

- Sap flow gauges are useful tools for verifying or adjusting K_{cb} curves. The pros are that it does not need any previous information from the field and can be installed any time in grown plants with continuous hourly measurements and no atmospheric conditions interfere with its measurements. It can also be used for any size of field. However, it needs to be installed correctly (location, number of sensors), the field has to be homogeneous because a reduced number of plants represent the entire field. It needs minimally trained personnel for data manipulation. There are low-cost sensors that can be used to estimate K_{cb} curves and that allow real time visualization

of the data. It is a plant-based direct method for estimating transpiration in the field, hence, there is no need of estimating soil evaporation.

Conclusion

We described the origin, advantages, and disadvantages of using the basal crop coefficients in a dual K_c approach. We highlighted the benefits of the use of the K_{cb} in a dual K_c approach in understanding the partitioning of the total ET_c and adjusting management practices to reduce the use of water in non-beneficial ways to enhance efficiency. We described how K_{cb} can be adjusted using new approaches with surface reflectance data and described the advantages of using technologies like sap flow sensors to derive or verify crop coefficients locally.

We were able to verify locally derived K_{cb} values from Trout and DeJonge (2018) for maize using sap flow sensors during 2019 and 2020 seasons. Locally derived K_{cb} for mid-season was 1.05. During 2019 the mean K_{cb} derived from the sap flow gauges (sap flow gauges described in Chapter 2) during a 17-day-period was 1.08 and 0.99 from the commercial sap flow gauges. For 2020 season, the mid-season K_{cb} derived from an 8-day-period sap flow data was 1.06. For the beginning of late-season from a 7-day-period, locally derived and sap flow values concurred (0.82) and for the end of late-period during a 7-day-period, sap flow K_{cb} was higher than the tabulated value (0.62 vs 0.4). We demonstrated the use of sap flow sensors for K_{cb} evaluation, and the use of low-cost sap flow sensors, which is especially beneficial for low budget and rapid evaluations. Sap flow sensors provide a unique value by estimating the actual plant transpiration from the field. We were able to show one of its most significant uses for validation of the site-specific K_{cb} functions.

References

- Abrisqueta, I.; Abrisqueta, J.; Tapia, L.; Munguia, J.; Conejero, W.; Vera, J.; Ruiz-sanchez, M. 2013. Basal crop coefficients for early season peach trees. *Agricultural Water Management*. V. 121: 158-163. <http://dx.doi.org/10.1016/j.agwat.2013.02.001> .
- Ainsworth, E.; Long, S. 2020. 30 years of free-air carbon dioxide enrichment (FACE): what have we learned about future crop productivity and its potential adaptation?. *Global Change Biology*. V.27: 27-49. DOI: 10.1111/gcb.15375.
- Allen, R.; Pereira, L.; Raes, D.; Smith, M. 1998. *Crop Evapotranspiration – guidelines for computing crop water requirements*. FAO Irrigation and Drainage paper No. 56. Rome, Italy. 299p.
- Allen, R. 2000. Using FAO-56 dual crop coefficient method over an irrigated region as part of an evapotranspiration intercomparison study. *Journal of Hydrology*. V. 229: 27-41.
- Allen, R.; Pereira, L.; Smith, M.; Raes, D.; Wright, J. 2005. FAO-56 dual crop coefficient method for estimating evaporation from soil and application extensions. *Journal of Irrigation and Drainage Engineering*. ASCE. V.131(1): 2-13.
- Allen, R.; Tasumi, M.; Trezza, R. 2007. Satellite-based energy balance for mapping evapotranspiration with internalized calibration (METRIC) – Model. *Journal of Irrigation and Drainage Engineering*. V. 133(4): 380-394. DOI: 10.1061/(ASCE)0733-9437(2007)133:4(380).
- Allen, R.; Wright, J.; Pruitt, W.; Pereira, L.; Jensen, M. 2007. Water requirements. In: Hoffman, G.J., Evans, R.G., Jensen, M.E., Martin, D.L., Elliot, R.L. (Eds.), *Design and Operation of Farm Irrigation Systems*, second ed. ASABE, St. Joseph, MI, USA, pp. 208–288.
- Allen, R.; Pereira, L.; Howell, T.; Jensen, M. 2011. Evapotranspiration information reporting: I. Factors governing measurement accuracy. *Agricultural Water Management*. V. 98: 899-920. doi:10.1016/j.agwat.2010.12.015 .
- Allen, R.; Pereira, L.; Howell, T.; Jensen, M. 2011b. Evapotranspiration information reporting: II. Recommended documentation. *Agricultural Water Management*. V. 98: 921-929. doi:10.1016/j.agwat.2010.12.016.
- Allen, R.; Kilic, A.; Robison, C. 2020. Current frameworks for reference ET and crop coefficient calculation. American Society of Agricultural and Biological Engineers. 6th Decennial National Irrigation Symposium, 6-8, December 2021, San Diego, California, 2020-070. DOI: <https://doi.org/10.13031/irrig.2020-070> .
- Al-Kaisi, M.; Brun, L.; Enz, J. 1989. Transpiration and Evapotranspiration from maize as related to leaf area index. *Agricultural and Forest Meteorology*, V.48: 111-116.
- Andales, A.; Straw, D.; Simmons, L.; Bartolo, M. 2014. Determination of Consumptive water use of corn in the Arkansas Valley of Colorado.

- Bausch, W.; Neale, C. 1987. Crop coefficients derived from reflected canopy radiation: a concept. *Transactions of the ASCE*. V. 30(3): 703-709.
- Bausch, W. 1993. Soil Background Effects on Reflectance-Based Crop Coefficients for Corn. *Remote Sensing and Environment*. V.46:213-222.
- Bausch, W. 1995. Remote sensing of crop coefficients for improving the irrigation scheduling of corn. *Agricultural Water Management*. V.27: 55-68.
- Bausch, W.; Neale, C. 1989. Spectral Inputs Improve Corn Crop Coefficients and Irrigation Scheduling. *Transactions of the ASAE*. V.32 (6): 1901-1908.
- Burman, R.; Wright, J.; Nixon, P.; Hill, R. 1981. Irrigation management – Water requirements and water balance. *Proceeding of the American Society of Agricultural Engineers*. Second National Irrigation Symposium. Oct. 1980: 141-153.
- Calera, A.; Campos, I.; Osann, A.; D'Urso, G.; Menenti, M. 2017. Remote sensing for crop water management: from ET modelling to services for the end users. *Sensors*. V. 17: 1104. doi:10.3390/s17051104.
- Campos, I.; Neale, C.; Calera, A.; Balbontin, C.; Gonzalez-Piqueras, J. 2010. Assessing satellite-based basal crop coefficients for irrigated grapes (*vitis vinifera* L.). *Agricultural Water Management*. V.98: 45-54. doi:10.1016/j.agwat.2010.07.011.
- Cancela, J.; Fandino, M.; Martinez, E. 2015. Automated irrigation system based on dual crop coefficient, soil and plant water status for *vitis vinifera* (cv Godello and cv Mencia). *Agricultural Water Management*. V.151: 52-63. <http://dx.doi.org/10.1016/j.agwat.2014.10.020> .
- Costa-Filho, E.; Chavez, J.; Andales, A.; Brown, A. 2022. Updating corn crop coefficients with remote sensing-based actual evapotranspiration algorithms. *World Environmental and Water Resources Congress 2022: Adaptive Planning and Design in an Age of Risk and Uncertainty*. Ed. Pierson, J.; Grubert, E. June 5-8, 2022. American Society of Civil Engineers. 1292 p.
- Cunningham, S.; Pullen, K.; Collof, M. 2009. Whole tree sap flow is substantially diminished by leaf herbivory. *Oecologia*. V.158: 633-640. DOI 10.1007/s00442-008-1170-3 .
- Damour, G.; Simonneau, T.; Cochard, H.; Urban, L. 2010. An overview of models of stomata conductance at leaf level. *Plant, Cell and Environment*. V.33: 1419-1438. doi: 10.1111/j.1365-3040.2010.02181.x .
- Delgado, J.; Groffman, P.; Nearing, M.; Goddard, T.; Reicosky, D.; Rattan, L.; Kitchen, N.; Rice, C.; Towery, D.; Salon, P. 2011. Conservation practices to mitigate and adapt to climate change. *Journal of Soil and Water Conservation*. V. 66(4): 118A-129A. doi:10.2489/jswc.66.4.118A
- Djaman, K.; Irmak, S. 2013. Actual crop evapotranspiration and alfalfa and grass reference crop coefficients of maize under full and limited irrigation and rainfed conditions. *Journal of Irrigation and Drainage Engineering*. V.139(6): 433-446; DOI: 10.1061/(ASCE)IR.1943-4774.0000559.

Doorenbos, J.; Priutt, W. 1977. Guidelines for predicting crop water requirements. FAO Irrigation and Drainage Paper No.24. Food and Agriculture Organization of the United Nations, Rome, 1977. 145pp.

Dragoni, D.; Lakso, A.; Piccioni, R. 2004. Transpiration of an apple orchard in a cool humid climate: measurement and modeling. *Acta Horticulturae*. V.664: 175-180. <https://doi.org/10.17660/ActaHortic.2004.664.19> .

Er-Raki, S.; Chebouni, A.; Guemouria, N.; Ezzahar, J.; Khabba, S.; Boulet, G.; Hanich, L. 2009. Citrus orchard evapotranspiration: Comparison between eddy covariance and the FAO-56 approach estimates. *Plant Biosystems*. V. 143(1): 201-208. DOI: 10.1080/11263500802709897 .

Fandino, M.; Cancela, J.; Rey, B.; Martinez, E.; Rosa, R.; Pereira, L. 2012. Using the dual-Kc approach to model evapotranspiration of Albarino vineyards (*vitis vinifera* L. cv. Albarino) with consideration of active ground cover. *Agricultural Water Management*. V.112:75-87. <http://dx.doi.org/10.1016/j.agwat.2012.06.008> .

Ferrerira, T.; Carr, M. 2002. Responses of potatoes (*Solanum tuberosum* L.) to irrigation and nitrogen in a hot, dry climate. I. water use. *Fields Crop Research*. V78:51-64.

Garcia, L.; Elhaddad, A.; Altenhofen, J.; Hattendorf, M. 2013. Developing corn regional crop coefficients using a satellite-based energy balance model (ReSET-Raster) in the South Platte river basin of Colorado. *Journal of Irrigation and Drainage Engineering*. V.139 (10): 821-832. DOI: 10.1061/(ASCE)IR.1943-4774.0000616.

Glenn, E.; Neale, C.; Hunsaker, D.; Nagler, P. 2011. Vegetation index-based crop coefficients to estimate evapotranspiration by remote sensing in agricultural and natural ecosystems. *Hydrological Processes*. V.25: 4050-4062. DOI: 10.1002/hyp.8392.

Gonzalez-Dugo, M.; Neale, C.; Mateos, L.; Kustas, W.; Prueger, J.; Anderson, M.; Li, F. 2009. A comparison of operational remote sensing-based models for estimating crop evapotranspiration. *Agricultural Forest Meteorology*. V. 149: 1843-1853. doi:10.1016/j.agrformet.2009.06.012.

Goodwin, I ; Cornwall, D ; Green, S. 2012. Pear transpiration and basal crop coefficients estimated by sap flow. *International Society for Horticultural Science. Acta horticulturae*. V.951: 183-190.

Gowda, P.; Chavez, J.; Colaizzi, P.; Evett, S.; Howell, T. Tolk, J. 2008. ET mapping for agricultural water management: present status and challenges. *Irrigation Science*. V. 26: 233-237. DOI 10.1007/s00271-007-0088-6.

Heinkle, S.; Gilley, J.; Watts, D. 1984. Improved crop coefficients for irrigation scheduling. USDA-ARS project report no. 58-9AHZ-9-454. Lincoln: Agricultural Engineering Dept., Univ. of Nebraska.

Hou, L.; Wenninger, J.; Shen, J.; Zhou, Y. 2014. Assessing crop coefficients for Zea mays in the semi-arid Hailiutu river catchment, northwest China. *Agricultural Water Management*. V. 140: 37-47. <http://dx.doi.org/10.1016/j.agwat.2014.03.016>.

Howell, T.; Evett, S.; Tolk, J.; Copeland, K.; Dusek, D.; Colaizzi, P. 2006. Crop coefficients developed at Bushland, Texas for corn, wheat, sorghum, soybean, cotton, and alfalfa. Proceedings of the ASCE-EWRI World Environmental Water Resources Congress 21-25 May 2006, Omaha Nebraska. Ed. Graham, R. DOI: 10.1061/40856(200)260.

Huete, A. 1988. A Soil-adjusted vegetation index (SAVI). Remote Sensing of Environment. V.25: 295-309.

Hunsaker, D.; Pinter Jr., P.; Cai, H. 2002. Alfalfa basal crop coefficients for FAO-56 procedures in the desert regions of the southwestern US. Transactions of the American Society of Agricultural Engineers. V. 45(6): 1799-1815.

Hunsaker, D.; Pinter Jr., P.; Barnes, E.; Kimball, B. 2003. Estimating cotton evapotranspiration crop coefficients with a multispectral vegetation index. Irrigation Science. V.22: 95-104. DOI 10.1007/s00271-003-0074-6.

Hunsaker, D.; Barnes, E.; Clarke, T.; Fitzgerald, G.; Pinter Jr., P. 2005. Cotton irrigation scheduling using remotely sensed and FAO-56 basal crop coefficients. Transactions of the American Society of Agricultural Engineers. V. 48: 1395-1407.

Jensen, M. 1968. Water consumption by agricultural plants. In. Water deficit and plant growth. T. Kozlowski, ed. V2, Academic Press, New York. 1-22.

Jensen, M. 1969. Scheduling irrigations with computers. Journal of Soil and Water Conservation. V.24 (5): 193-195.

Jensen, M.; Wright, J.; Pratt, B. 1971. Estimating soil moisture depletion from climate, crop and soil data. Transactions of the ASCE. V. 14 (5): 954-959.

Jensen, M.; Allen, R. 2016. Evaporation, evapotranspiration and irrigation water requirements. ASCE Manual and Reports on Engineering Practice No.70. Second edition. American Society of Civil Engineering. Virginia, USA. 744p.

Jiang, X.; Kang, S.; Tong, L.; Fusheng, L.; Li, D.; Ding, R.; Qiu, R. 2014. Crop coefficient and evapotranspiration of grain maize modified by planting density in an arid region of Norwest China. Agricultural Water management. V. 142: 135-143. <http://dx.doi.org/10.1016/j.agwat.2014.05.006>

Johnson, L.; Trout, T. 2012. Satellite NDVI Assisted Monitoring of Vegetable Crop Evapotranspiration in California's San Joaquin Valley. Remote Sensing. V.4: 439-455; doi:10.3390/rs4020439.

Jones, H. 2004. Irrigation scheduling: advantages and pitfalls of plant-based methods. Journal of Experimental Botany, Water-Saving Agriculture Special Issue. V. 55(407). 2427–2436. doi:10.1093/jxb/erh213.

Juhasz, A.; Sepsi, P.; Nagy, Z.; Tokei, L.; Hrotko, K. 2013. Water consumption of sweet cherry trees estimated by sap flow measurement. Scientia Horticulturae. V. 164: 41-49. <http://dx.doi.org/10.1016/j.scienta.2013.08.022> .

Kang, S.; Gu, B.; Du, T.; Zhang, J. 2003. Crop coefficient and ratio of transpiration to evapotranspiration of winter wheat and maize in a semi-humid region. *Agricultural Water Management*. V.59: 239-254.

Kington, J.; Collison, A. Scene level normalization and harmonization of Planet Dove imagery. 2022. chrome-extension://efaidnbnmnibpcjpcglclefindmkaj/https://assets.planet.com/docs/scene_level_normalization_of_planet_dove_imagery.pdf.

Kullberg, E.; DeJonge, K.; Chavez, J. 2017. Evaluation of thermal remote sensing indices to estimate crop evapotranspiration coefficients. *Agricultural Water Management*. V.179: 64-73.

Li, Y.; Cui, J.; Zhang, T.; Zhao, H. 2003. Measurement of evapotranspiration of irrigated spring wheat and maize in a semi-arid region of north China. *Agricultural Water Management*. V.61: 1-12.

Lopez-Urrea, R.; Sanchez, J.; de la Cruz, F.; Gonzalez-Piqueras, J.; Chavez, J. 2020. Evapotranspiration and crop coefficients from lysimeter measurements for sprinkler-irrigated canola. *Agricultural Water Management*. V. 239: 106260. <https://doi.org/10.1016/j.agwat.2020.106260> .

Lopez-Urrea, R.; Martin de Santa Olalla, F.; Montoro, A.; Lopez-Fuster, P. 2009. Single and Dual crop coefficients and water requirements for onion (*Allium cepa* L.) under semiarid conditions. *Agricultural Water Management*. V. 96: 1031-1036. doi:10.1016/j.agwat.2009.02.004 .

Lovelli, S.; Pizza, S.; Caponio, T.; Rivelli, A.; Peroniola, M. 2005. Lysimetric determination of muskmelon crop coefficients cultivated under plastic mulches. *Agricultural Water Management*. V.72: 147-159. doi:10.1016/j.agwat.2004.09.009 .

Marcial-Pablo, M.; Ontiveros-Capurata, R.; Jimenez-Jimenez, S.; Ojeda-Bustamante, W. 2021. Maize crop coefficient estimation based on spectral vegetation indices and vegetation cover fraction derived from UAV-based multispectral images. *Agronomy*. V.11: 668. <https://doi.org/10.3390/agronomy11040668> .

Marek, G.; Marek, T.; Evett, S.; Bell, J.; Colaizzi, P.; Brauer, D.; Howell, T. 2020. Comparison of lysimeter-derived crop coefficients for legacy and modern drought-tolerant maize hybrids in the Texas High Plains. *Transactions of the ASABE, American Society of Agricultural and Biological Engineers*. V. 63 (5): 1243-1257. <https://doi.org/10.13031/trans.13924> .

Martinez-Cob, A., Playan, E., Zapata, N., Cavero, J., Medina, E. T., and Puig, M. (2008). "Contribution of evapotranspiration reduction during sprinkler irrigation to application efficiency". *J. Irrig. Drain. Eng.*, 10.1061/(ASCE)0733-9437(2008)134:6(745), 745–756.

Martins, J.; Rodrigues, G.; Paredes, P.; Carlesso, R.; Oliveira, Z.; Knies, A.; Petry, M.; Pereira L. 2013. Dual crop coefficients for maize in southern Brazil: Model testing for sprinkler and drip irrigation and mulched soil. *Biosystems Engineering*. V.115: 291-310. <http://dx.doi.org/10.1016/j.biosystemseng.2013.03.016> .

Miner, G.; Ham, J.; Kluitenberg, G. 2017. A heat-pulse method for measuring sap flow in corn and sunflower using 3Dprinted sensor bodies and low-cost electronics. *Agricultural and Forest Meteorology*. V. 246: 86-97.

Moller, M.; Tanny, J.; Li, Y.; Cohen, S. 2004. Measuring and predicting evapotranspiration in an insect-proof greenhouse. *Agricultural and Forest Meteorology*. V. 127: 35-51. doi:10.1016/j.agrformet.2004.08.002 .

Monteith, J. 1965. Evaporation and environment. *Symposia of the Society for Experimental Biology*. V.19: 205-234.

Monteith, J.; Szeicz, G.; Waggoner, P. 1965. The measurement and control of stomata resistance in the field. *Journal of Applied Ecology*. V2(2): 345-355.

Neale, C.; Geli, H.; Kustas, W.; Alfieri, J.; Gowda, P.; Evett, S.; Prueger, J.; Hipps, L.; Dulaney, W.; Chavez, J.; French, A.; Howell, T. 2012. *Advances in Water Resources*. V. 50: 152-161. <http://dx.doi.org/10.1016/j.advwatres.2012.10.008> .

Paco, T.; Ferreira, M.; Rosa, R.; Paredes, P.; Rodrigues, G.; Conceicao, N.; Pacheco, C.; Pereira, L. 2012. The dual crop coefficient approach using a density factor to simulate the evapotranspiration of a peach orchard: SIMDualKc model versus eddy covariance measurements. *Irrigation Science*. V.30: 115-126. DOI 10.1007/s00271-011-0267-3 .

Paco, T.; Pocas, I.; Cunha, M.; Silvestre, J.; Santos, F.; Paredes, P.; Pereira, L. 2014. Evapotranspiration and crop coefficients for super intensive olive orchard. An application of SIMDualKc and METRIC models using ground and satellite observations. *Journal of Hydrology*. V.519: 2067-2080. <http://dx.doi.org/10.1016/j.jhydrol.2014.09.075> .

Paco, T.; Paredes, P.; Pereira, L.; Silvestre, J.; Santos, F. 2019. Crop coefficients of a super intensive Arbequina olive orchard using the Dual Kc approach and the Kcb computation with the fraction of ground cover and height. *Water*. V. 11: 383. doi:10.3390/w11020383 .

Paredes, P.; Rodrigues, G.; Petry, M.; Severo, P.; Carlesso, R.; Pereira, L. 2018. Evapotranspiration partition and crop coefficients of Tifton 85 bermudagrass as affected by the frequency of cuttings. Application of the FAO-56 dual Kc model. *Water*. V.10: 558. doi:10.3390/w10050558 .

Planet Labs PBC. 2022. Planet imagery product specifications. chrome-extension://efaidnbmnnnibpcajpcgclefindmkaj/https://assets.planet.com/docs/Planet_Combined_Imagery_Product_Specs_letter_screen.pdf.

Penman. Natural evaporation from open water, bare soil and grass. *Proceedings of the Royal Society of London. Series A, Mathematical and Physical Sciences*. V.193(1032):120-145.

Pereira, L.; Perrier, A.; Allen, R.; Alves, I. 1999. Evapotranspiration: Concepts and future trends. *Journal of Irrigation and Drainage Engineering*. V. 125: 45-51.

Pereira, L.; Paredes, P.; Melton, F.; Johnson, L.; Wang, T.; Lopez-Urrea, R.; Cancela, J.; Allen, R. 2020. Prediction of crop coefficients from fraction of ground cover and height. *Background and*

validation using ground and remote sensing data. *Agricultural Water Management*. V. 241: 106197. <https://doi.org/10.1016/j.agwat.2020.106197> .

Pereira, L.; Paredes, P.; Lopez-Urrea, R.; Hunsaker, D.; Mota, M.; Mohammadi Shad, Z. 2021. Standard single and basal crop coefficients for vegetables crops, an update of FAO56 crop water requirements approach. *Agricultural Water Management*. V. 243: 106196. <https://doi.org/10.1016/j.agwat.2020.106196>.

Phogat, V.; Simunek, J.; Skewes, M. Cox, J. McCarthy, M. 2016. Improving the estimation of evaporation by the FAO-56 dual crop coefficient approach under subsurface drip irrigation. *Agricultural Water anagement*. V.178: 189-200.

Poblete-Echeverria, C.; Ortega-Farias, S. 2013. Evaluation of single and dual crop coefficients over a drip-irrigated Merlot vineyard (*Vitis vinifera* L.) using combined measurements of sap flow sensors and an Eddy covariance system. *Australian Journal of Grape and Wine Research*. V. 19: 249-260. doi: 10.1111/ajgw.12019.

Pocas, I.; Calera, A.; Campos, I.; Cunha, M. 2020. Remote sensing for estimation and mapping single and basal crop coefficients: A review on spectral vegetation indices approaches. *Agricultural Water Management*. V. 233: 106081. <https://doi.org/10.1016/j.agwat.2020.106081>.

Puig-Sirera, A.; Rallo, G.; Paredes, P.; Paco, T.; Minicapilli, M.; Provenzano, G.; Pereira, L. 2021. Transpiration and wáter use of an irrigated traditional olive grove with sap flow observations and the FAO-56 dual crop coefficient approach. *Water*. V. 13:2466. doi.org/10.3390/w13182466.

Puppo, L.; Garcia, C.; Bautista, E.; Hunsaker, D.; Beretta, A.; Girona, J. 2019. Seasonal basal crop coefficient pattern of Young non-bearing olive trees grown in drainage lysimeters in a temperate sub-humid climate. *Agricultural Water Management*. V.226: 105732. <https://doi.org/10.1016/j.agwat.2019.105732> .

Rallo, G.; Paco, T.; Paredes, P.; Puig-Sirera, A.; Massai, R.; Provenzano, G.; Pereira, L. 2021. Updated single and dual crop coefficients for tree and vine fruit crops. *Agricultural Water Management*. V. 250: 106645. <https://doi.org/10.1016/j.agwat.2020.106645> .

Rana, G.; Ferrara, R.; Cona, F.; De Lorenzi, F. 2021. Actual transpiration and canopy resistance in a Mediterranean vineyard irrigated with saline water. *Irrigation Science*. V. 39: 469-481. <https://doi.org/10.1007/s00271-021-00723-5> .

Razzaghi, F.; Plauborg, F.; Jacobsen, A.; Jensen, C.; Andersen, M. 2012. Effect of nitrogen and wáter availability of three soil types on yield, radiation use efficiency and evapotranspiration in field grown quinoa. *Agricultural Water Management*. V.109: 20-29. doi:10.1016/j.agwat.2012.02.002 .

Ritchie, J.; Burnett, E. 1971. Dryland evaporative flux in a subhumid climate. II. Plant Influences. *Agronomy Journal*. V63: 56-62.

- Rosa, R.; Paredes, P.; Rodrigues, G.; Alves, I.; Fernando, R.; Pereira, L.; Allen, R. 2012. Implementing the dual crop coefficient approach in interactive software. 1. Background and computational strategy. *Agricultural Water Management*. V.103: 8-24. doi:10.1016/j.agwat.2011.10.013 .
- Senock, R.; Ham, J.; Loughin, T.; Kimball, B.; Hunsaker, D.; Pinter, P.; Wall, G.; Garcia, R.; LaMorte, R. 1996. Sap Flow in wheat under free-air CO₂ enrichment. *Plant, Cell and Environment*. V. 19: 147-158.
- Shrestha, N.; Shukla, S. 2014. Basal crop coefficients for vine and erect crops with plastic mulch in a subtropical region. *Agricultural Water Management*. V. 143: 29-37. <http://dx.doi.org/10.1016/j.agwat.2014.05.011> .
- Sinclair, T. 2019. "Natural Evaporation from Open Water, Bare Soil and Grass" by Harold L. Penman, *Proceedings of the Royal Society of London* (1948) A193:120–146. *Crop Science*. V.59: 2297-2299. doi: 10.2135/cropsci2019.05.0292 .
- Singh, R.; Irmak, A. 2009. Estimation of crop coefficients using satellite remote sensing. *Journal of Irrigation and Drainage Engineering*. V. 135(5): 597-608. DOI: 10.1061/(ASCE)IR.1943-4774.0000052.
- Steduto, P.; Hsiao, T. 1998. Maize canopies under two soil water regimes. II. Seasonal trends of evapotranspiration, carbon dioxide assimilation and canopy conductance, and as related to leaf area index. *Agricultural and Forest Meteorology*. V.89: 185-200.
- Tasumi, M.; Allen, R.G.; Trezza, R. 2006. Calibrating satellite-based vegetation indices to estimate evapotranspiration and crop coefficients. In *Proceedings of the USCID Water Management Conference*, Boise, ID, USA, 25–28 October 2006.
- Trout, T.; Johnson, L.; Gartung, J. 2008. Remote sensing of canopy cover in horticultural crops. *Horticultural Science*. V. 43(2): 333-337.
- Trout, T.; DeJonge, K. 2018. Crop water use and crop coefficients of maize in the Great Plains. *Journal of Irrigation and Drainage Engineering*. V 144(6): 04018009; DOI: 10.1061/(ASCE)IR.1943-4774.0001309.
- Van Bavel, C.; Newman, J.; Hilgeman, R. 1967. Climate and estimated water use by an orange orchard. *Agricultural Meteorology*. V.4: 27-37.
- Wang, T.; Melton, F.; Pocas, I.; Johnson, L.; Thao, T.; Post, K.; Cassel-Sharma, F. 2021. Evaluation of crop coefficient and evapotranspiration data for sugar beets from landsat surface reflectances using micrometeorological measurements and weighing lysimetry. *Agricultural Water Management*. V. 244: 106533. <https://doi.org/10.1016/j.agwat.2020.106533> .
- Wei, Z.; Paredes, P.; Liu, Y.; Chi, W.; Pereira, L. 2015. Modelling transpiration, soil evaporation and yield prediction of soybean in North China Plain. *Agricultural Water Management*. V. 147: 43-53. <http://dx.doi.org/10.1016/j.agwat.2014.05.004> .

Wright, J. 1981. Crop coefficients for estimates of daily crop evapotranspiration. American Society of Agricultural Engineers. The proceedings of the Irrigation Scheduling Conference, Irrigation scheduling for water and energy conservation in the eighties. December, 1981: 16-26.

Wright, J. 1982. New evapotranspiration crop coefficients. Proceedings of the American Society of Civil Engineers. V.108: 57-73.

Zhao, W.; Liu, B.; Zhang, Z. 2010. Water requirements of maize in the middle Heihe river basin, China. Agricultural Water Management. V.97:215-223.

Zhao, N.; Liu, Y.; Cai, J.; Paredes, P.; Rosa, R. Pereira, L. 2013. Dual crop coefficient modelling applied to the winter wheat-summer maize crop sequence in North China Plain: basic crop coefficients and soil evaporation component. Agricultural Water Management. V.117: 93-105. <http://dx.doi.org/10.1016/j.agwat.2012.11.008> .

Zhao, L.; Zhao, W. 2014. Canopy transpiration obtained from leaf transpiration, sap flow and FAO-56 dual crop coefficient method. Hydrological Processes. V.29: 2983-2993. DOI: 10.1002/hyp.10417.

CHAPTER 4

A SIMPLE ARTIFICIAL DRY REFERENCE SURFACE FOR REAL-TIME CANOPY CONDUCTANCE AND TRANSPIRATION ESTIMATION IN MAIZE USING INFRARED SENSORS

Summary

Thermal methods are a useful tool for determination of water use and stress detection in crop fields. They have a potential use for site-specific irrigation scheduling and for improvements in water productivity. The objective of this study was to design an artificial reference surface (ARS) that mimics the temperature from a non-transpiring maize canopy and use it for estimating maize transpiration and canopy conductance continuously and in real-time with low-cost sensors. A simple water stress detection method of using relative temperatures was also analyzed. A hemispherical 3D-printed prototype with a light green color was deployed in a well irrigated and a deficit irrigated maize (*Zea mays* L.) field in northern Colorado, USA. Mean daily transpiration estimates were compared to maize transpiration using the tall reference ASCE equation and a local crop coefficient curve showing a coefficient of determination (R^2) of 0.82, RMSE of 0.61 mm and MAE of 0.53 mm, representing a 12% and a 10% error. Transpiration was also compared to sap flow data showing an RMSE and MAE of 0.78 mm and 0.73 mm, respectively, and showed a strong correlation ($R^2 = 0.7$) for hourly rates. Mean canopy conductance estimates showed an R^2 of 0.57, an RMSE and MAE of 0.72 mm/s and 0.51 mm/s, representing a 11.6% and 8.1% error from the mean canopy conductance values, respectively, when compared to sap flow data. Canopy conductance estimates were able to show the effects of soil water depletion on the crop

water status. The simple approach for stress detection was linearly correlated to conductance ($R^2 = 0.7$) and can adequately detect stress. We proved that the method estimated absolute values of actual transpiration, canopy conductance and detection of water stress continuously. The simple calculations and limited weather data needed make it an attractive technique for estimating crop water requirements.

Introduction

The search for improved irrigation management practices, plant water use monitoring and accurate irrigation decision support tools are prominent topics in irrigation studies. The use of thermal methods can contribute to this area of research. Their application in the determination of transpiration and water deficit of irrigated crops has been demonstrated in many experiments (Allen et al., 2007; Bastiaanssen et al., 1998; Jackson et al., 1981; Idso et al., 1981; Jones, 1999, Jones 2018, Maes et al., 2011; DeJonge et al., 2015). Thermal methods have shown to be useful tools for automating irrigation scheduling (Jones et al., 2009; O'Shaughnessy et al., 2012). They can be used to match water application with actual crop water needs, in time and in quantity and map the variation of the crop water status in site-specific irrigation schedules (Cohen et al., 2005; Berni et al., 2009; Colaizzi et al., 2012; O'Shaughnessy et al., 2020). They are strongly correlated to water use efficiency, crop yield, ET, leaf water potential or stomatal conductance, factors that are not easily visualized or measured. Hence, they provide valuable information for improvement of irrigation management and crop water productivity even if automated management is not chosen (Colaizzi et al., 2012).

Thermal methods can be used for direct determination of transpiration and detection of water deficit through thermal indices or canopy conductance estimations. Measuring the actual canopy conductance and plant transpiration from the field may help to develop or improve modeling and

prediction of crop water requirements (Katerji and Rana, 2006) or can be used directly for irrigations scheduling (Blonquist et al., 2009). For irrigation purposes, the use of thermal methods has advantages compared to other plant-based methods. They allow continuous, long-term monitoring and are less labor-intensive. On the other hand, gas-exchange measurements such as porometry or leaf water potential are not practical since they would need to sample a large number of leaves, need physical contact with the leaves and can interfere with stomatal responses. They are not automatic and are time consuming (Leinonen et al., 2006; Cohen et al., 2005). Thermal data has the potential to replace direct plant or leaf measurements especially at large scales and provide a robust indicator of water status within a field, with the great advantage of rapidly providing a spatial representation of large areas (Leinonen et al., 2006).

However, plant temperature by itself is not an indicator of plant water status (Jones, 2004; Colaizzi et al., 2012) because canopy temperature is a component of the energy balance of the soil-plant-atmosphere, and it is the result of interactions between the crop and micrometeorological conditions and soil water content.

In well-watered crops transpiration rate is at its potential, or very near (Blonquist et al., 2009). The canopy temperature is relatively low due to the cooling effect of transpiration. When the soil available water is limiting, the stomates begin to close and the evaporative cooling effect diminishes. Thus, latent heat flux (ET) is reduced, thermal dissipation decreases, and canopy temperature rises. Eventually, sensible heat becomes a greater component in the energy balance equation of the canopy (Blonquist et al., 2009). Canopy temperature's sensitivity to changes in stomatal conductance can be used for direct estimation of canopy conductance; detection of changes in stomatal conductance can be used as a measure of plant response to water deficit (Jones et al., 2009). However, plant temperature is also affected by environmental factors such as solar radiation, wind speed, air temperature and humidity, which are constantly changing,

besides canopy conductance (Jones, 1999; Jones, 2004, Maes and Steppe, 2012). Therefore, it requires direct or indirect observations of these factors. The leaf temperature does not provide information about plant water status unless it is normalized in relation to references that account for the changes in meteorological conditions (Jones 2009; Costa et al., 2013, Maes and Steppe, 2012). A solution to the observation of weather variables has been to develop estimations that involve the relation between plant and reference temperatures (Leinonen et al., 2006).

Canopy conductance can be derived from the energy balance formulae using actual canopy temperature and weather variables (Jones, 2004; Berni et al., 2009; Blonquist et al., 2009) and there are also several approaches for its determination derived from the full energy balance equation. One approach developed and described by Jones (2004), Leinonen et al. (2006) involves the use of canopy temperature and the temperature from a dry artificial reference surface (ARS) for its estimation. This approach has been used to estimate conductance in cotton (Jones et al., 2018), grapevines (Petrie et al., 2019) and strawberries (Grant et al., 2012), however, there are no studies performed for maize that we were able to detect.

For this purpose, the use of reference surfaces for temperature are valuable since they are well-defined, reproducible and they require less calculations and weather data for their use. The use of a stationary ARS in the field using ground-based infrared thermometers (IRTs) is a practical approach, even when using thermography, because having an ARS available in every image may be impractical (Alchanatis et al., 2010, Maes and Steppe, 2012).

The goal of this work was to develop a simple, low-cost, and user-friendly temperature-based tool for irrigation water management. The objective was to design and test a hemispherical 3-D printed dry ARS for estimation of absolute maize transpiration and canopy conductance, continuously

and in real time. Additionally, the use of the ARS and canopy temperatures for detecting maize stress was also tested.

Background

An alternative to measuring weather variables or empirical approaches: reference surface temperatures

There is a wide variety of approaches to get reference or baseline temperatures representing either a crop transpiring at its highest rate (wet or lower baselines) or representing a non-transpiring crop (dry or upper baselines).

Several studies have used wet reference temperatures (T_{wet}) and dry reference temperatures (T_{dry}) theoretically determined from the energy balance using weather data (Alchanatis et al., 2010; Jones, 1999). The disadvantage is the need of a weather station in the field, since the closer the weather measurements to the field, the more accurate estimation of the reference is made (Alchanatis et al., 2010). Other studies have used an estimation for dry reference surface temperature as ($T_{air} + 5\text{ °C}$) (Cohen et al.; 2005, Alchanatis et al., 2010, Meron et al., 2010). An alternative to measuring weather variables such as net radiation (R_n), vapor pressure deficit (VPD), air temperature and wind speed, is to use reference leaves, that is, surfaces with the same radiative and aerodynamic properties (Jones, 2004). Such references would mimic the leaf in everything except the water vapor conductance. Radiative and aerodynamic properties have to be similar and the reference should be situated in the same conditions (Jones, 1999a). The main requirement is to measure the relative temperature between the reference surface and the leaf of interest, not the absolute temperature.

Several studies have successfully used physical references, dry (Qiu et al., 2003, Maes et al., 2011), wet (Maes et al., 2016) and both (Leinonen et al., 2006; Apolo-Apolo et al., 2020, Pou et al., 2014). A physical reference surface can be a natural leaf from the canopy covered with petroleum jelly for a dry reference (Leinonen et al., 2006, Jones 1999b), or a leaf sprayed with water and detergent as a wet reference surface (Leinonen et al., 2006; Jones 1999b). The disadvantage is that it is labor-intensive, impractical, destructive, and the measurements need to be done a certain time after the application of the fluid, and therefore, not useful for large scale nor automated applications (Maes et al., 2016).

Artificial reference surfaces are an alternative to leaves or plants used as references and can be constructed with different materials, shapes, and sizes. ARS temperatures for dry and wet references have been used in stress detection, implementing them directly as the thresholds in thermal indices (Katimbo et al., 2022; Apolo-Apolo, et al., 2020; Qiu et al., 2003). Studies have used horizontal absorbent paper (Brenner and Jarvis, 1995), green florist styrofoam bricks (Katimbo et al., 2022) or microporous membranes for wet references (Jones 1999b), a cloth floating in water (Alchanatis et al., 2010; Meron et al., 2010) or with leaf-shapes and orientation similar to the leaves for wet references (Maes et al., 2016), black metal or a heated metal for dry reference (Pou et al., 2014, Brenner and Jarvis, 1995, respectively) or an evaporimeter as a wet reference (Pou et al., 2014, Grant et al., 2016); or hemispherical shapes made with colored paper for wet and dry references (Apolo-Apolo et al., 2020) or hemispherical plastic for dry references (Jones et al., 2018).

The use of reference surfaces in the estimation of stomatal conductance eliminates the need for measurement of some meteorological variables, especially those difficult to measure correctly, such as net radiation. The advantage of using wet and dry references together, is that there is no

need to measure humidity. Nevertheless, humidity measurements are easy to acquire with reasonable precision (Leinonen et al., 2006). The advantage of only using the dry reference is that it is much simpler in practice because there is no wet reference to maintain in the correct conditions. Using only a dry reference was recommended by Leinonen et al., (2006) after evaluating the wet and dry reference approach. Additionally, mimicking temperature from a well-watered crop is harder than a non-transpiring one. Artificial wet references (Apolo-Apolo et a., 2020) and even wetting leaves from the same canopy have not shown an exact imitation and need a transformation for its use.

In terms of scale, working with natural, single leaves is not feasible at field scale (Maes and Steppe, 2012). Jones et al. (2018) introduced the use of an artificial hemispherical dry reference surface that has an advantage compared with a living reference surface and it better mimics the radiative properties of crop canopies given the hemispherical shape.

In irrigation studies reference surfaces are often applied as the upper and lower baselines in water stress indices (Maes and Steppe, 2012). However, their use can be extended for the estimation of the canopy conductance and transpiration rates of the crop in the field (Jones et al., 2018).

Crop water needs estimation using a dry reference and canopy temperatures

Estimation of evapotranspiration (ET) or transpiration from the crop is a critical component in an irrigation management plan. Traditionally these can be calculated with well-known approaches like the Penman Monteith (PM) standardized equation (Allen et al., 1998; ASCE, 2005) and crop coefficient curves. Their calculation requires weather data, commonly measured by a proximal standard weather station.

Plant water needs can also be estimated directly using canopy temperature. Water stress indices such as the crop water stress index (CWSI) or others derived from the energy balance can be used for this purpose. Usually, CWSI has been used for crop stress detection, indicating the onset of irrigation requirement by setting thresholds, but it can also be used to estimate how much to irrigate (Taghvaeian et al., 2012). The relationship: $ET = ET_p (1 - CWSI)$ can be used to estimate crop actual transpiration. It determines the transpiration reduction, K_s , as $(1 - CWSI)$ from the actual field, and estimates actual ET (Kullberg, et al., 2017). The simplicity of the estimation of actual transpiration compared to a remote sensed ET estimation positions CWSI as a promising practical way for actual crop transpiration estimation (Taghvaeian et al., 2012).

A different approach is to estimate plant transpiration using temperature from a leaf and a reference surface (Jones, 2004, Jones et al., 2018). Using a dry reference surface mimicking a non-transpiring leaf, and the energy balance formulae from a leaf, we can estimate the evaporation rate. The derivation considers the sensible heat equation (C) for a dry surface and the evaporation rate from the surface of a leaf (E), considers the soil heat flux (G) as zero and introduces the net isothermal radiation of a surface (R_{ni}), which is defined as the net radiation that would be received by an identical surface if it were at air temperature. It follows (Jones, 2004):

Considering a non-transpiring leaf:

$$R_{n\ dry} = C_{dry} = c_p \rho g_{ah} (T_{dry} - T_a) \quad [1]$$

where ρ_a is air density, C_p is specific heat of air, g_{ah} is aerodynamic conductance, $R_{n\ dry}$ is the net radiation of the dry leaf, T_{dry} is the dry reference temperature, and T_a is air temperature.

For an evaporating leaf surface:

$$R_{n\ leaf} = C_{leaf} + \lambda E = c_p \rho g_{ah} (T_{leaf} - T_a) + E \quad [2]$$

where, $R_{n\ leaf}$ is the net radiation from the active leaf and λ is the latent heat of vaporization of water.

Defining net radiation, R_n , as:

$$R_n = R_{ni} - c_p \rho g_r (T_{leaf} - T_{air}) \quad [3]$$

Substituting R_n using the R_{ni} in the equations and introducing the R_{ni} from the non-transpiring leaf for the evaporating surface, it can be rearranged for transpiration rate (J/m^2s) as (Jones. 2004):

$$E = c_p \rho g_{hr} (T_{dry} - T_{leaf}) \quad [4]$$

$$g_{hr} = g_{ah} + g_r \quad [5]$$

where g_{hr} is parallel conductance to heat (Equation 15 in Appendix C) and g_r is radiative transfer (Equation 14 in Appendix C).

It can be appreciated that evaporation rate from a surface is proportional to the temperature difference between the surface and the reference dry surface, that is, a similar surface to a leaf that is dry (Jones, 2004). Therefore, we can estimate transpiration rate using wind speed, air temperature and humidity, the dry reference surface temperature and the leaf temperature. This approach has the advantage of not using net radiation, which is difficult to estimate accurately.

Canopy conductance estimation using a dry reference and canopy temperatures

The theory behind the estimation of the canopy conductance to water vapor (g_w) from canopy temperature has been described by Jones (2014), Leinonen et al. (2006) and Giullioni et al., 2008.

It is derived from the full energy balance equation (Jones, 2014; Jones et al., 2018):

$$g_w = \frac{\gamma \left[\left(\frac{R_{ni}}{\rho C_p} \right) - g_{hr} (T_{canopy} - T_{air}) \right]}{\Delta (T_{canopy} - T_{air}) + VPD} \quad [6]$$

where T_{canopy} is temperature from the infrared sensors pointing at the maize canopy and T_{air} is air temperature in Kelvin, VPD is the vapor pressure deficit in Pa, Δ is rate of change of saturation vapor pressure with temperature, and γ is the psychrometric constant (Pa/K).

As cited by Jones (2004) this equation is difficult to implement because it needs accurate values for boundary layer conductance, R_{ni} , VPD and temperatures.

A simpler approach is to use a dry reference, with similar aerodynamic and optical properties to the crop, defined as a non-transpiring plant, hence (Leinonen et al., 2006):

$$T_{dry} - T_{air} = \frac{R_{ni}}{g_{hr} C_p \rho} \quad [7]$$

where T_{Dry} is the temperature from the dry reference dome.

Then, replacing R_{ni} , canopy conductance can be rearranged to (Jones et al., 2018):

$$g_w = \frac{g_{hr} \gamma (T_{dry} - T_{canopy})}{\Delta (T_{canopy} - T_{air}) + VPD} \quad [8]$$

Use of dry ARS in simple approaches for stress detection

The use of ARS has a potential capability of standardizing approaches using thermography methods (Grant et al., 2006; Grant et al., 2016). It can be used as the upper limit temperature in stress indices, such as the popular crop water stress index (CWSI). CWSIs can be used for water stress detection and to estimate actual ET_c , being a powerful tool for water use monitoring, however, Katimbo et al. (2022) show that CWSI is very sensitive to the baselines.

Water stress to the plant can be used strategically or as a consequence of water shortages (Comas et al., 2019). Water stress indices can be used as a tool for stress detection to avoid or to control the impacts on yield through irrigation management. It can be used with the purpose of water savings or monitoring the performance of the crop irrigation over the season. However, the use of water stress indices can be cumbersome for farmers to use given the number of factors to take into account for its derivation (Singh et al., 2021). Hence it is of interest to simplify calculations as much as possible yet inform the presence of water stress in the field.

One of the first parameterizations, and the simplest, is to use the difference between canopy and air temperatures, called the stress degree day, but it has constraints because it does not account for changes in VPD, wind speed or solar radiation (Costa et al., 2013). Singh et al (2021) discussed the use of the $(T_c - T_a)$ as an indicator of stress for future studies given the simplicity of its determination in relation to the empirical CWSI for practical purposes for farmers. This is because, while CWSI is more informative for irrigation timing as it takes into account micrometeorological variables, the applicability is restricted to the complexity of the stress and non-stress baselines and calculations (Singh et al., 2021). However, plant temperature for short periods of time can be greatly impacted by the variation in weather conditions, in addition to changes in stomata closure (Grant et al., 2016). Maes et al. (2011) found that the difference (T_{leaf}

– T_a) was very sensitive to the incoming short-wave radiation, its use is limited to meteorological conditions that are not stable. Data from Grant et al (2016) show that $(T_{\text{canopy}} - T_{\text{air}})$ is not a good indicator of plant water status because T_{canopy} is affected by other weather variables and not only air temperature. This is the reason why more complex approaches have been developed.

Other stress indices only use an upper baseline for temperature. Two simple approaches are the one called “ h_{at} ” developed by Qiu et al., (2003), that uses temperature from the dry reference, canopy and air; or the one used by Poirier-Pocovi and Bailey (2020) and Poirier-Pocovi et al (2020), using only canopy and dry reference temperatures. They are appealing methods to detect irrigation needs given their simplicity. Nevertheless, a much simpler approach of just comparing the canopy temperature against a dry reference can also be used to detect stress. The difference between a dry ARS and canopy temperatures has been found to be less sensitive to incoming shortwave radiation and low stomatal conductance, therefore, it could be used as a stress indicator (Grant et al., 2006; Maes et al., 2011). They found that it is almost linearly and strongly correlated with stomatal conductance.

Materials and Methods

The study was conducted during summer 2020 at the Irrigation Innovation Consortium Headquarters (IIC), Research Farm, Colorado, USA (40°33'26"N, 106°59'43"W, 1426 m). The study site consists of two large plots: one that was fully irrigated (6.6 ha) and another that was deficit irrigated (8.3 ha). The two fields were contiguous and irrigated by siphon tubes and graded furrows. Irrigation amount and timing were estimated using the Water Irrigation Scheduler for Efficient application (WISE; Andales et al., 2014, 2020) that estimates daily crop ET and net irrigation requirement (soil water deficit). The well irrigated corn field was maintained in a fully irrigated condition, satisfying 100% of the ET demands for the period with each irrigation. The

deficit field was irrigated during sensitive growth phases of corn to guarantee an adequate plant stand and pollination for ear development. The irrigations consisted of one irrigation in the vegetative period and irrigations on the mid-season period, starting around VT until R4.

Planting was on May 13, 2020, with a plant population of 80,000 plants ha⁻¹ and 76 cm of row spacing, using the G02K39-3120 maize variety from Syngenta. Management practices, herbicide applications and fertilization ensured a good stand of maize and prevented weed competition and nutrient deficiencies.

Weather, plant transpiration and soil monitoring

An automatic weather station was installed next to the maize plots over a grass pasture. Maize water use was estimated using the ASCE standardized tall reference Penman Monteith equation (ASCE, 2005) and a local crop coefficient curve (Trout and DeJonge, 2018).

Maize transpiration was measured using 8 sap flow gauges deployed in each field from August to September 2020. Plant transpiration was estimated using a heat pulse technique upscaled with plant population to calculate actual maize transpiration from the field. Data used were one-hour averages of 15-minute readings. The sensors allow plant transpiration estimation with precision of ± 1.04 mm SD and a MAE of 0.48mm.

Soil moisture was monitored using 4 soil moisture sensors in each field, installed at 20 and 50 cm depth in the corn row. Capacitance sensors were used for continuous monitoring (TEROS12, METEK, Pullman, USA), using a CR1000 datalogger (Campbell Scientific, Inc.; Logan, USA).

Temperature sensing

Plant canopy and reference surface temperatures were measured using IRTs with a field of view of 10 degrees (Melexis 90614-ESF-BCF, Melexis, Ypres, Belgium). The same type of IRT was used in studies by Jones et al. (2018) and the performance was assessed by O'Shaughnessy et al. (2011) with satisfactory results. Sensors had a resolution of 0.02 °C and an accuracy of 0.5 °C, from 0 to 50 °C. The same type of IRTs were used to measure canopy temperature in the field and inside the dry ARS.

There are important considerations when working with thermal methods using ground infrared sensors, such as the field of view and the orientation (Jones et al., 2018). Each plot had 4 IRTs installed at 45 degrees from a vertical reference and 2 m above canopy height, in sets of two, facing north-east and north-west, the same field of view of the sun, to measure sunlit canopy. For optimizing the sensitivity of the IRT for water stress detection the view angle should be close to the solar direction and without shading of the leaves (Jones et al., 1997). The canopy was already at full effective cover when our experiment started. Hence, influences of soil temperature in the measurements should be minimal.

Melexis sensors were calibrated against a Fluke 4180, Precision Infrared Calibrator (Fluke Corporation, Everett, USA) using 6 temperatures (5, 15, 25, 35, 45 and 55 °C) and 3 emissivities (0.93, 0.95, 0.97) and a calibration curve was generated for each sensor. Field sensors were also calibrated for surface emissivity and background temperature.

Calculations for the corrections are shown in Appendix C. Fractional ground cover (f_c) was estimated using NDVI from ground scouting of surface reflectance using the MSR5 multispectral

radiometer (Cropscan Inc.; Rochester, USA) and the relation developed by Johnson and Trout (2012). Ground cover for the days between measures were modeled with linear interpolation.

Dry reference surface temperature was compared with temperature from non-transpiring leaves. For this comparison, four corn leaves were covered with Vaseline. Two leaf temperatures were measured using thermocouples. The thermocouples were built using a T type, 36-gauge thermocouple wire, WNJR082447, TT-T-36, insulated wire (OMEGA Engineering, Inc.), a thermocouple amplifier Breakout (MAX31856, Adafruit®) and connected to a CR1000 Campbell Scientific datalogger. Thermocouples wires were attached to the abaxial side of the second leaf, in the middle with electrical tape (white color, 1 cm x 5 cm). Data used were 15-minute averages of five-minute readings.

Dry artificial reference surface

Artificial reference surfaces (ARS) are an alternative to the use of actual plants or leaves as references. The characteristics of the surface, the position in the canopy and orientation have a great impact on the resulting temperature of the surface (Jones, 2004).

Three main characteristics should be considered in the design of an ARS: the thermal mass, spectral properties, and orientation.

- 1) The same time constants and thermal mass. The heat capacity of the reference surface needs to be similar to the leaves of interest. If this is the case, the temperature changes in response to environmental changes would be similar. This would vary according to leaf thickness, size, conductance and wind speed. The larger mass redounds in a large thermal inertia or thermal time constant, and temperature responds slower to changes in

the environment. Therefore, it might not represent the energy balance of a leaf. Jones (2004).

- 2) The same spectral properties. Given that temperature relies on the energy balance, the short-wave absorptance and long-wave emissivity have to be similar between both, the reference surface and crop leaves.
- 3) The same orientation. The radiant load of a surface has great impact on its temperature. Leaf temperature is a function of absorbed radiation and linearly increases with irradiance (Jones et al., 2009). Therefore, the sun angle and the view angle of the leaves of interest (leaf orientation) and the exposed surface of the reference surface are subject to attention. The distribution of the illumination over the reference surface would also have to mimic the targeted leaves for the same radiant load (Jones et al., 2018).

We developed an artificial hemispherical surface (Figure 16) with a shape similar to a light bulb that was 3D-printed in a thin white plastic similarly to Jones et al. (2018). Considering that the shape proposed in this study would better imitate the radiant exposure of a maize canopy. The prototype was printed using white PETG (glycolized polyester). It was printed using a Lulzbot TAZ6 (Lulzbot, Loveland, USA) with a 25% infill, 0.28mm filament. An IRT was situated inside, facing upward, in the base of the 7.5 cm void plastic bulb.

The ARS was installed in the field from August 24, 2020, until a snowstorm event on September 8. Three replicas were installed inside the well irrigated corn field at 2.3 m height, mounted at 25cm above canopy height, avoiding shading of the leaves and inflorescences, but close to the canopy to maintain similar aerodynamic properties. It was located inside the maize field. The ARS measurement should be simultaneous with the plant temperature measurements and located

within the same field for instantaneous local conditions for the surface to be identical to the canopy (Alchanatis et al., 2010). Crop temperature, plant transpiration and soil moisture were measured at the same location.

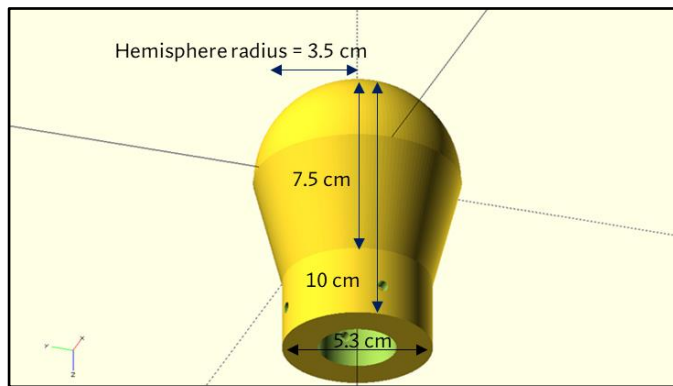


Figure 16. Dry artificial reference surface prototype

The data acquisition from the canopy and dry ARS IRTs used an LTE Boron microprocessor board (Boron LTE, Particle Industries Inc., San Francisco, USA) microcontroller with cellular connectivity. Ubidots (Ubidots, Medellin, Colombia) was used as an Internet of Things provider, a cloud platform for real-time data visualization and storage.

The system was backed up with a 12 V battery (Duracell, Sealed Lead Acid battery of 7 Amp or a Duracell Ultra, sealed lead acid battery 35 Amp) and a 10 W solar panel and a lipo battery (Lithium ion polymer battery of 3.7 V-DC and 1,800 mAh.) for the microprocessor board.

Data collected from the IRTs every 5 minutes was sent via cellular connectivity to the Particle cloud and then the data was sent to the IoT provider, Ubidots. Data was stored in the Ubidots cloud and was also available for real time visualization from any device and from any place in the world. One-hour averages were used for calculations.

Preliminary tests for different colors of paint for the dry ARS were conducted to find the adequate color, which temperature represented a dry maize canopy. Temperatures from the ARS with eight different brush-painted colors were compared to the mean temperature of non-transpiring leaves obtained by covering them with petroleum jelly (See Figure C4 in Appendix C for an example of the temperature variation of the dry ARS with three different colors). This approach was used by Jones et al (2018) and also used in studies as dry references themselves, by using its temperature straightforward (Leinonen et al., 2006, Jones 1999b). However, using plant leaves as references has the drawback of not being suited for large scale and automated applications. On the other hand, the use of an ARS represents a more logical approach than using an arbitrary temperature, such as (air temperature + 5°C) commonly used as a dry reference (Cohen et al.; 2005, Alchanatis et al., 2010, Meron et al., 2010).

Calculations

Canopy transpiration was calculated using the tall reference ASCE PM approach (ASCE, 2005) and the basal crop coefficient for maize. A basal crop coefficient curve was estimated using Trout and DeJonge (2018) local values and the maize transpiration was calculated. Results were compared with the estimated transpiration using equation 4. Transpiration measured from the dry ARS is referred to as T_{dry} .

Plant transpiration was monitored using sap flow gauges simultaneously in the well irrigated and deficit fields. Transpiration for the deficit treatment was normalized for calculation and the relative transpiration was calculated as the ratio of transpiration from the well irrigated and the deficit field, measured with sap flow gauges.

Soil moisture was also monitored. The 50 cm depth soil water content was used as an indicator of soil moisture deficit in the deficit treatment. The water availability in the soil was calculated as the fraction of transpirable soil water or relative extractable water (Verhoef and Egea, 2014; She et al., 2013).

Extractable soil water was estimated as the fraction of transpirable soil water (FTSW) remaining in the soil at 50 cm soil depth, as:

$$Extractable\ soil\ water \begin{cases} \left[\frac{\theta - \theta_{WP}}{\theta_{FC} - \theta_{WP}} \right] & \begin{matrix} \theta \geq \theta_{FC} \\ \theta_{WP} < \theta < \theta_{FC} \\ \theta \leq \theta_{WP} \end{matrix} \end{cases} \quad [9]$$

where θ is volumetric soil water content, θ_{WP} is volumetric soil water content at wilting point and θ_{FC} is volumetric soil water content at field capacity.

A simple approach for water stress detection was tested using the difference (dry ARS temperature – Canopy temperature) (Grant et al., 2006; Maes et al., 2011).

Results were evaluated using a time frame from 9 AM to 5 PM.

Results and Discussion

Results from this study show the evaluation of the performance of a dry ARS developed for the imitation of the temperature of a non-transpiring maize leaf and the potential uses for the estimation of actual maize transpiration and canopy conductance using Jones et al., (2018) and

Leinonen et al. (2006) approaches. A simple approach for water stress detection was also tested using the approach from Grant et al. (2006) and Maes et al. (2011), linearly related to canopy conductance.

Reference surface development

Colors tested in the preliminary tests for the dry ARS were a set of green colors: airy green, sap green, frog, green neon, Anime, lime tree, reviving green (MQ3-47, M350-3M, M350-6D, P340-6O, P340-5D, P340-4TMED, P340-3M) from Behr (Behr, Santa Ana, USA; <https://www.behr.com/>). The colors that best represented a non-transpiring leaf were reviving green and airy green (figure 17, A), a light green color named 'airy green' was chosen. Comparison of the temperatures showed similar values and pattern for the entire day (Figure 17, A). A student paired t test showed that the temperatures for the 4 leaves and the ARS were not different, and the regression line showed a coefficient of determination close to 1 (Figure 17, B). Preliminary tests also examined a 90-degree field of view Melexis IRT. However, it was observed that temperatures were higher when the wider field of view sensor was used, therefore, the 10-degree FOV IRT mounted in the reference surface was a better option.

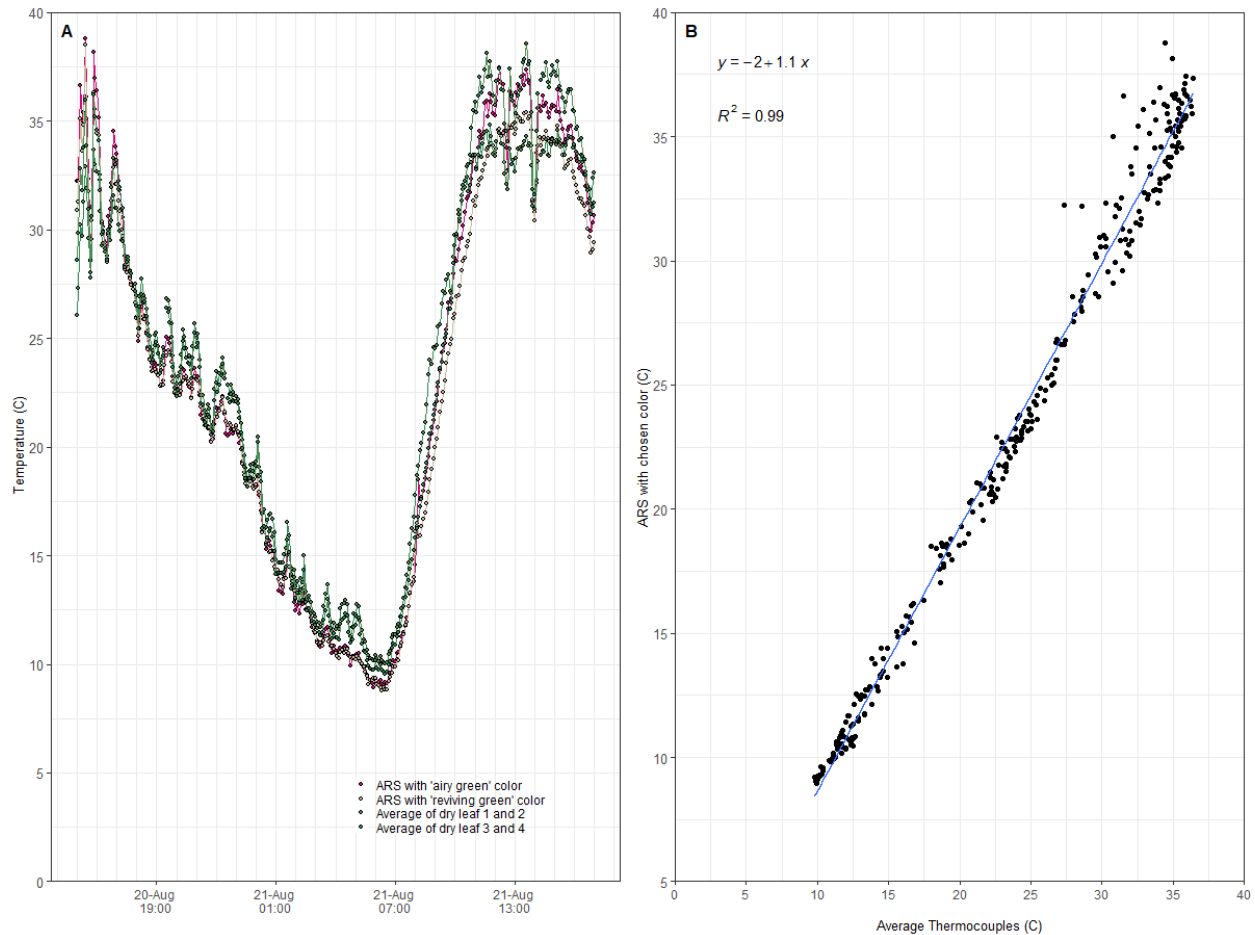


Figure 17. A. Temperature of dry artificial reference surfaces painted with two different colors compared to 4 non-transpiring leaves. B. Regression with the average temperature from four leaves and the temperature from the ARS painted with the “airy green” color.

It was assumed that second leaves from maize plants covered with petroleum jelly represented the canopy temperature from non-transpiring plants. Previous studies carried out by Jones et al. (2018) demonstrated that a plastic hemispherical dome was able to represent the thermal variability of a non-transpiring canopy during the day if an appropriate color was used. Our preliminary data of the dry ARS temperature showed that the designed geometry of the prototype used was able to match the diurnal thermal behavior of a non-transpiring maize leaf. This indicated that thermal mass, spectral properties, and orientation of the dome can represent the maize canopy.

Transpiration estimation using dry ARS temperature

Most of the studies using reference temperatures were focused on the calculation of thermal indices for water stress detection (Apolo-apolo et al.; 2020, Poirier-Pocovi et al, 2020, Pou et al., 2014; Katimbo et al., 2022). However, a dry ARS temperature has alternative uses such as the determination of absolute values for transpiration or estimation of the actual canopy conductance.

Hourly transpiration was calculated using sap flow sensors and the widely accepted Penman-Monteith (P-M) approach with the basal crop coefficient curve, for transpiration estimation. For the latter calculation, we used the tall reference ASCE Penman-Monteith standardized equation (ASCE, 2005) and basal crop coefficient values estimated from Trout and DeJonge (2018), who developed a local function with historical local data for maize. The method will be referred as “Maize ASCE-PM” in this study. The sap flow data were the upscaled mean values from 8 sensors deployed in the field. We compared the transpiration values from these two methods against the transpiration estimated with the dry reference approach (equation 4), referred as “Dry reference transpiration or TDry”. Calculations were performed for hourly (Figure 19) and daily timesteps (Table 1).

Hourly values of TDry were a subset of daytime values, when $R_s > 0$, the timeframe useful for transpiration calculations. This was from 6AM to 7PM, however, the method showed negative values systematically at the beginning and end of the day. Negative values were associated with the sun angle above the horizon (beta, factor estimation from ASCE (2005)) below 0.21 radians, this is because the distribution of irradiance over a surface depends on solar elevation, thus related to the shape of the ARS. The timeframe was then changed to 9AM - 5PM (Figure 19). The few negative values left with this subset (from 3PM to 5PM on 8/31, 9AM on 8/29, 4PM and 5PMhs on 8/28 and 3PMhs on 8/26) were due to low relative cloudiness and they were set to zero.

Relative cloudiness refers to the ratio between locally measured solar radiation (R_s) and calculated clear sky radiation (R_{so}). The ratio stays between 1 and 0.3 according to the ASCE manual (ASCE, 2005), for clear sky to cloudy or dusk conditions, respectively. It was observed that TDry data showed spikes for some days during August. Weather parameters were studied to understand possible causes and it was found that the relative cloudiness (R_s/R_{so}) had great influence on these values (Figure 18). This affected both, transpiration determination and canopy conductance estimation, suggesting that this approach may have constraints in locations of the world where cloudiness is often present during the crop season. This constraint also exists for thermal indices, (Grant et al., 2009; Taghvaeian et al. 2012; Jackson 1981). Clear sky conditions have been found to be a condition for adequate estimation of thermal methods because clouds have a significant effect on crop temperature. Taghvaeian et al. (2012), used the ratio between relative shortwave radiation and clear sky solar radiation (R_s/R_{so}) larger than 0.70, as an assumption for cloud-free conditions, considering it a threshold for their calculations. This is a limitation of thermal methods in humid climates. However, if relative cloudiness is monitored, precautions can be taken when interpreting values under these conditions.

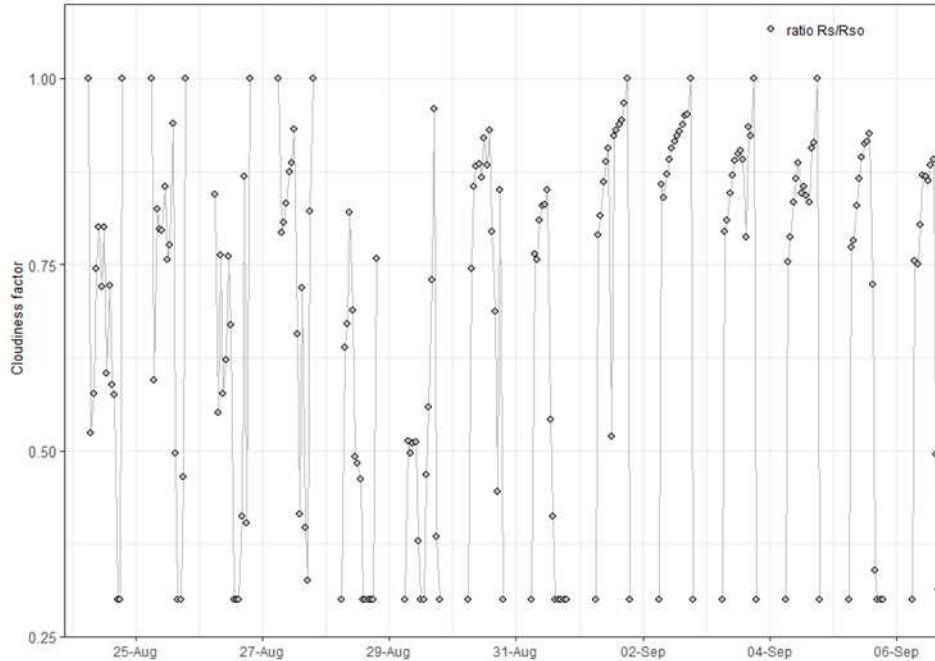


Figure 18. Relative cloudiness for the study period.

Hourly transpiration using TDry method agreed with the diurnal transpiration from maize (Figure 19A). However, there was systematic underestimation at the beginning and the end of each day. Nonetheless, hourly TDry data and the maize transpiration measured with sap flow gauges were strongly correlated, showing a coefficient of determination (R^2) of 0.70, $p < 0.005$. Comparisons with maize ASCE P-M transpiration also showed a strong relationship, $R^2 = 0.83$, $p < 0.005$. Transpiration rates for TDry ranged from 0 to 1.27 mm/h and for the maize ASCE P-M values ranged from 0.17 mm/h to 1.04 mm/h, for the 14-day period. Sap flow transpiration rates for the 6-day period during September, ranged from 0.09 mm/h to 0.7 mm/h. During the 6-day period the TDry transpiration ranges were higher (0 to 1.13 mm/h) than values from sap flow and maize ASCE P-M (0.2 mm/h to 0.93 mm/h).

Daily transpiration was also calculated as the sum of the transpiration from 9AM to 5PM (Table 4). Estimation of Maize ASCE P-M transpiration using this timeframe accounts for 90% of the

diurnal T on average, therefore, values are a good representation of the daily maize transpiration. Total transpiration for the 14-day period estimated with TDry and maize ASCE P-M methods were highly correlated, with an R^2 of 0.87. Root mean squared error (RMSE) and mean absolute error (MAE) were 0.95 mm and 0.74 mm respectively, representing a 20% and a 16% error from the actual value, respectively. However, when errors and weather variables were analyzed, it was found that there is a tendency to find larger errors with low atmospheric demand and median relative cloudiness below 0.55. When values for mostly cloudy days, 8/28, 8/29 and 8/31, were removed, the methods better correlate attributed to the impact of radiation conditions to temperature. The R^2 was then 0.82, RMSE was 0.61 mm and MAE of 0.53 mm, representing a 12% and a 10% error of the method in relation to the actual maize transpiration. Without the 3 cloudy days, the total transpiration for the 11-day-period was 51 mm from the TDry method and 56mm with the ASCE P-M maize transpiration estimation, showing an underestimation of 9%. The mean daily transpiration was 5.1 mm. If the complete period is included the difference increases to 10 mm, meaning a 15% underestimation for the 14-day-period (56 mm vs 66 mm). The TDry method tends to underestimate daily maize transpiration.

When results were compared to the sap flow, the RMSE was 0.78 mm and the MAE was 0.73 mm which represented a 17% and a 16% error, respectively. Measurements were from 1st to 6th of September with a daily mean transpiration of 4.5 mm. The R^2 was low (0.2) due to the few datapoints available from the sap flow gauges for the comparison and the small range of values for that period (maximum and minimum transpiration was 4.8 mm and 4.3 mm respectively). However, a paired student test revealed that data from sap flow and TDry are not different. The total transpiration for the 6-day period calculated with TDry was 25 mm and the measured with sap flow was 26.9 mm. There was an underestimation of 2 mm from the Tdry respect to sap flow estimates, representing an underestimation of 7.3%.

It was also noted that the largest transpiration underestimations from the dry reference method (of 1.5 mm and 2.3 mm per day) were found when relative cloudiness was below 0.55, the solar radiation was low and the VPD was very small, at values of 0.8 KPa and 1.3 KPa, for 8/29 and 8/31. It was observed that for these two days the dry reference temperature and the canopy temperature from the well irrigated maize were very similar and much lower than the rest of the days, with a mean value of 21.7°C. The TDry method showed sensitivity to the ARS temperature.

| Date | Dry reference transpiration | Sap Flow transpiration (mm) | Maize transpiration ASCE-PM (mm) | Transpiration difference (mm) | Daytime Maize transpiration ASCE-PM (mm) | Wind speed (m/s) | VPD (Kpa) | Solar radiation (W/m ²) | Relative cloudiness |
|------------|-----------------------------|-----------------------------|----------------------------------|-------------------------------|--|------------------|-----------|-------------------------------------|---------------------|
| 08/24/2020 | 5.29 | | 5.10 | -0.19 | 5.82 | 1.46 | 3.88 | 539.76 | 0.72 |
| 08/25/2020 | 5.96 | | 6.34 | 0.37 | 7.16 | 2.22 | 3.66 | 564.97 | 0.78 |
| 08/26/2020 | 3.92 | | 4.34 | 0.42 | 4.92 | 2.33 | 2.54 | 311.34 | 0.58 |
| 08/27/2020 | 4.72 | | 4.92 | 0.20 | 5.61 | 1.64 | 3.35 | 508.67 | 0.72 |
| 08/28/2020 | 3.00 | | 3.88 | 0.88 | 4.91 | 3.29 | 2.06 | 403.19 | 0.46 |
| 08/29/2020 | 1.08 | | 2.60 | 1.53 | 2.94 | 1.51 | 0.83 | 329.78 | 0.51 |
| 08/30/2020 | 6.17 | | 7.09 | 0.93 | 8.00 | 4.44 | 3.79 | 622.69 | 0.88 |
| 08/31/2020 | 1.00 | 3.10 | 3.33 | 2.33 | 3.96 | 2.89 | 1.34 | 437.17 | 0.54 |
| 09/01/2020 | 3.40 | 4.31 | 4.42 | 1.02 | 4.91 | 2.20 | 1.98 | 618.32 | 0.92 |
| 09/02/2020 | 3.96 | 4.59 | 4.84 | 0.88 | 5.28 | 2.26 | 2.83 | 650.88 | 0.92 |
| 09/03/2020 | 3.82 | 4.32 | 4.67 | 0.85 | 5.25 | 3.30 | 2.10 | 599.78 | 0.89 |
| 09/04/2020 | 4.09 | 4.79 | 4.58 | 0.50 | 4.93 | 2.10 | 3.66 | 594.75 | 0.85 |
| 09/05/2020 | 3.88 | 4.33 | 4.17 | 0.29 | 4.54 | 2.06 | 3.59 | 589.98 | 0.86 |
| 09/06/2020 | 5.80 | 4.59 | 5.63 | -0.17 | 6.14 | 3.86 | 4.96 | 595.47 | 0.86 |

Table 4. Daily transpiration estimation using the dry reference, maize ASCE P-M and sap flow approaches and median values for wind speed, vapor pressure deficit (VPD) and solar radiation.

Daily maize transpiration can be adequately estimated with the dry ARS temperature using the TDry method (Equation 4). The method works well with near clear sky conditions and when the same weather requirements for any thermal stress index method are satisfied. No scaling factor was used with our data to adjust values to the maize ASCE P-M transpiration. Jones et al. (2018) used an arbitrary scaling factor of 0.5 to fit estimates of ET to reference ET (Equation 25 in Appendix C) because they found an over-estimation of the method attributed to the higher solar absorptance of the reference to that of the canopy. In our study, using a different shape of the ARS and a lighter color, the tendency was to underestimate transpiration.

Transpiration from the deficit field was also estimated and it was observed that values were greatly underestimated when the maize showed water stress, during September (Figure 21B). This was due to the similarity of temperatures between the stressed canopy and the Dry ARS (Figure C2 in Appendix C). This could mean that the assumption that the second leaf from the maize plant representing the temperature of the canopy was not adequate. The temperatures were similar, yet the deficit maize was still transpiring, therefore, higher temperatures than the measured with the ARS were found in a non-transpiring canopy. Similarly, Berni et al. (2009) found differences when they compared stomatal conductance from plant measurements with canopy estimations, assuming that limited number of measured leaves represented the average population. This underlines findings by Jones et al. (2018), that transpiration and canopy conductance estimates using these approaches are very sensitive to the dry ARS temperature and good estimates of temperature are needed.

On the other hand, the similarity of the temperature dynamic during the day (Figure C2 in Appendix C) shows that the shape of the ARS allowed a proper radiant load that imitated that of the canopy. It was observed that when the maize canopy was not stressed (August), the TDry closely represented the hourly values from the field when compared to the sap flow measurements. However, the negative values early and late in the day and the larger differences at 9AM and 5PM, suggests that testing a flatter shape of the sides of the ARS could be a future study.

This simple thermal method approach to estimate maize actual transpiration could be used as an alternative to the use of atmometers for the estimation of reference ET (Gleason et al., 2013, Irmak et al., 2010) and crop coefficients, when local weather data is limited. Local weather variables needed for transpiration calculation using the dry ARS approach are wind speed, VPD (humidity), air temperature and dry ARS and leaf temperature. These variables are easy to

measure locally, the sensors required are not expensive nor difficult to acquire and the calculations are simple and suitable for real time and continuous data acquisition systems.

Canopy conductance estimation using dry ARS temperature

Well Irrigated field

Simultaneous temperature data collected from the well irrigated maize field and the dry ARS temperature were used to calculate canopy conductance using equation 8 (Figure 19A). Results were compared against the conductance derived from sap flow transpiration. Canopy conductance estimations were performed from 9AM to 5PM given the findings for the performance of the dry ARS described previously.

Conductance pattern during the day for the two methods is shown in figure 19A. In the same way as for transpiration, canopy conductance with the dry reference temperature underestimated values at the beginning and at the end of the day. It was also seen that conductance derived from the sap flow data showed a peak at the beginning of the day, which is not revealed with the dry ARS method. Overall, the daily patterns are similar specially around noon, from 11AM to 3PM.

Canopy conductance estimated from a dry ARS temperature was also tested in studies by Petrie et al (2019) and Grant et al. (2012) where canopy conductance for different species and environments agreed with the measured in the field. Their work highlights the benefits of using a dry reference temperature, in the rapid screening of the crop's conductances, elimination of the need for high absolute accuracy of plant temperature and the need of solar radiation measurements. However, weather variables affect the estimates of conductance. The sensitivity of stomatal conductance estimation increases with temperature, vapor pressure deficit, radiation,

and lower wind speed (Jones, 1999b). The straightforward use and simple maintenance of a dry ARS are advantages and enables easier maintenance of good quality data through time.

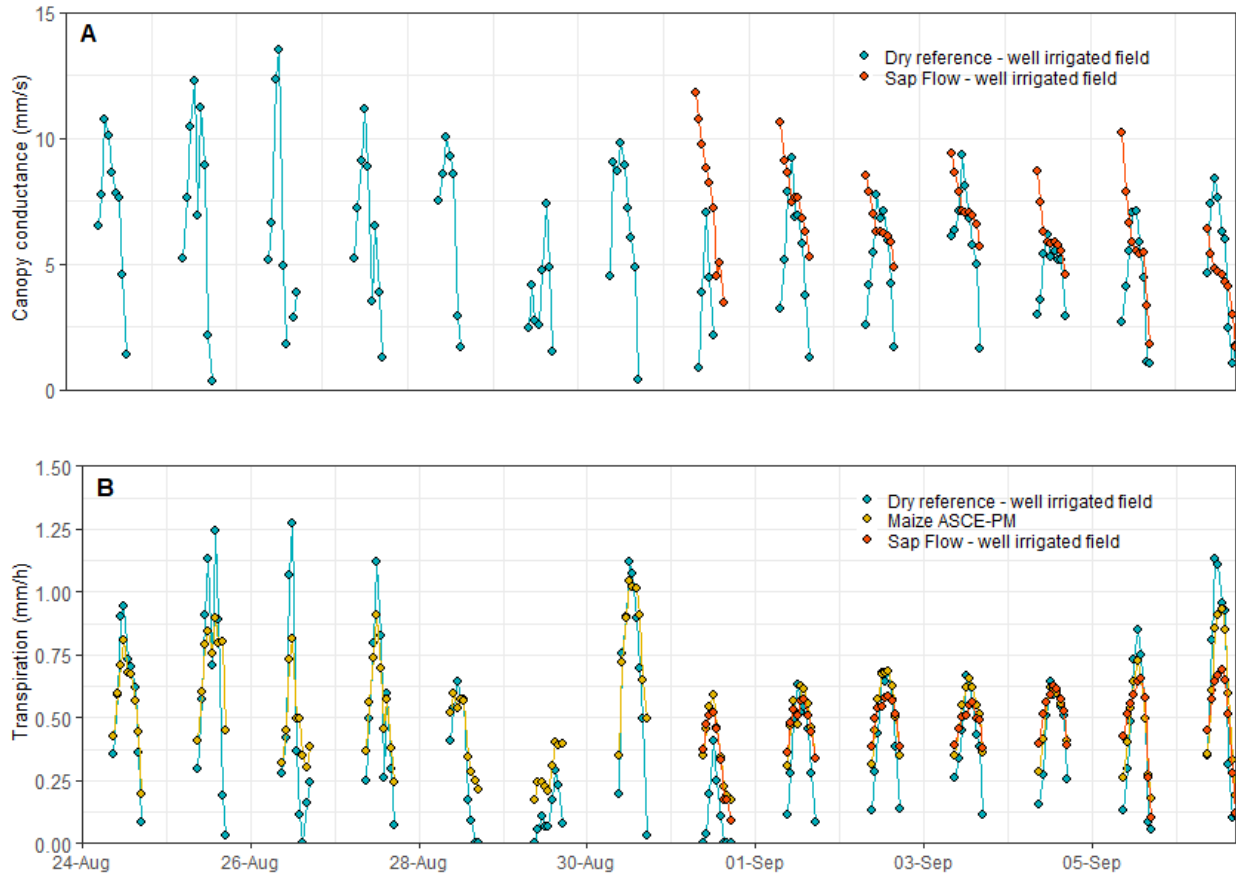


Figure 19. Hourly values for canopy conductance and transpiration estimation for the well irrigated field using the dry reference method using the maize ASCE P-M approach and sap flow estimations. Daily data from 9AM to 5PM.

Boundary layer conductance is a critical variable for the derivation of ET and canopy conductance (Jones et al., 2018). Two boundary layer conductance methods were tested for canopy conductance estimation: using Allen et al. (1998) approach and using Monteith and Unsworth (2013). The latter resulted in an overestimation of the conductance when compared against the conductance derived from sap flow measurements (figure C1 in Appendix C). The aerodynamic conductance estimated with Allen (1998) approach, assuming neutral conditions for the

atmosphere, resulted in canopy conductance and transpiration estimations that were comparable to the maize conductance and transpiration from the sap flows and in a better agreement with ASCE P-M maize transpiration.

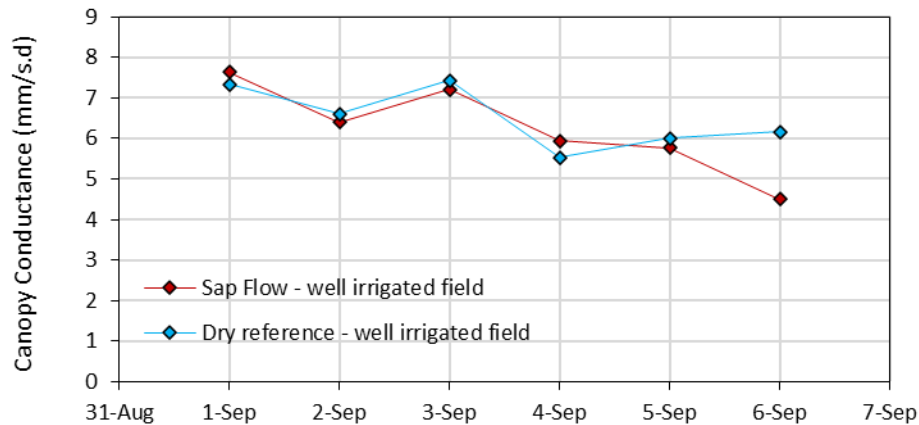


Figure 20. Mean daily canopy conductance from the well irrigated maize derived from sap flow data and from the Dry ARS method. Daily data from 11AM to 3PM.

Mean values for each day were compared between the methods. Dry reference conductance showed an underestimation of the values (data not shown). However, the pattern was similar. Canopy conductance derived from the sap flow sensors ranged from 7.7 mm/s.d to 4.3 mm/s.d. When the 6 values for conductance from sap flow were compared to the dry ARS conductance the MAE was 1.41 mm/s.d and RMSE, 1.5 mm/s.d, however, just like it was seen for transpiration, R^2 was low (0.34), and a paired student test showed no statistical difference ($p > 0.05$) between means from both methods. If the dry reference conductance method could give improved estimates at the beginning and the end of the day, the model would perform better.

When the analysis was performed with mean daily values around noon (from 11AM to 3PM), canopy conductance from the dry ARS showed a better agreement to the sap flow (Figure 20). Regression showed an R^2 of 0.57. The RMSE was 0.72 mm/s and the MAE was 0.51 mm/s, representing a 11.6% and 8.1% error, respectively, from the mean canopy conductance values.

Canopy conductance from sap flow ranged from 7.6 mm/s to 4.5 mm/s, these values were not much different from the mean values from 9AM to 5PM, however, the estimation of conductance from the dry ARS performed better at around noon. Results showed that the dry ARS could be an adequate tool for mid-day canopy conductance estimations.

Most of the water stress indices are indirectly or empirically related to stomatal conductance (Guilloni et al., 2008). In contrast, the proposed method in this study enabled calculation of absolute values of stomatal conductance. Estimates of canopy conductance values can be used as a direct indicator of water stress in the field (Blonquist et al., 2009), with the additional benefit of the continuous calculation and the possible implementation in the automation of irrigation triggering.

Additionally, canopy conductance estimation can be used as input in different models for crop water needs calculation (Li et al., 2015). Berni et al., (2009) for example, used canopy conductance values in an analytical solution of the CWSI. The use of complex models as the full energy balance for estimation of canopy conductance has the drawback of the additive errors on each of the parameters of the equation, and the need for very accurate canopy temperature estimation (Jones, 1999b). The methodology used in our study allows the estimation of canopy conductance and avoids the complexity of using some parameters, especially calculation for net radiation, and does not require as many weather parameters.

Deficit irrigated field

Estimations of the canopy conductance with the dry ARS method in the deficit field were carried out simultaneously with the well irrigated field (Figure 21A). Hourly estimates were compared showing clear differences during the period from 9/1 to 9/6, where lower values were observed

for the deficit maize compared to the well irrigated maize. Mean values for the period were near zero (0.11 mm/s, conductance mean value around noon). A large difference in conductance after August 31st was observed. On this date only the well irrigated field was irrigated, and the deficit field showed a continuous soil water depletion that caused water stress as shown in Figure C4 in Appendix C. During the five clear-sky days before the irrigation event, canopy conductance was also lower than the well irrigated maize. The canopy conductance was 8.3 mm/s for the well irrigated field and 5.3 mm/s for the deficit field, however, during this period the soil depletion data did not suggest water deficits. Results reveal an underestimation of the canopy conductance using the dry reference method; however, it demonstrates a high sensitivity to canopy temperatures. Data suggests that this approach has a potential use for early detection of water stress.

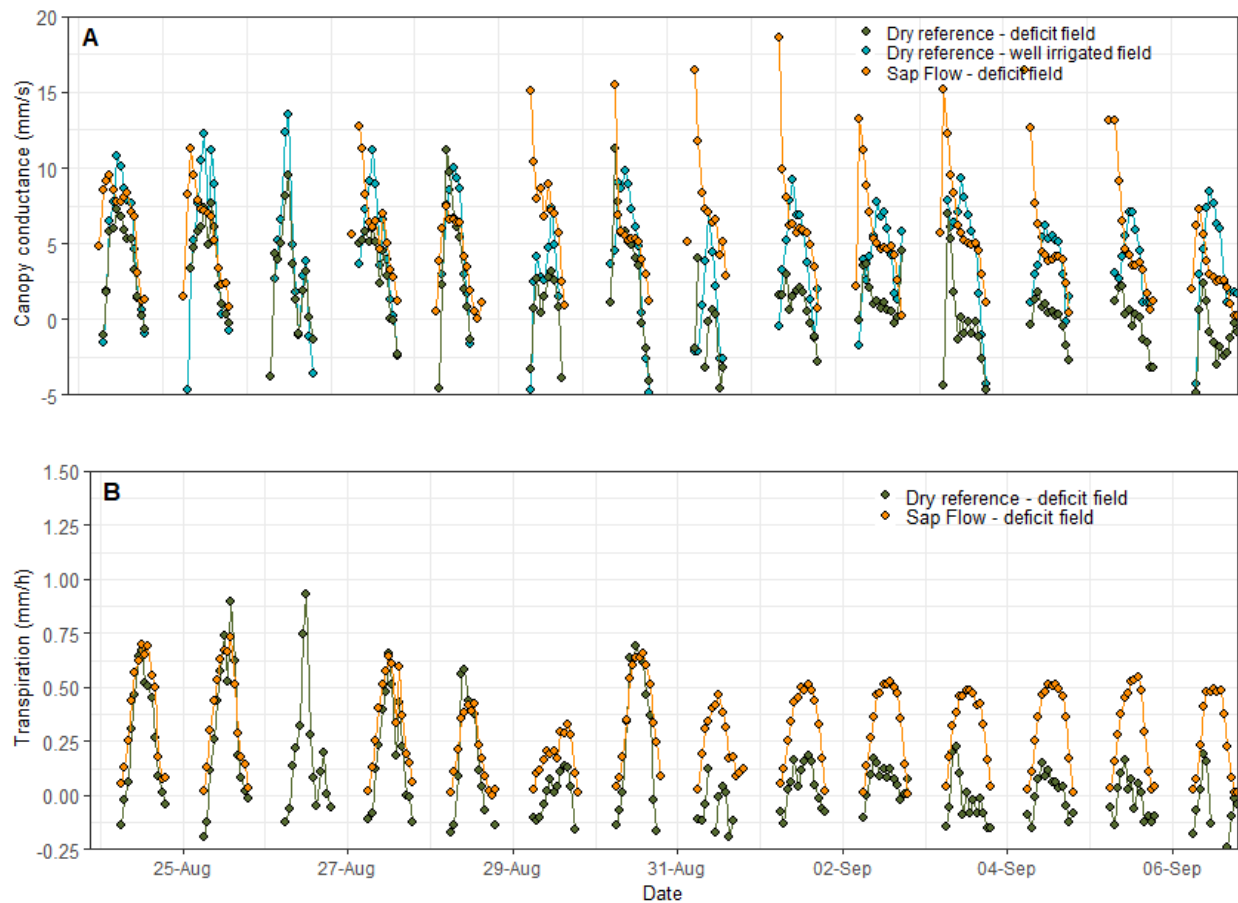


Figure 21. Hourly values for canopy conductance and transpiration estimation for the deficit field using the dry ARS method and sap flow measures. Daily data from 6AM to 7PM.

Hourly patterns from 6AM to 7PM from the deficit field revealed that sap flow data showed a peak at the beginning of each day, which was also observed in the well irrigated field. The canopy conductance from the dry ARS method for the deficit field also revealed this peak (Figure 21A).

Mean values from 11AM to 3PM for each day were compared to the sap flow derived canopy conductance (Figure 22), showing an R^2 of 0.69. Daily canopy conductance estimated with sap flow data ranged from 7.8 mm/s to 2.7 mm/s for the measured period. However, great differences were manifested after 8/31, where water deficit was present. The RMSE and MAE were 3.4 mm/s and 2.9 mm/h, respectively. Errors showed to be overly large for a desired accurate measure for any purpose, nevertheless the error is mainly due to the large differences in deficit period during

September (Figure 22). RMSE and MAE for the measures during August were 0.93 mm/s and 1.15mm/s, respectively, and for the deficit period were over 4mm/s for both parameters.

From analyzing the temperature from the maize and from the ARS (Figure A2B, in Appendix C) it was observed that the temperature from the ARS was too close to that of the canopy, especially during September, when the errors got larger. This explains the canopy conductance values close to zero during this period. These findings suggest that the color used for the reference did not represent a non-transpiring leaf, but the actual canopy. Additional research with a darker color for the ARS needs to be performed to study a better imitation of higher temperatures to represent a non-transpiring canopy. In addition, a different IRT orientation in the field, towards shaded leaves, could be also performed to study if the underestimation could also be due to a higher sensitivity of the method to this factor.

The canopy temperature measured by a sensor varies greatly depending on the direction of the view of the sensor in relation to the direction of the sun light (Jones et al., 2009). Therefore, in this study most of the leaves were sunlit. Temperature increases with increases in absorbed radiation of the canopy. Studies have proven that measurements of leaves exposed to direct sun radiation are more representative of stomatal changes because of the greater difference between air and plant temperature, when compared to measurements in the shade side of the canopy (Maes and Steppe, 2012) and there is less shading in the field of view of the sensor. Sensors pointing in similar or opposite direction of the sun (sensing sunlit or shaded canopy) can give substantially different measured canopy temperature between them (Jones et al., 2018). Sun-exposed leaves are more sensitive to changes in water status (Jones, 1999) and the sensitivity of IRTs to detect water stress is improves if temperature is measured with full sun and with a view of the solar radiation, avoiding shading of the leaves (Jones et al., 1997). However, some studies found that temperature measurements in the shade may be slightly more accurate respect to

those in the sun given a lower standard deviation of the values (Craparo et al., 2017). This should be considered in the implementation of any stress index.

Nevertheless, this study showed that early water stress could be detected using canopy conductance estimates. This avoids indirect or empirical approaches for stress determination, the latter, often used in stress detection indices (Idso et al., 1981; DeJonge et al., 2015) and allows for a direct estimation of canopy conductance.

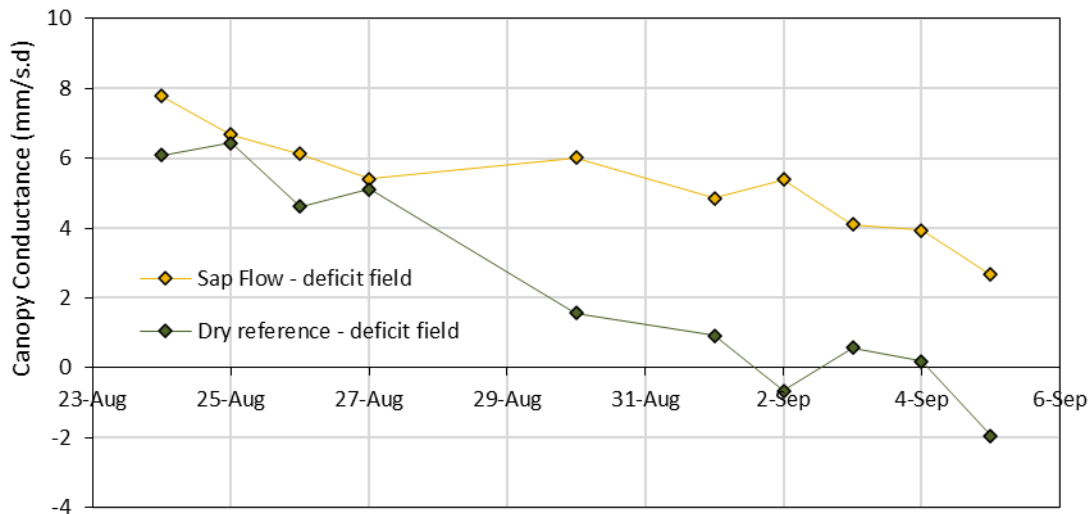


Figure 22. Mean daily canopy conductance from the deficit irrigated maize derived from sap flow data and from the Dry ARS method. Daily data from 11AM to 3PM.

In search for an even simpler solution for canopy conductance and transpiration estimations, we tested the use of a popular procedure to estimate a dry reference temperature, which is adding 5°C to the air temperature. We used this arbitrary approach of a dry reference temperature and performed the calculations for the TDry method. Results showed large spikes for conductance and for transpiration estimations and diurnal trends were different from the sap flow measurements (Figure C3 in Appendix C). We also found that this calculated temperature was not higher than the under-irrigated maize canopy, therefore it does not represent the temperature of a non-transpiring crop. Results agree with Jones et al. (2018), showing that this simple

approximation was not appropriate for canopy conductance or transpiration estimations. The performance of the physical reference was better for transpiration and conductance calculations with the proposed method.

The comparison between canopy conductance from the well irrigated and the deficit irrigated fields demonstrates that the method could be suitable for estimation of temporal (real-time) and spatial variation of canopy conductance, allowing detection of water stress locations in maize fields. However, it is known that the sensitivity of leaf temperature to changes in stomatal conductance increases with solar radiation (Jones et al., 1997) and meteorological conditions. We were able to verify the sensitivity of the method to such conditions, especially presence of clouds affecting incident radiation. Temperature from the sunlit leaves also vary as a function of orientation (Jones, 2004; Jones et al., 2009) and surface temperature from the ARS would also vary with the radiant load.

This experiment provided a basis for further canopy conductance monitoring studies in maize with a novel technique, using a dry ARS with a hemispherical shape in field conditions.

Potential use for crop water stress detection using a Dry ARS with a simple approach

An additional use of the dry ARS would be in the implementation of a simple method to detect crop water stress. The simple comparison of canopy temperatures against the dry ARS has been suggested previously as a potentially useful stress indicator (Grant et al., 2006; Maes et al., 2011) in grapevines and *Jatropha curcas* crops.

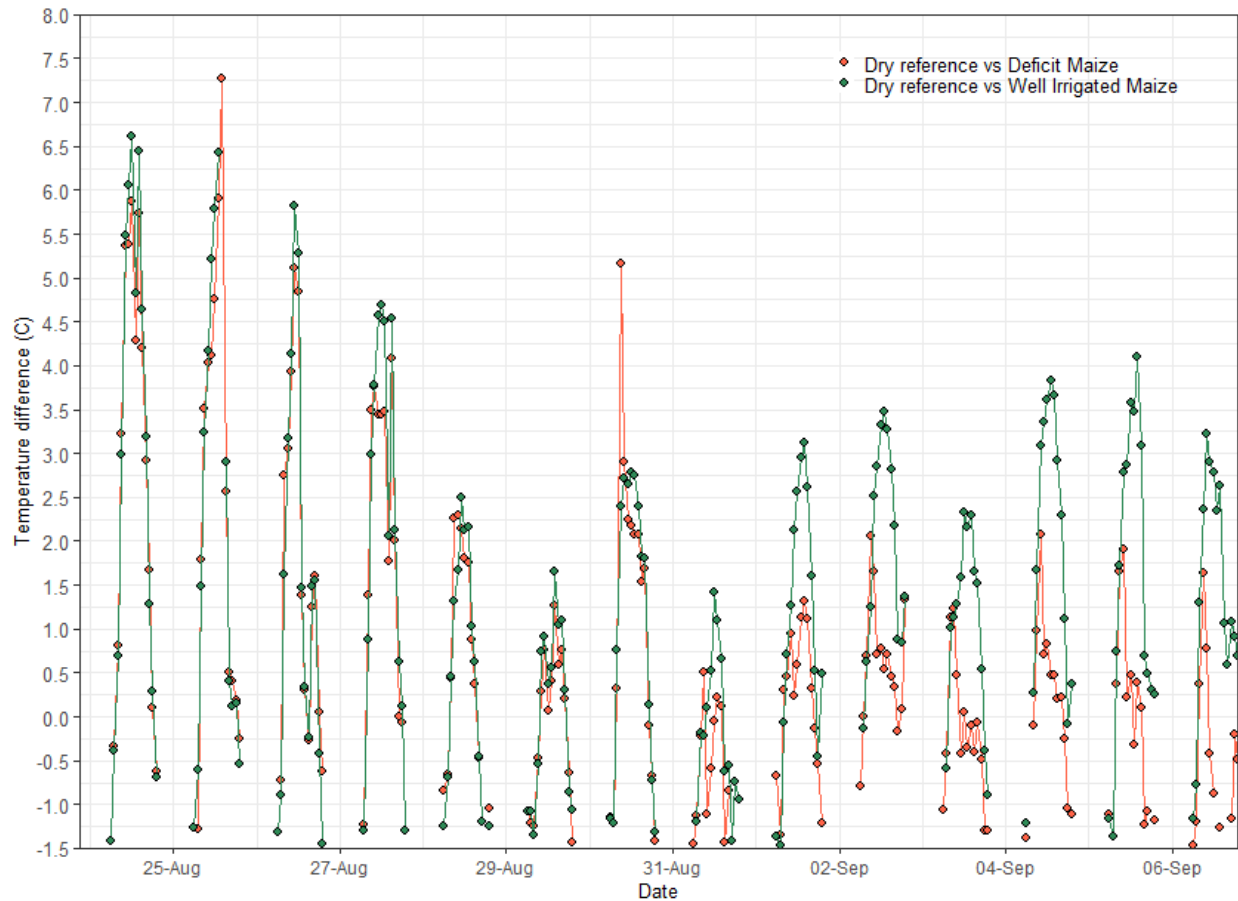


Figure 23. Use of relative temperatures as a simple approach to detect water stress. Daily data from 6AM to 7PM.

Results of the implementation of this simple approach are shown in Figure 23, for the deficit and the well irrigated maize. The temperature difference between the dry ARS and the crop temperatures (dT_{dry}) for both fields were similar during August and showed clear differences in September. From an independent set of measures using relative transpiration from the sap flow data and relative extractable water in the soil (Figure in C5 in Appendix C) a deficit event was detected around August 30th. The dT_{dry} showed a steady decline of the values for both fields. After August 31st the dT_{dry} showed lower values for the deficit maize in comparison to the well irrigated field. Results suggest this method could be able to track the water status of maize and be used as a stress indicator.

It was observed that values for August 29 and August 31 for the dTDry were low in both fields, probably due to cloudiness and the low atmospheric demand. Cloudiness is an important factor that needs to be considered in all interpretations that involve the use of the ARS temperature. The underestimation could give the wrong sense of water stress presence in the field. However, if this limitation is understood, it could be an adequate alternative for water stress detection. The relative temperature of the dry ARS and the under-irrigated maize showed a clear tendency of reduction as the soil water depletion increases. The tendency can be appreciated either using hourly or mean dTDry values for the day. A threshold would need to be defined in order to use this approach to trigger irrigation.

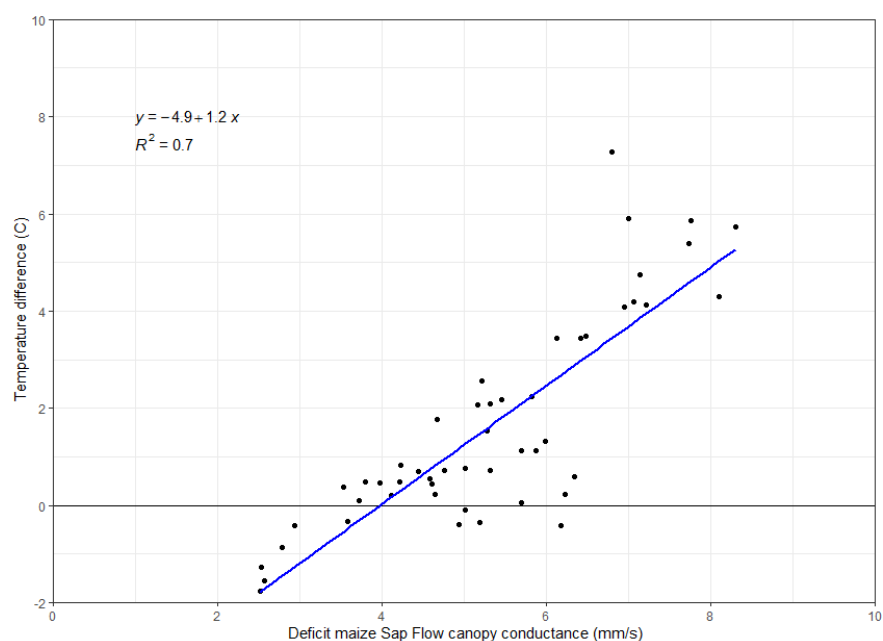


Figure 24. Temperature difference between the dry ARS and canopy temperature against canopy conductance from the deficit irrigated maize measured with sap flow gauges. Hourly daily values from 11AM to 3PM, where the highest differences in temperature are present and without the two days with low VPD.

When the dTDry for the deficit maize was compared to the hourly canopy conductance from the sap flow gauges (Figure 24), it showed a strong correlation with $R^2 = 0.7$, $p < 0.005$, proving to be a robust indicator of water stress. Days with low atmospheric demand were removed for the

reasons mentioned above and the time frame was reduced to 11AM to 3PM, given that the greatest differences in temperature are found near solar noon. This strong correlation confirmed our hypothesis for using the dTdry as an adequate approach for water stress detection.

A larger dataset with additional water deficit events and different weather conditions would need to be tested for a better assessment and validation of the dTdry as stress detector and to define temperature thresholds for practical applications. Nevertheless, our findings support previous studies by Grant et al., 2006 and Maes et al. (2011) who suggested that a simple comparison of temperature from the canopy to the dry ARS are able to detect stress. We contribute to the idea of Singh et al (2021) of using simple approaches as indicators of water stress to avoid the complexity of numerous measurements and complicated calculations, which limits the applicability to farmers. Other simple approaches considering the comparison of the canopy temperature against a fixed critical value or against air temperature, have also been suggested (Colaizzi et al., 2012; DeJonge et al., 2015; Singh et al., 2021). However, while they would be simple to use, we preferred to use a normalization of the temperature and avoid absolute values to minimize the effects of calibration of IRTs and orientation of the IRTs in relation to the sun. In addition, when environmental conditions change it may be difficult to distinguish an increase in water stress from the leaf temperature changes to increasing air temperature or other weather parameters. The dTdry method linear correlation with canopy conductance proves its strong sensitivity for detecting plant stress and will also be able to measure the severity of the water deficit.

The approaches shown in this study aim to improve the estimations of crop water use. We provide evidence that actual absolute maize transpiration and canopy conductance can be estimated using our designed dry ARS temperature, canopy temperature and limited weather data.

The dry ARS temperature has also other potential uses by directly using the temperature from the dome in comparison with the canopy or used as an upper baseline in water stress indices (Apolo-Apolo, 2020; Maes et al., 2011).

Conclusions

We developed a 3D-printed dry reference surface that has a potential use for real time monitoring of actual maize transpiration, canopy conductance and water stress in field conditions. The low-cost structure and electronic components make it feasible to reproduce and deploy in the field without much need for maintenance during the season. The use of the IoT allowed continuous, real-time monitoring of the temperatures and could be used for long-term observations. The dry ARS temperature followed diurnal temperature of non-transpiring leaves in plant studies. However, it was observed that the dry ARS temperatures during water-stressed periods were too close to that of the stressed canopy, hence, a darker color should be tested in further studies.

Actual maize transpiration was adequately estimated with the dry ARS temperature approach, when compared to the transpiration calculated from sap flow and ASCE standardized tall reference ET (ASCE, 2005) and local Kcb curve for maize. Daily values considered the timeframe between 9AM and 5PM, a timeframe that accounts for 90% of the diurnal maize transpiration, and that could represent the total daily water needs. TDry showed underestimation of the daily transpiration values. When the TDry method was compared to the ASCE P-M maize transpiration, the RMSE was 0.61mm and MAE of 0.53mm, representing a 12% and a 10% error of the method in relation to the actual Maize transpiration. The total transpiration for the 12-day-period using the TDry method was 51 mm and 56mm with the P-M approach. Comparisons for sap flow data for the 6-day period showed the RMSE was 0.78 mm and MAE of 0.73 mm, representing a 17% and 16% error, respectively. Transpiration was 25 mm with the TDry and 27mm measured with sap

flow gauges. Hourly rates estimated with TDry were highly correlated to hourly values from the ASCE PM maize transpiration and from sap flow gauges with an R^2 of 0.83 and 0.7, respectively.

Canopy conductance was modeled during the day with the dry ARS approach. The pattern and values were similar to the canopy conductance derived from sap flow sensors for a well irrigated maize, with a tendency to underestimate the daily values. Conductance calculated with the dry reference method showed a good performance. The regression between dry reference conductance and conductance from sap flow gauges showed an R^2 of 0.57 mm/s, MAE of 0.51 mm/s. (8.1% from mean daily values) and a RMSE of 0.72 mm/s. (11.6 %error). Canopy conductance from sap flow ranged from 7.6 mm/s to 4.5 mm/s.

When the method was used for deficit-irrigated maize, it clearly showed a reduction in transpiration and canopy conductance due to soil water depletion. This demonstrated the sensitivity of the method for detecting water stress in the field. However, great underestimation of the values was found, attributed mainly to the color of the dry ARS. Comparisons of the conductances from the well irrigated and the deficit maize fields showed the onset of water stress.

Limited local weather variables are needed for transpiration and canopy estimation using the proposed method. Therefore, it is an appealing practical approach to use, especially in locations where ET weather station data is not available. Nevertheless, the method is restricted to days with relative cloudiness above 0.55 to avoid large errors in the calculations.

A simple thermal method for water stress detection was also tested. Results showed that it could be used as an indicator of water stress in the field. The dTDry method was strongly correlated to canopy conductance ($R^2 = 0.7$) and was able to detect the onset of water stress in the field.

Proving it as a robust indicator for rapid screening of stress in the field. Additional data is needed to evaluate the use of this approach under different weather conditions.

We provide evidence that actual transpiration and canopy conductance can be monitored continuously and in real-time using the designed dry ARS, low-cost sensors and the proposed method. It requires measuring temperatures from the ARS and the canopy simultaneously and limited weather data. In addition, there is a potential use of this method for detecting changes in canopy conductance due to water deficit. Comparing conductances from different locations or using the straight-forward temperature comparisons of canopy and the dry ARS could indicate water stress in the field. Further studies would need to be carried out to fine-tune the determination of the absolute values for canopy conductance and transpiration with the Dry ARS method. However, this technique proves to be an attractive low-cost tool for irrigation management purposes and could also be used as a validation tool of complex models for transpiration estimation.

Future research

- Evaluate the use of a dry ARS in different growth stages, especially during the developmental stages, where controlled water stress can be of interest.
- Evaluate different colors for the dry ARS to be used in different growth stages. Evaluate a different shape and materials with different thermal conductivity for the hemisphere.
- Evaluate the “dTdry” approach for a larger dataset with frequent situations of water stress to test sensitivities and absolute estimations with different weather conditions.
- Evaluate approaches/corrections for cloudy days.

References

- Alchanatis, V.; Cohen, Y.; Moller, M.; Sprinstin, M.; Meron, M.; Tsipris, J.; Saranga, Y.; Sela, E. 2010. Evaluation of different approaches for estimating and mapping crop water status in cotton with thermal imaging. *Precision Agriculture*. V. 11: 27-41. DOI 10.1007/s11119-009-9111-7.
- Allen, R.; Pereira, L.; Raes, D.; Smith, M. 1998. *Crop Evapotranspiration – guidelines for computing crop water requirements*. FAO Irrigation and Drainage paper No. 56. Rome, Italy. 299p.
- Allen, R.; Tasumi, M.; Trezza, R. 2007. Satellite-based energy balance for mapping evapotranspiration with internalized calibration (METRIC) model. *Journal of Irrigation and drainage engineering*. V.133(4): 380-394. 10.1061/ASCE0733-94372007133:4380 .
- Andales, A. A., Bartlett, A. C., Bauder, T. A., & Wardle, E. M. 2020. Adapting a Cloud-Based Irrigation Scheduler for Sugar Beets in the High Plains. *Applied Engineering in Agriculture*, 36(4), 479–488. <https://doi.org/10.13031/aea.13902>.
- Andales, A. A., Bauder, T. A., & Arabi, M. 2014. A Mobile Irrigation Water Management System Using a Collaborative GIS and Weather Station Networks. In L. R. Ahuja, L. Ma, & R. J. Lascano (Eds.), *Advances in Agricultural Systems Modeling* (pp. 53–84). American Society of Agronomy and Soil Science Society of America. <https://doi.org/10.2134/advagricsystmodel5.c3>
- ASCE. Walter, I.; Allen, R.; Elliot, R.; Itenfisu, D.; Brown, P.; Jensen, M.; Mecham, B.; Howell, T.; Snyder, R.; Eching, S.; Spofford, T.; Hattendorf, M.; Martin, D.; Cuenca, R.; Wright, J. Task Committee on Standarization of Reference Evapotranspiration of the Environmental and Water Resources Institute of the American Society of Civil Engineers. 2005. *The ASCE standardized reference evapotranspiration equation*. Final Report. 59p.
- Apolo-Apolo, O.; Martinez-Guanter, J.; Perez-Ruiz, M.; Egea, G. 2020. Design and assesment of new artificial reference surfaces for real time monitoring of crop water stress index in maize. *Agricultural Water Management*. V. 240: 106304. <https://doi.org/10.1016/j.agwat.2020.106304> .
- Bastiaanssen, W.; Menenti, M.; Feddes, R.; Holtslag, A. 1998. A remote sensing surface energy balance algorithm for land (SEBAL). *Journal of Hydrology*. V.212-213: 198-212.
- Berni, J.; Zarco-Tejada, P.; Sepulcre-Canto; Fereres, E.; Villalobos, F. 2009. Mapping canopy conductance and CWSI in olive orchards using high resolution thermal remote sensing imagery. *Remote Sensing of Environment*. V.113: 2380-2388. doi:10.1016/j.rse.2009.06.018 .
- Blonquist Jr., J.; Norman, J.; Bugbee, B. 2009. Automated measurement of canopy stomatal conductance based on infrared temperature. *Agricultural and Forest Meteorology*. V. 149:1931-1945.
- Brenner, A.; Jarvis, P. 1995. A heated replica technique for determination of leaf boundary layer conductance in the field. *Agricultural and Forest Meteorology*. V. 72: 261-275.

Brunsell, N.; Gillies, R. 2002. Incorporating emissivity into a thermal atmospheric correction. *Photogrammetric Engineering and Remote Sensing*. V.68(12): 1263-1269.

Chavez, J. 2015. Using canopy temperature as an indicator of plant stress. In: *Proceedings of the 26th Annual Central Plains Irrigation Conference*. pp. 61–70.

Cohen, Y.; Alchanatis, V.; Meron, M.; Saranga, Y.; Tsipris, J. 2005. Estimation of leaf water potential by thermal imagery and spacial analysis. *Journal of Experimental Botany*. V. 56(417): 1843-1852. doi:10.1093/jxb/eri174.

Colaizzi, P.; O'Shaughnessy, S.; Evett, S.; Howell, T. 2012. Using plant canopy temperature to improve irrigated crop management. In: *24th Annual Central Plains Irrigation Conference, CPIA, Colby KS*.

Costa, J.; Grant, O.; Chaves, M. 2013. Thermography to explore plant-environment interactions. *Journal of Experimental Botany*. V. 64 (13): 3937-3949. doi:10.1093/jxb/ert029 .

DeJonge, K.; Taghvaeian, S.; Trout, T.; Comas, L. 2015. Comparison of canopy temperature-based water stress indices for maize. *Agricultural Water Management*. V.156: 51-62.

Evangelisti, L.; Guattari, C.; Asdrubali, F. 2019. On the sky temperature models and their influence on buildings energy performance: A critical review. *Energy and Buildings*. V. 183: 607-625. <https://doi.org/10.1016/j.enbuild.2018.11.037> .

Gholipour, M.; Sinclair, T.; Raza, M.; Cooper, M.; Messina, C. 2013. Maize hybrid variability for transpiration decrease with progressive soil drying. *Journal of Agronomy and Crop Science*. V. 199: 23-29. doi:10.1111/j.1439-037X.2012.00530.x

Gleason, D.; Andales, A.; Bauder, T.; Chavez, J. 2013. Performance of atmometers in estimating reference evapotranspiration in a semi-arid environment. *Agricultural Water Management*. V. 130: 27-35.

Grant, O.; Chaves, M.; Jones, H. 2006. Optimizing thermal imaging as a technique for detecting stomatal closure induced by drought stress under greenhouse conditions. *Physiologia Plantarum*. V. 127: 507-518. doi: 10.1111/j.1399-3054.2006.00686.x .

Grant, O.; Ochagavia, H.; Baluja, J.; Diago, M.; Tardaguila, J. 2016. Thermal imaging to detect spacial and temporal variation in the water status of grapevine. *The Journal of Horticultural Science and Biotechnology*. V. 91(1): 43-54. <https://doi.org/10.1080/14620316.2015.1110991> .

Guilioni, L.; Jones, H.; Leinonen, I.; Lhomme, J. 2008. On the relationships between stomatal resistance and leaf temperatures in thermography. *Agricultural and Forest Meteorology*. V. 148: 1908-1912.

Ham, J. 2005. Useful equations and tables in micrometeorology. In: *Micrometeorology in Agricultural Systems, Agronomy Monograph No. 47*. American Society of Agronomy, Crop Science Society of America, Soil Science Society of America, 677 S. Segoe Rd., Madison, WI 53711, USA.

- Idso, S.; Jackson, R.; Pinter, P.; Reginato, R.; Hatfield, J. 1981. Normalizing the stress-degree-day parameter for environmental variability. *Agricultural Meteorology*. V. 24: 45-55.
- Irmak, S.; Rees, J.; Zoubek, G.; van DeWalle, B.; Rathje, W.; DeBuhr, R.; Leininger, D.; Siekman, D.; Schneider, J.; Christiansen, A. 2010. Nebraska Agricultural water management demonstration network (NAWMDN): Integrating research and extension/outreach. *Applied Engineering in Agriculture*. American Society of Agricultural and Biological Engineers. V. 26(4): 599-613.
- Jackson, R.; Idso, S.; Reginato, R.; Pinter Jr., P. 1981. Canopy temperature as a crop water stress indicator. V. 17(4): 1133-1138.
- Jones, H.; Aikman, D.; McBurney, T. 1997. Improvements to infrared thermometry for irrigation scheduling in humid climates. *Acta Horticulturae* 449. V. 1: 259-266.
- Jones, H. 1999. Use of infrared thermometry for estimation of stomatal conductance as a possible aid to irrigation scheduling. *Agricultural and Forest Meteorology*. V. 95: 139-149.
- Jones, H. 1999b. Use of thermography for quantitative studies of spatial and temporal variation of stomatal conductance over leaf surfaces. *Plant, Cell and Environment*. V. 22: 1043-1055.
- Jones, H. 2004. Application of thermal imaging and infrared sensing in plant physiology and ecophysiology. *Advances in Botanical Research*. V 41: 107-163.
- Jones, H.; Serraj, R.; Loveys, B.; Xiong, L.; Wheaton, A.; Price, A. 2009. Thermal infrared imaging of crop canopies for the remote diagnosis and quantification of plant responses to water stress in the field. *Functional Plant Biology*. V. 36: 978-989.
- Jones, H. 2014. *Plant and Microclimate: A quantitative approach to environmental plant physiology*. 3rd edition. 407pp.
- Jones, H.; Hutchinson, P.; May, T.; Jamali, H.; Deery, D. 2018. A practical method using a network of fixed infrared sensors for estimating crop canopy conductance and evaporation rate. *Biosystems Engineering*. V. 165: 59–69. <https://doi.org/10.1016/j.biosystemseng.2017.09.012> .
- Johnson, L.; Trout, T. 2012. Satellite NDVI assisted monitoring of vegetable crop evapotranspiration in California's San Joaquin Valley. *Remote Sensing*. V.4: 439-455. doi:10.3390/rs4020439.
- Katimbo, A.; Rudnick, D.; DeJonge, K.; Lo, T.; Qiao, X.; Franz, T.; Nakabuye, H.; Duan, J. 2022. Crop water stress index computation approaches and their sensitivity to soil water dynamics. *Agricultural Water Management*. nV.266: 507575. <https://doi.org/10.1016/j.agwat.2022.107575> .
- Kullberg, E.; DeJonge, K.; Chavez, J. 2017. Evaluation of thermal remote sensing indices to estimate crop evapotranspiration coefficients. *Agricultural Water Management*. V.179: 64-73.
- Leinonen, I.; Grant, O.; Tagliavia, C.; Chaves, M.; Jones, H. 2006. Estimating stomatal conductance with thermal imagery. *Plant, Cell and Environment*. V. 29: 1508-1518. doi: 10.1111/j.1365-3040.2006.01528.x .

Li, S.; Zhang, L.; Kang, S.; Tong, L.; Du, T.; Hao, X.; Zhao, P. 2015. Comparison of several surface resistance models for estimating crop evapotranspiration over the entire growing season in arid regions. *Agricultural and Forest Meteorology*. V. 208: 1-15. <http://dx.doi.org/10.1016/j.agrformet.2015.04.002> .

Maes, W.; Achten, W.; Reubens, B.; Muys, B. 2011. Monitoring stomatal conductance of *Jatropha curcas* seedlings under different levels of water shortage with infrared thermography. *Agricultural and Forest Meteorology*. V. 151: 554-564. doi:10.1016/j.agrformet.2010.12.011 .

Maes, W.; Steppe, K. 2012. Estimating evapotranspiration and drought stress with ground-based thermal remote sensing in agriculture: a review. *Journal of Experimental Botany*. V. 63(13): 4671-4712. doi:10.1093/jxb/ers165 .

Maes, W.; Baert, A.; Huete, A.; Minchin, P.; Snelgar, W.; Steppe, K. 2016. A new wet reference target method for continuous infrared thermography of vegetations. *Agricultural and Forest Meteorology*. V.226-227: 119-131. <http://dx.doi.org/10.1016/j.agrformet.2016.05.021> .

Meron, M.; Tsipris, J.; Orlov., V.; Alchanatis, V.; Cohen, Y. 2010. Crop water stress mapping for site-specific irrigation by thermal imagery and artificial reference surfaces. *Precision Agriculture*. V.11: 148-162. DOI 10.1007/s11119-009-9153-x .

O'Shaughnessy, S.; Hebel, M.; Evett, S.; Colaizzi, P. 2011. Evaluation of a wireless infrared thermometer with a narrow field of view. *Computers and Electronics in Agriculture*. V.76: 59-68.

O'Shaughnessy, S.; Evett, S.; Colaizi, P.; Howell, T. 2012. A crop water stress index and time threshold for automatic irrigation scheduling of grain sorghum. *Agricultural Water Management*. V. 107: 122-132. doi:10.1016/j.agwat.2012.01.018 .

O'Shaughnessy, S.; Kim, M.; Andrade, M.; Colaizzi, P. 2020. Site-specific irrigation of grain sorghum using plant and soil water sensing feedback – Texas High Plains. *Agricultural Water Management*. V.240: 106273. Sensor <https://doi.org/10.1016/j.agwat.2020.106273> .

Pou, A.; Diago, M.; Medrano, H.; Baluja, J.; Tardaguila, J. 2014. Validation of thermal indices for water status identification in grapevine. *Agricultural Water Management*. V. 134: 60-72. <http://dx.doi.org/10.1016/j.agwat.2013.11.010> .

Qiu, G.; Sase, S.; Shi, P.; Ding, G. 2003. Theoretical analysis and experimental verification of a remotely measurable plant transpiration transfer coefficient. *Japan Agricultural Research Quarterly (JARQ)* V. 37(3): 141-149.

Sadras, V.; Milroy, S. 1996. Soil-water thresholds for the responses of leaf expansion and gas exchange: a review. *Field Crops Research*. V.47: 253-266.

She, D.; Xia, Y.; Shao, M.; Peng, S.; Yu, S. 2013. *Agroforestry Systems*. V. 87: 667-678. DOI 10.1007/s10457-012-9587-4 .

Singh, J.; Ge, Y.; Heeren, D.; Walter-shea, E.; Neale, C.; Irmak, S.; Woldt, W.; Bai, G.; Bhatti, S.; Maguire, M. 2021. Inter-relationships between water depletion and temperature differential in row crop canopies in a sub-humid climate. *Agricultural Water Management*. V.256: 107061. <https://doi.org/10.1016/j.agwat.2021.107061> .

Taghvaeian, S.; Chavez, J.; Hansen, N. 2012. Infrared thermometry to estimate Crop Water Stress Index and water use of irrigated maize in northeastern Colorado. *Remote Sensing*. V. 4: 3619-3637. doi:10.3390/rs4113619 .

Trout, T.; DeJonge, K. 2018. Crop water use and crop coefficients of maize in the Great Plains. *Journal of Irrigation and Drainage Engineering*. V. 144(6): 04018009; DOI: 10.1061/(ASCE)IR.1943-4774.0001309.

Verhoef, A.; Egea, G. 2014. Modeling plant transpiration under limited soil water: comparison of different plant and soil hydraulic parametrizations and preliminary implications for their use in land surface models. *Agricultural and Forest Meteorology*. V. 191: 22-32. <http://dx.doi.org/10.1016/j.agrformet.2014.02.009> .

CHAPTER 5

GENERAL CONCLUSIONS

We provided evidence that actual transpiration, canopy conductance and crop water stress can be monitored continuously using the newly designed low-cost IoT sap flow sensors and artificial reference surface.

- A new Heat Ratio method for a heat pulse technique was successfully developed and coupled with a new gauge design created with 3D-printed parts and low-cost sensors. The gauges are easy to build and adaptable to a range of stem sizes. The sap flow sensors were calibrated for maize in the greenhouse resulting in a calibration coefficient of $1.28 \pm \text{SD } 0.2$, used to convert heat velocity to transpiration flow. This coefficient was higher during 2019 due to the effect of a longer heating time, confirming that calibration coefficients also account for sources of errors such as wound effects on the plants. Results showed that they were in good agreement with estimated transpiration from plants on scales from greenhouse studies, from field measurements with commercially available sap flow gauges and with estimations with the P-M approach in field conditions. In 2019 greenhouse validation studies showed an RMSE of 12.4% and MAE of 10.2% from the mean T value. In field conditions, when sap flow gauges were compared to the reference transpiration for daily transpiration estimation with the P-M approach the RMSE and MAE were 0.70 mm and 0.56 mm, a 13.2% and 11% error from the mean T value respectively. When compared to commercially available sap flow gauges, the RMSE and MAE were 0.66 mm and 0.54 mm (12.4% and 10.2% from the mean T value respectively). In 2020 daily plant transpiration validation study in the greenhouse showed an RMSE of 15.4% and a MAE of 12.1% of mean transpiration value with a strong coefficient of determination

($R^2 = 0.87$). Sap flow gauges underestimated transpiration a 5.8%. At field conditions, in a well irrigated maize sap flow gauges showed a plant transpiration estimation precision of ± 1.04 mm (SD). When compared to the P-M approach, the MAE was 0.48 mm and RMSE was 0.62 mm. Differences were within 10%. The total transpiration for the period was 72 mm from the reference transpiration and 75 mm measured with the gauges, overestimating water use a 4.4 %. The accuracy of the transpiration measurement varies with the number of sensors deployed in the field. More than 4 sensors should be deployed in the field to obtain estimations of corn transpiration with less than 20% error. Measured accuracy with a ME for a 95% certainty was 0.87 mm/day using 8 sensors. The number of gauges that need to be deployed for more than 80% confidence of finding a difference of 1 mm between treatments and a Standard Error around 0.3 mm of corn transpiration would be 12. The combination of the sensor design, model for heat velocity, calibration factor and the use procedure is a reliable approach to measure crop water use for various purposes and a useful option for small plots or field scale.

- The use of the sap flow sensors for site-specific basal crop coefficients derivation was described. Locally derived Kcb values from Trout and DeJonge (2018) for maize was verified using our low-cost sap flow sensors for a period of 17 days in 2019 and 22 days in 2020. In season 2019 the period measured was situated in the mid-season maize phase and the mean Kcb derived was 1.08 from the sap flow gauges (sap flow gauges described in chapter two) and 0.99 from the commercial sap flow gauges. The locally derived Kcb was 1.05. In season 2020 the period was divided into mid-season, beginning of late-season and end late-season. Mid-season Kcb derived from sap flow data (8/16/2020 to 8/24/2020) was 1.06 while locally derived Kcb was 1.05. For beginning of late-season (8/31 to 9/6), both values concur (0.82) and for the end of late-period (9/17/2020 to 9/23/2020) flow Kcb was higher than the tabulated value (0.62 vs 0.4). However, this is

probably due to the fixed end-of-cycle-date for maize cycle (using GDD). This approach is especially useful for low budget and rapid evaluations. We reviewed the benefits and constraints of using basal crop coefficients in a dual K_c approach for better estimation of crop water requirements and management. The use of K_{cb} could allow for better understanding of the partition of the total ET_c into transpiration and soil water evaporation, enabling adjustment of management practices to reduce the use of water for non-beneficial purposes and improve water use efficiency. It can also bring valuable information by quantifying the impacts of changes in local agronomic management practices such as inter-row cropping, changes in crop varieties, pest affectation or reductions of leaf area functioning, salinity effects or environmental changes on in the transpiration component of the evaporating surface, hence, improving the estimation of crop water requirements.

- A 3D-printed plastic hemispherical artificial reference surface (ARS) was developed and tested for continuous monitoring of actual maize transpiration and canopy conductance. The dry ARS allowed very close imitation of actual temperatures of non-transpiring maize leaves ($R^2 = 0.99$). Actual maize transpiration was adequately estimated with the dry ARS temperature approach during a 14-day period, when compared to the transpiration calculated from sap flow and ASCE standardized tall reference ET (ASCE, 2005) with a local K_{cb} value for maize. The daily RMSE was 0.61 mm and margin of error (ME) of 0.53 mm, representing a 12% and a 10% error of the method in relation to the Penman-Monteith approach for a 12-day period. The daily RMSE and ME was 0.78 mm and 0.73 mm in relation to actual maize transpiration from sap flow gauges, for a 6-day period, representing a 17% and 16% error, respectively. The total transpiration for the 12-day-period using the proposed method was 51 mm compared to 56 mm using the ASCE P-M approach. Transpiration was 25 mm with the dry ARS method and 27mm measured with

sap flow gauges. Differences to the total transpiration were within 7.5%. Absolute hourly values of canopy conductance showed similarity to the conductance derived from the sap flow gauges during a six-day period. However, the model underestimated values early in the morning and late afternoon. When mean daily mid-day values were compared, MAE and RMSE were 0.51 mm/s. and 0.72 mm/s, representing a 8.1% and an 11.6% error respectively. The method was also tested in a deficit-irrigated maize field, revealing that it was able to show reductions in transpiration and canopy conductance due to soil water depletion, demonstrating its sensitivity to water stress in the field. However, absolute values were greatly underestimated, attributed mainly to the similarity of the temperature from the ARS and the stressed canopy and suggesting the color of the reference should be darker. The method can be a practical approach to estimating maize transpiration and canopy conductance since it requires less weather data. Its simplicity of fabrication and implementation and its low requirements for maintenance during the season are also advantages. Nevertheless, the method is restricted to days with relative cloudiness above 0.55 to avoid large errors in the calculations. In addition, we showed the device can also be used for water stress detection using a simple comparison of canopy temperature to that of the reference. Results indicated a strong linear correlation ($R^2=0.7$) between the temperature comparison (ARS temperature – canopy temperature) and canopy conductance derived from the sap flow sensors. This provided evidence that the device could be used for monitoring and detection of water stress in a crop field.

The fabrication of the tools for this study used a modern approach of utilizing low-cost sensors and electronics coupled with the IoT technology. Both the sap flow gauge and the dry ARS can be low-cost options for real time continuous calculation of crop water use and monitoring of crop water stress. The complementary use of the sap flow gauges and the dry ARS, has a potential

use for supporting water use decision making and could aid in improving irrigation management practices.

In addition, sap flow sensors measure plant transpiration directly, capturing environmental and plant effects on transpiration rate. They provide a unique and valuable information for ground-truthing complex multi-layer and remote sensing ET models and simulations that aim to estimate actual transpiration from the field.

Future research recommendations

- Continue to research the implementation of the dry ARS for estimation of maize transpiration and canopy conductance. Mainly testing different colors for the reference surface and explore the use of new materials with different thermal conductivity. Test its use in different growth stages, especially during the developmental stages, where controlled water stress can be of interest and continue to evaluate its use for stress detection with a larger dataset with water deficit events.
- Continue to test if changes in the heating time and heat velocity equations improve the sap flow precision using the new design for the gauge. Test the probes for different species and in a complete crop season. Maximize the number of days the gauges can be attached to a plant. Develop a printed circuit board for the hardware components for quicker fabrication process and test for improvements in real time data visualization of transpiration rates.

- Further studies to investigate the potential use of the complementary real time data of both tools, the sap flow gauges and dry ARS in the field. Assessing real-time decision-making with case studies using data from these low-cost sensors would demonstrate practical applications in irrigation management.
- Exploit the potential of the combined use of sap flow data with the remote sensing techniques for ground truthing more complex models that are being developed for crop evapotranspiration estimation at the field scale.

Appendix A

Derivation for the approximations to estimate heat-pulse velocity with the new heat ratio method, presented in equations 4 and 5 is shown below.

Approximations are derived from the instantaneous heated line solution from Marshall (1958).

$$T(x, y, t) = \frac{q}{4\pi\rho ckt} \exp\left[-\frac{(x-vt)^2+y^2}{4kt}\right] \quad \text{A1}$$

The maximum temperature rise satisfies the expression

$$\Delta T_m(x, y) = \frac{q}{2\pi\rho c(x+y)^2} \left[1 + \sqrt{1 + \frac{v^2(x+y)^2}{4k^2}} \right] \exp\left[\frac{vx}{2k} - \sqrt{1 + \frac{v^2(x+y)^2}{4k^2}}\right] \quad \text{A2}$$

Thus, the maximum temperature rise at $(x,y) = (L_d,0)$ is given by

$$\Delta T_{m,d} = \frac{q}{2\pi\rho cL_d^2} \left[1 + \sqrt{1 + \left(\frac{vL_d}{2k}\right)^2} \right] \exp\left[\frac{vL_d}{2k} - \sqrt{1 + \left(\frac{vL_d}{2k}\right)^2}\right] \quad \text{A3}$$

And the maximum temperature rise at $(x,y) = (0, L_u)$ is given by

$$\Delta T_{m,u} = \frac{q}{2\pi\rho cL_u^2} \left[1 + \sqrt{1 + \left(\frac{vL_u}{2k}\right)^2} \right] \exp\left[-\frac{vL_u}{2k} - \sqrt{1 + \left(\frac{vL_u}{2k}\right)^2}\right] \quad \text{A4}$$

The ratio of the maximum temperature rise at the downstream and upstream locations is obtained by combining Equation A3 and A4 to write

$$\frac{\Delta T_{m,d}}{\Delta T_{m,u}} = \frac{\frac{q}{2\pi\rho c L_d^2} \left[1 + \sqrt{1 + \left(\frac{V L_d}{2k}\right)^2} \right] \exp\left[\frac{V L_d}{2k} - \sqrt{1 + \left(\frac{V L_d}{2k}\right)^2}\right]}{\frac{q}{2\pi\rho c L_u^2} \left[1 + \sqrt{1 + \left(\frac{V L_u}{2k}\right)^2} \right] \exp\left[-\frac{V L_u}{2k} - \sqrt{1 + \left(\frac{V L_u}{2k}\right)^2}\right]} \quad \text{A5}$$

$$\ln\left(\frac{L_d^2 \Delta T_{m,d}}{L_u^2 \Delta T_{m,u}}\right) = \ln\left[\frac{1 + \sqrt{1 + \left(\frac{V L_d}{2k}\right)^2}}{1 + \sqrt{1 + \left(\frac{V L_u}{2k}\right)^2}}\right] + \frac{V L_d}{2k} \left(1 + \frac{L_u}{L_d}\right) + \sqrt{1 + \left(\frac{V L_u}{2k}\right)^2} - \sqrt{1 + \left(\frac{V L_d}{2k}\right)^2} \quad \text{A6}$$

This is an implicit relationship in V, so that the value of V that satisfies this equation can be determined using numerical methods, provided the other constants are known or determined independently. Unfortunately, this approach may be too complicated for routine implementation. Therefore, approximations of equation A6 that yield relatively simple expressions of V can be derived using the dimensionless variables:

$$\alpha = \frac{L_u}{L_d} ; v = \frac{V L_d}{2k}$$

$$\ln\left(\frac{\Delta T_{m,d}}{\alpha^2 \Delta T_{m,u}}\right) = v (1 + \alpha) + \ln\left[\frac{1 + \sqrt{1 + v^2}}{1 + \sqrt{1 + \alpha^2 v^2}}\right] + \sqrt{1 + \alpha^2 v^2} - \sqrt{1 + v^2} \quad \text{A7}$$

Equation A7 can be written in the form

$$\ln\left(\frac{\Delta T_{m,d}}{\alpha^2 \Delta T_{m,u}}\right) = v(1 + \alpha) - \frac{1}{4}v^2(1 - \alpha^2) + \frac{1}{32}v^4(1 - \alpha^4) - \frac{1}{96}v^6(1 - \alpha^6) + \frac{5}{1024}v^8(1 - \alpha^8) - \frac{7}{2560}v^{10}(1 - \alpha^{10}) + \dots \quad \text{A8}$$

Truncating terms of order two and greater in equation A8 yields the explicit approximation

$$v \approx \frac{1}{1 + \alpha} \ln\left(\frac{\Delta T_{m,d}}{\alpha^2 \Delta T_{m,u}}\right) \quad \text{A9}$$

Truncating terms of order four and greater in equation A8 yields the approximation

$$\frac{1}{4}v^2(1 - \alpha^2) - v(1 + \alpha) + \ln\left(\frac{\Delta T_{m,d}}{\alpha^2 \Delta T_{m,u}}\right) \approx 0 \quad \text{A10}$$

Which simplifies to

$$\frac{1}{4}v^2(1 - \alpha) - v + \frac{1}{1 + \alpha} + \ln\left(\frac{\Delta T_{m,d}}{\alpha^2 \Delta T_{m,u}}\right) \approx 0 \quad \text{A11}$$

By making use of the identity $(1 - \alpha^2) = (1 - \alpha)(1 + \alpha)$. Solving this quadratic equation yields the explicit approximation

$$v \approx \frac{2}{1-\alpha} \left[1 - \sqrt{1 - \left(\frac{1-\alpha}{1+\alpha}\right) \ln\left(\frac{\Delta T_{m,d}}{\alpha^2 \Delta T_{m,u}}\right)} \right]$$

A12

Which is correct to order three.

The first order approximation from equation A9 yields equation 4, and the third-order correction approximation from equation A12 yields equation 5.

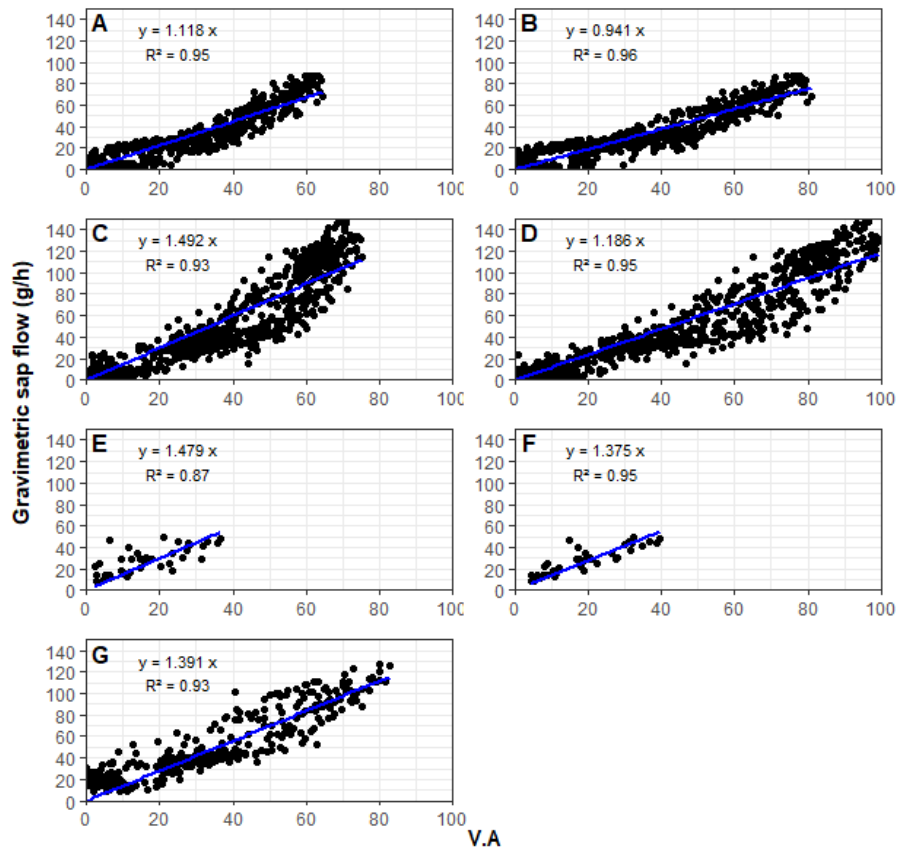


Figure A1. Calibration factors derivation per each sensor (A to G) in four maize plants, from greenhouse studies. Two sensors were installed per plant.

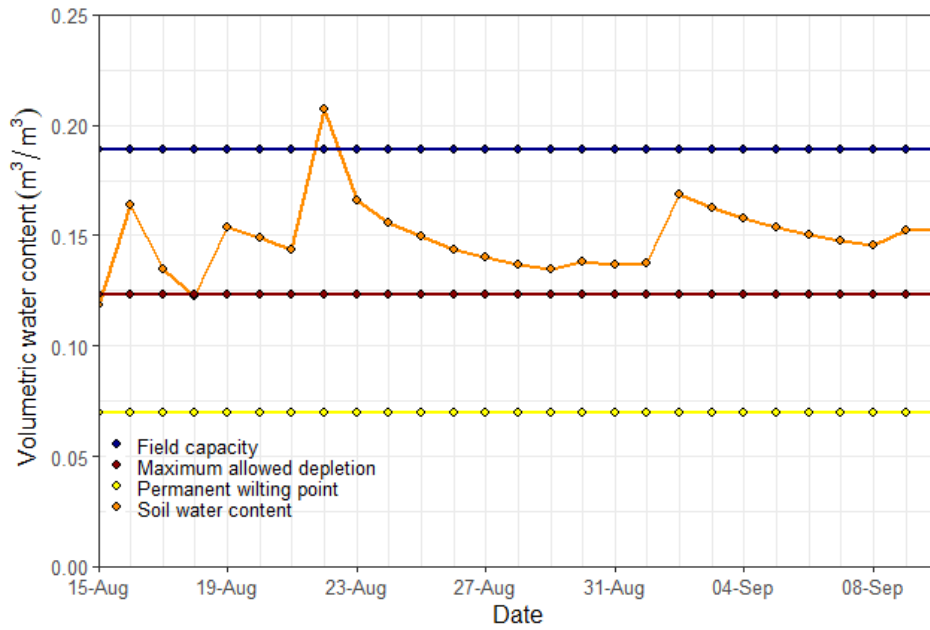


Figure A2. Soil volumetric water content monitoring in the maize field for the sap flow measurement period.

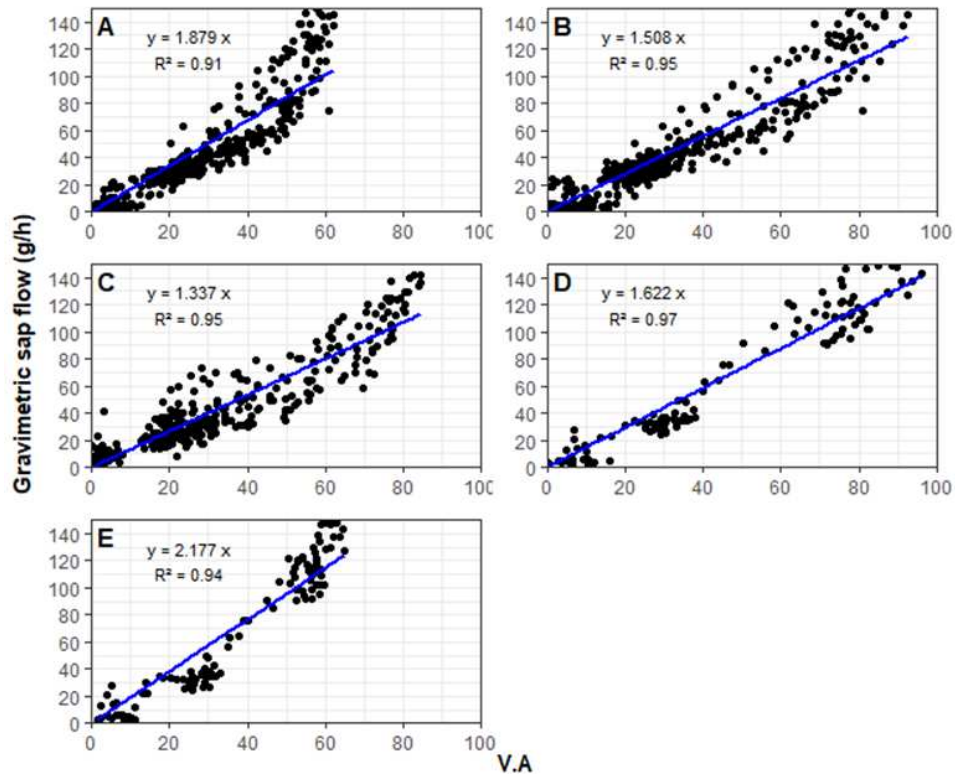


Figure A3. Calibration factors derivation per each sensor (A to E) in three maize plants, from greenhouse studies. Two sensors were installed in two plants and one sensor in the third plant.

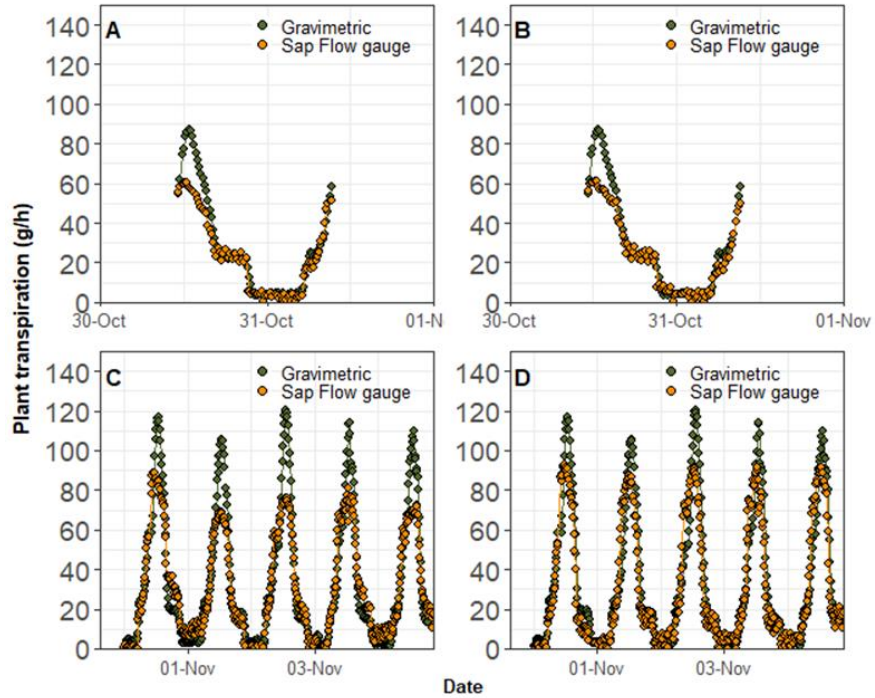


Figure A4. Time series of the validation of the calibration coefficient in greenhouse studies using two plants, with two sensors per plant. Letters A to F correspond to the results of each sensor.

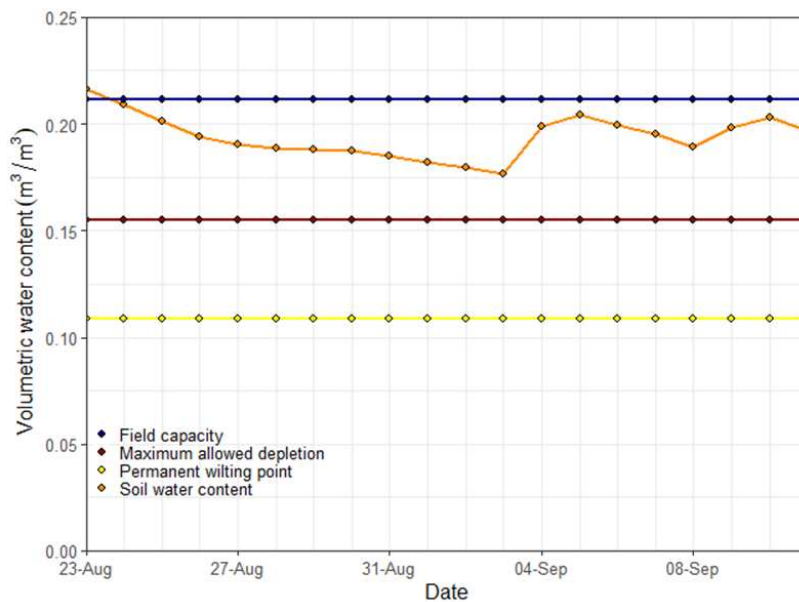


Figure A5. Mean soil moisture condition for the maize field in 2019 for a soil profile of 1m.

Appendix B

Materials and Methods

The research was carried out at two locations. In 2019 the study was conducted at USDA-ARS Limited Irrigation Research Farm (LIRF), Colorado, USA (40°26'54"N, 104°38'21"W, 1426 m). The site comprises a large plots of 190 m x 110 m, with a subsurface drip irrigation system. In 2020 it was at the Irrigation Innovation Consortium (IIC) Headquarters, Research Farm, Fort Collins, Colorado, USA (40°33'26"N, 106°59'43"W, 1426 m), in a plot of 6 ha with a surface irrigation system.

Two type of sap flow sensors were deployed in the field, a new developed type of sensor (see chapter two) and a commercial version of sap flow gauge. Four commercial version of sap flow gauges were installed (Sap flow – commercial). These gauges use the heat balance approach (Dynagage SGB25, Dynamax Inc., Houston, USA). Eight Sap flow gauges were installed in each field, using a heat pulse technique. Sap flow sensors used the heat pulse technique and a new algorithm based on Kluitenberg and Ham (2004) approach and Miner et al. (2017), described in the second chapter of this thesis.

Sap flow gauges were moved to different plants weekly to avoid any risk of effect of heat damage on stems that could interfere with sampling. Measures of plant transpiration were taken every 15 minutes and were hourly averaged. Then were added for daily results. Results from individual plants were upscaled to estimate field transpiration using maize field population (80,000 pl/ha). Transpiration measures with 8 gauges were taken into account for the calculations.

Data collection consisted in measures of frequent leaf area index (LAI) using the Licor canopy analyzer, LAI-2000 (Licor Inc., Lincoln, USA). Weekly measures of reflectance using a multispectral radiometer, MSR5 (Cropscan Inc.; Rochester, USA). The sensor measures surface reflectance in five bandwidths (between 485 nm and 1650 nm). Near infrared (NIR) and red bandwidths were used for this study, NIR corresponds to 830 nm and Red corresponds to 660 nm for the MSR5. From PlanetScope multispectral imager (Planet Labs, PBC, San Francisco, USA) daily images were used unless cloud interference. Phenology and crop height were also monitored throughout the season.

Images from Planet Labs PBC are collected and processed in different formats (Planet Labs PBC, 2022) for a daily frequency and a 3m pixel size. Planet surface reflectance is determined from top of the atmosphere and then follows several processing steps for sensor data correction and corrections for the effect of earth atmosphere. They combined the use of MODIS water vapor, ozone and aerosol data and atmospheric models for corrections (Planet Labs PBC 2022).

There are different generations of Planet Labs satellites, hence, the number of spectral and bandwidth diverge, nevertheless, together they all provide daily images of earth. Therefore, in addition to the other corrections, Planet made a normalization and harmonization of the surface reflectance data (for blue, green, red and near infrared bands) from their different satellites because they have different relative spectral responses. For the normalization and harmonization, they used Sentinel-2 as the target sensor, making all data approximately comparable to Sentinel-2. For this, they fitted a linear model for each band, transforming the PlanetScope reflectance coefficients to match Sentinel-2 spectral response and minimize ambient effects (Kington and Collison, 2022.). The result improves temporal and spatial consistency of data between sensors for different satellites. The corrections reduced the variability between images and between the

generations of Planet satellites and maintained compatibility with Sentinel-2 data (Kington and Collison, 2022).

The data used in this work was a combination of the satellite reflectance data available, hence different satellites were used in order to have daily images. We evaluated the availability of daily images as more important than working with the latest satellite generation because tendency was valued as more important than a exact absolute value and the “normalization and harmonization” corrections reduced large differences between sensors.

NDVI it is the most common VI for estimating Kc or Kcb (Glenn et al., 2011), the NDVI VI is highly correlated to agronomic variables and canopy cover (Bausch and Neale, 1987). Normalized difference vegetation index (NDVI) was calculated using the red and near infrared (NIR) spectral reflectance, 660nm and 850nm wavelengths, respectively.

$$NDVI = \frac{NIR - Red}{NIR + Red}$$

SAVI developed by Huete (1988) as in Bausch (1993), is claimed to minimize the brightness of soil in the red and near infrared wavelengths. It includes a coefficient L, which was estimated that varies with LAI, nevertheless, a value of L=0.5 shows that minimizes soil influence with good results for crop coefficient estimation (Bausch, 1993).

$$SAVI = \frac{NIR - Red}{NIR + Red + L} (1 + L)$$

$$L = 0.5$$

The adjustment factor used for intermediate vegetation of $L=0.5$ improves the results when compared to NDVI for the entire range of vegetation cover (from sparse to dense vegetation cover, planophile and erectophile), soil type and condition (wet or dry) (Huete, 1988).

Data from Planet satellites (CubeSats) and from the MSR5 multispectral radiometer were used for NDVI calculation of the area of interest. We used this vegetation index to estimate f_c following Johnson and Trout (2012) function and the two-step procedure and the K_{cb} values from. The f_c was estimated as Johnson and Trout (2012):

$$F_c = 1.26 NDVI - 0.18$$

The relationship between NDVI and f_c , was developed for 18 different crops (annual and perennial crop types, including row crops, grains, orchard, vineyard) of varying maturity, over 11 satellite overpass dates (Johnson and Trout, 2012). This function was used to determine f_c from the MSR5 radiometer and satellite reflectance data.

When the crop is above or below full effective cover ($f_c < 0.8$) the relationship is linear; when f_c is over 0.8, there is no relationship, but the average K_{cb} corresponds to the mean season K_{cb} value (Trout and DeJonge, 2018):

$$K_{cb_{before R1}} = 1.08f_c + 0.17$$

$$K_{cb_{after R1}} = 1.21f_c + 0.10$$

$$K_{cb_{all season}} = 1.1f_c + 0.17$$

Regression fits to the data for $f_c \leq 0.8$. Fractional ground cover correlates well with K_{cb} and these data indicate that this relationship is linear up to an f_c saturation value of about 0.8. Values of f_c

above 0.8, where held as 0.8. We used the Kcb function for period after R1 or before R1 according to the phenology of maize in each field.

With the NDVI data from the MSR5 and satellite images, f_c was estimated and the relationship with Kcb was used to estimate the Kcb for the location where the sap flow gauges were installed in the field.

Kcb was calculated using reflectance from MSR5 and Planet, using functions from DeJonge and Trout (2018), Bausch and Neale (1990) and Bausch (1995).

Bausch and Neale (1989):

$$Kcb = 1.181 * NDVI - 0.026$$

Bausch (1993) and Bausch (1995):

$$Kcb = 1.416 * SAVI + 0.017$$

The growing degree days were calculated after emergence until 2500 GDD for this maize variety.

Hourly reference evapotranspiration was estimated, and hourly values were added for daily results. We used the standardized tall reference evapotranspiration equation (ASCE, 2005):

$$ET_r = \frac{0.408 \Delta (Rn - G) + \gamma \frac{Cn}{T + 273} u (es - ea)}{\Delta + \gamma (1 + Cd u)}$$

Where, R_n is the calculated net radiation at the crop surface, G is soil heat flux density at the soil surface, T is mean hourly air temperature at 1.5 to 2.5-m height, u is the mean hourly wind speed at 2-m height, e_s and e_a are the saturation vapor pressure and the mean actual vapor pressure at 1.5 to 2.5-m height, Δ is the slope of the saturation vapor pressure-temperature curve, γ is the psychrometric constant. C_n and C_d are constants derived to simplify terms in the ASCE-PM equation and round the result. C_n considers the aerodynamic roughness of an alfalfa vegetation and C_d considers the surface resistance an aerodynamic roughness of an alfalfa field. For alfalfa reference C_n is 66 and C_d is 0.25 for daytime and 1.7 for nighttime values.

The dual crop coefficient approach (Allen et al., 1998) refers to:

$$ET_c = ET_r K_{cb}$$

Maize K_{cb} was determined with transpiration measures from the sap flow gauges. The latter relationship was used for its derivation.

In this study the basal crop coefficient curve is represented by four linear segments, each representing a crop stage from planting to harvest, identified as initial, development, mid-season and late-season growth stages (Allen et al., 1998).

We constructed a 4-linear segment curve with values from Trout and DeJonge (2018) for initial, mid-season and late season phases.

The 4-segment K_{cb} curve was delineated considering available field data from different sensors. Instead of using fixed number of days for the duration of each of the 4 phases, the periods were determined using a combination of different measurements during the crop season to better mimic the maize growth curve. The length of the 4 phases were custom modified for the season based

on phenology, LAI, fc and crop height measurements from the field. LAI and fc estimations were used to directly observe and determine crop development, without the need of idealized maize stage assumptions. However, the beginning and the end of the curve was determined with GDD. Maize cycle length for 2500 GDD, a hypothesized value, according to the maize variety, and cumulative 100 GDD for the onset of emergence, determined the slope of the late season period and the beginning of the curve.

The rationale for the determination of each of the 4-segment phases is described below.

Determination of Emergence

Emergence is usually set at 90 to 120 GDD from planting, in this case was set on 5/20/2020, around 100 GDD.

Determination of the crop development period

The development phase was set to start on 6/4, 23 days after planting, when the crop was on V6-V7 and with a 20cm maize height. Similar to Andales et al. (2014), for Rocky Ford in Colorado, who found the start of the development phase as 25 days after planting, when maize was between V4 and V5, with 25cm.

Determination of the end of the full effective canopy cover period

According to the MSR5 fc measurements the beginning of the reduction of the effective cover would be after 8/21 and before 9/5. Probably closer to 8/21 than 9/5, given that fc is 0.8 and 0.54, respectively. The date was set to 8/25, DOY 238, 104 days after planting, 49 days after full effective canopy cover, between R3 and R4. This is similar to results found by Andales et al. (2014). DeJonge and Trout (2018) showed a decrease on Kcb after 40 days after effective cover, a few days before R4, in a 6-year study at Greeley, Colorado.

Determination of period for 100% of effective canopy cover

Measured data:

- V11, 7/6, LAI= 2.7. This is 54 days after planting (DOY 188).
- V13, 7/15, LAI=3.5. This is 63 days after planting (DOY 197).
- On the 7/15, the Trout and Johnson (2012) canopy ground cover index, $fc = 0.94$.

Effective full canopy cover it is reached at an $fc = 0.8$ and additional ground cover does not increase transpiration significantly (Trout and DeJonge, 2018). It was observed that on 7/15 the fc is larger than 0.8; hence, we can assume that full effective cover was before 7/15. (on 7/24 maize pollinizing). As a general guideline, effective full canopy cover can be determined when LAI=3 (Allen et al., 1998, Nielsen and Hinkle, 1996; Jensen and Allen, 2016, Bausch, 1995) or after 2.7 (Ritchie and Burnett, 1971). Some studies have found that crop coefficient arrived at a max value when the crop was around an LAI of 3 and remained constant with an LAI larger than 3 (Kang et al, 2003, Zhao et al., 2010). Adjusting a polynomial function for the LAI data from the field, an LAI=3 was estimated to be at DOY= 189, corresponding to 7/7/2020, 55 days after planting, around V11.

Therefore, the day for beginning of $K_{c_{mid}}$ is similar to Andales et al., (2014), 58 DAP, at V10 and continued for 48 days (until around R4-R5). Trout and DeJonge (2018) found that full effective cover was around 70 days after planting and 10-15 days before VT, at V14, for a study of 6 years in Greeley, Colorado. Li et al. (2003) showed similar results, where $K_{c_{mid}}$ was set at 11 weeks after sowing and after LAI reached 3. Steduto and Hsiao (1998) also showed that crop coefficient increased as LAI and found a max around 60 days after sowing. A schematic view of the K_{cb} curve was delineated (Figures B2 and B3).

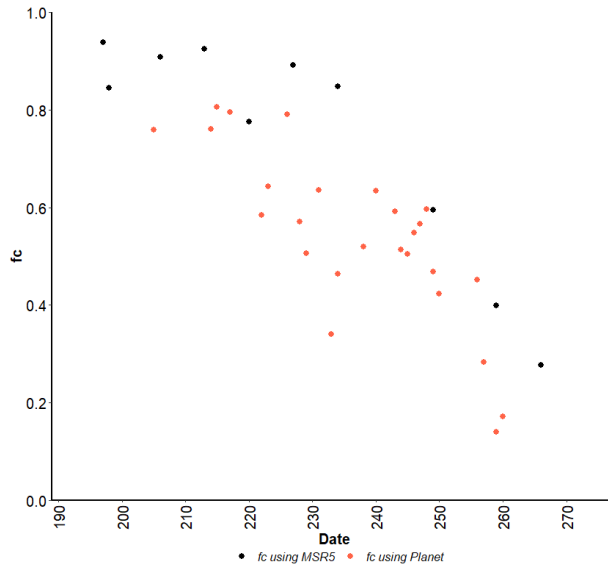


Figure B1. Calculated f_c (Johnson and Trout, 2012) with NDVI from spectral reflectance from manual scouting with MSR5 and satellite imagery from PlanetLabs.

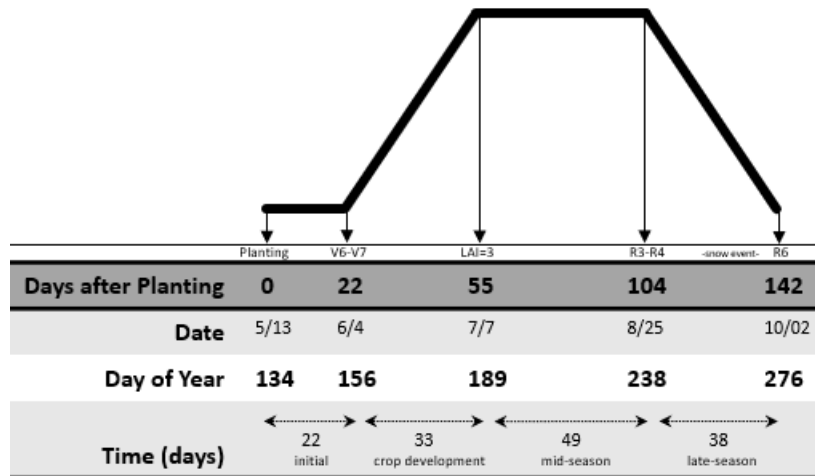


Figure B2. Maize growth stages defined following the FAO-56 methodology (Allen et al., 1998) and field data for 2020.

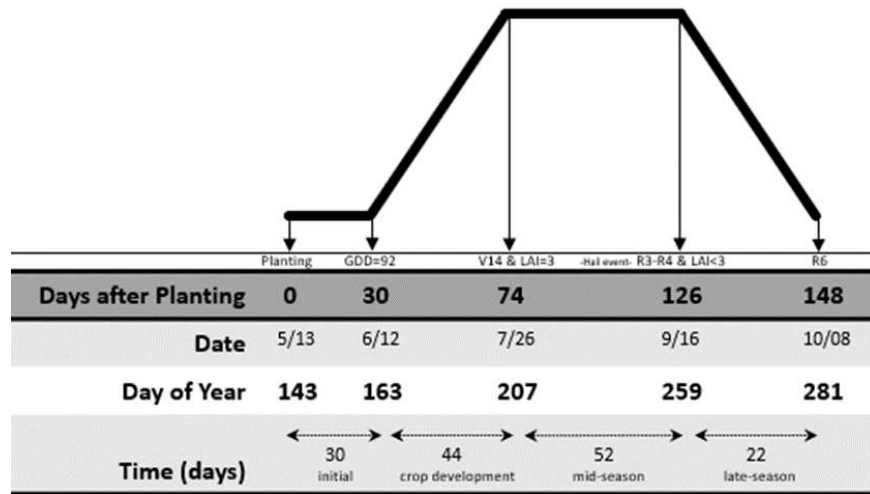


Figure B3. Maize growth stages defined following the FAO-56 methodology (Allen et al., 1998) and field data for 2019.

Appendix C

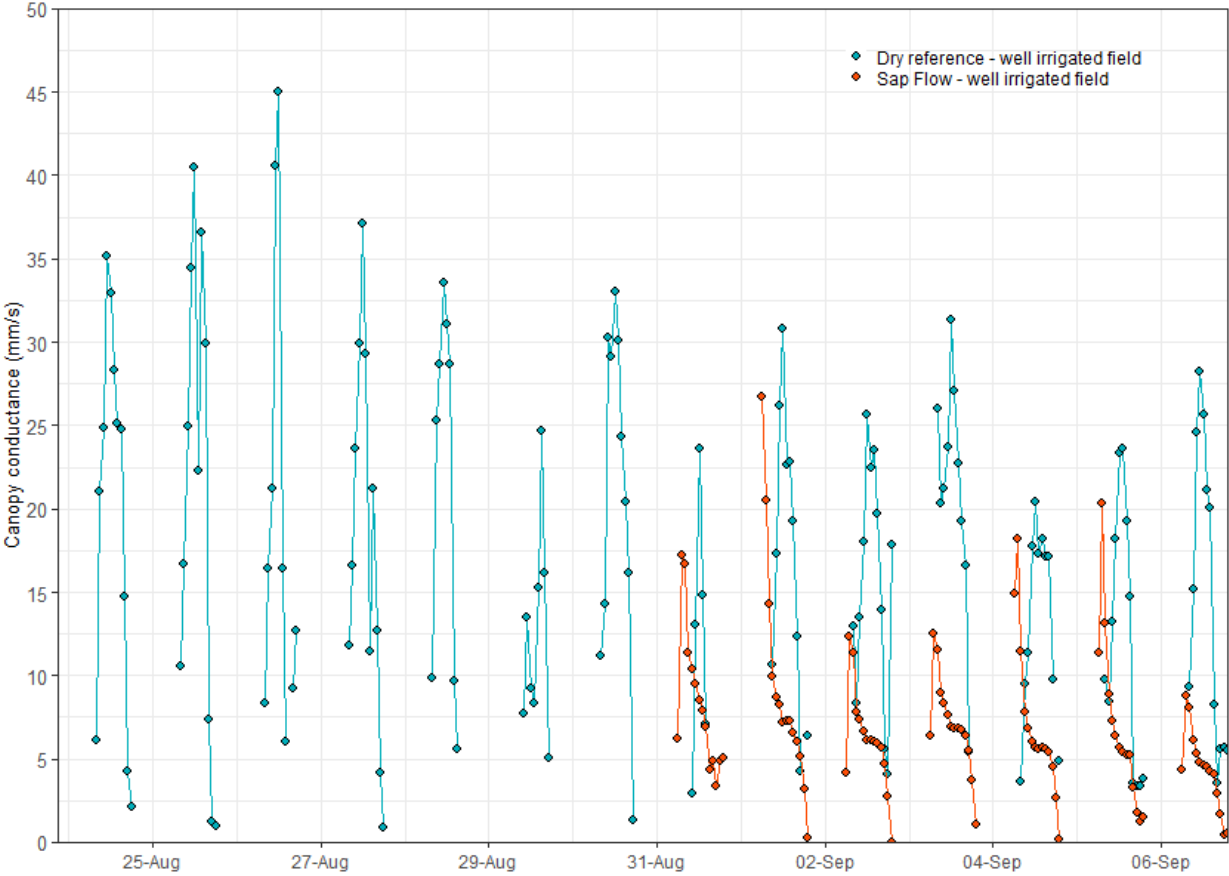


Figure C1. Canopy conductance determined with two different methods using Monteith and Unsworth (2013) boundary layer conductance approach.

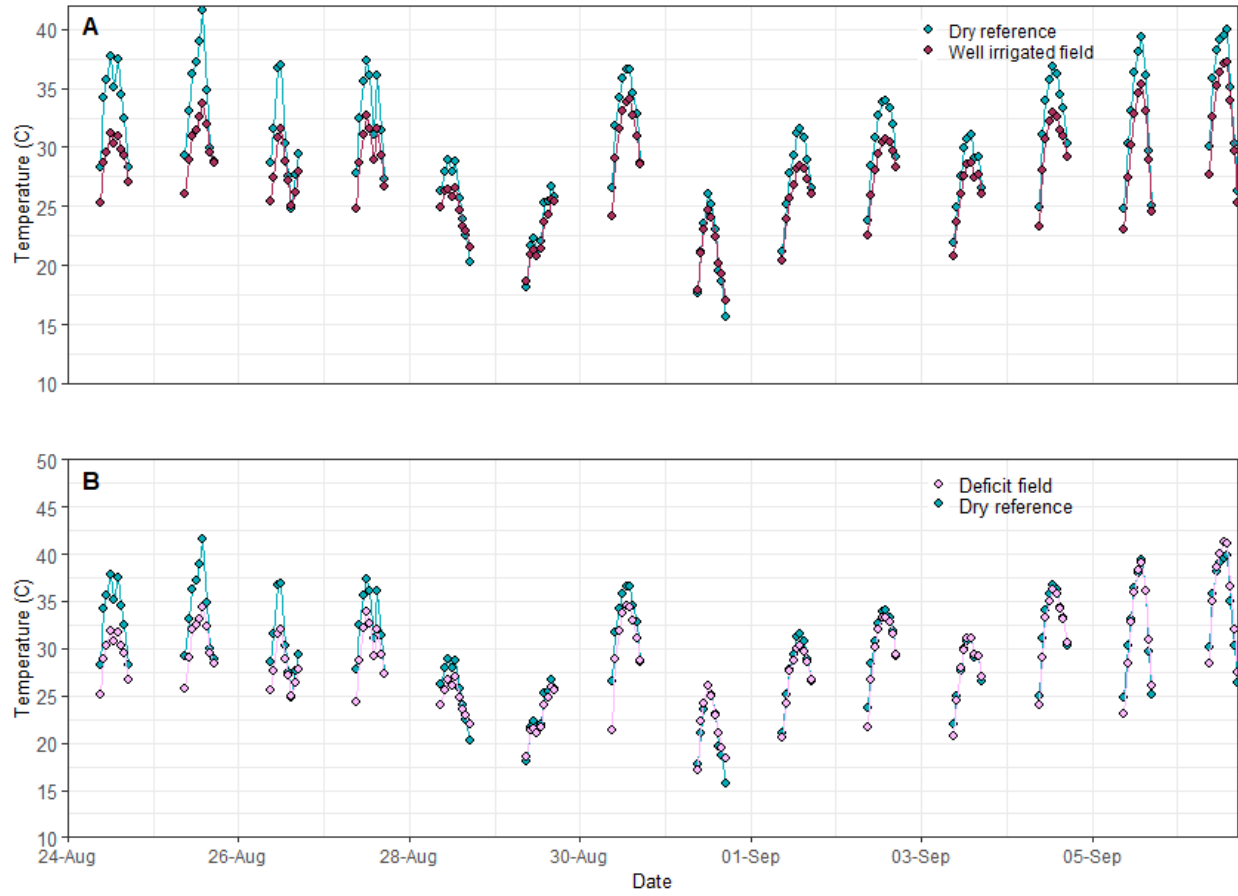


Figure C2. Temperatures from the Dry ARS and from the canopy of the well irrigated and the deficit field.

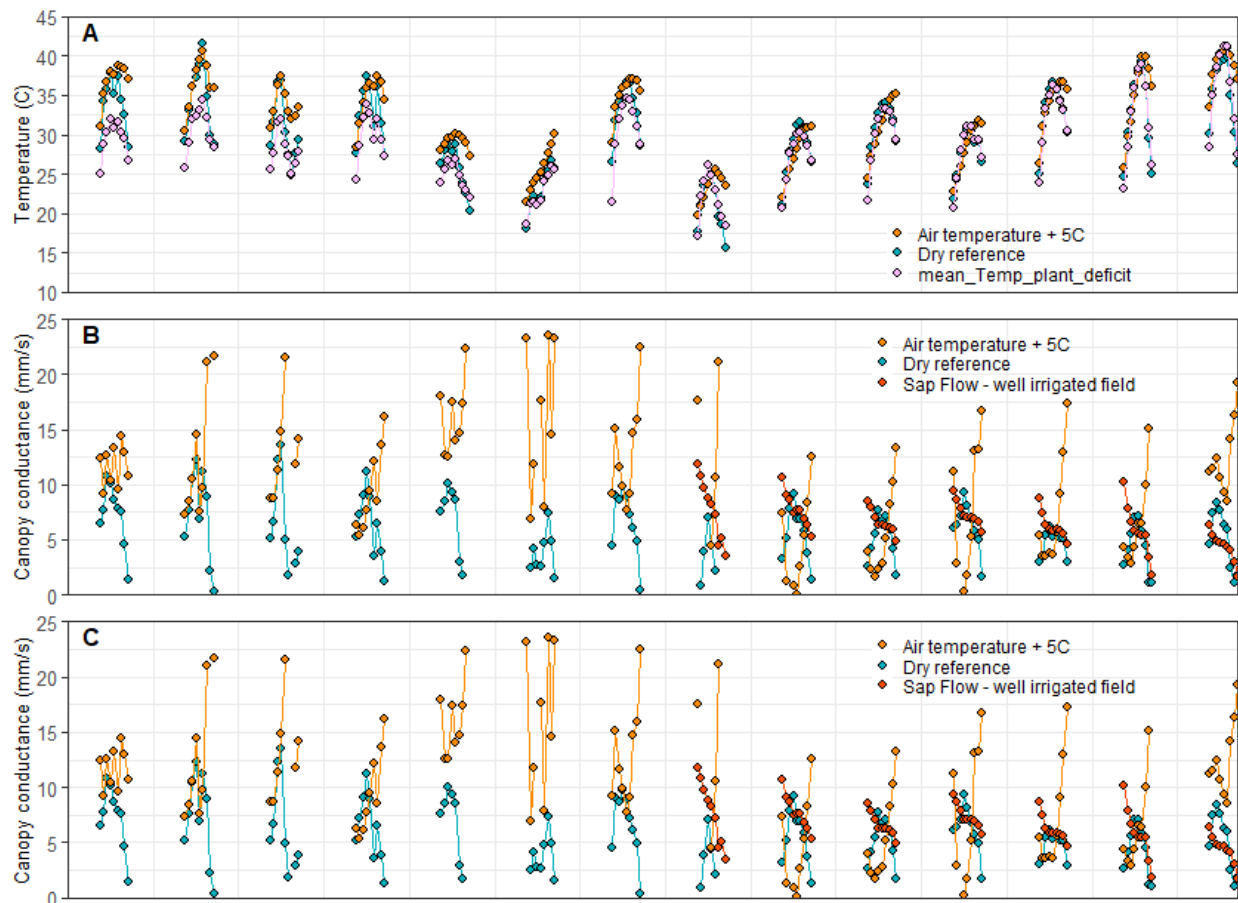


Figure C3. Comparison of temperature, canopy conductance and transpiration using air temperature plus 5C as the dry reference temperature in the TDry approach. Values showed are from 9AM to 5PM.

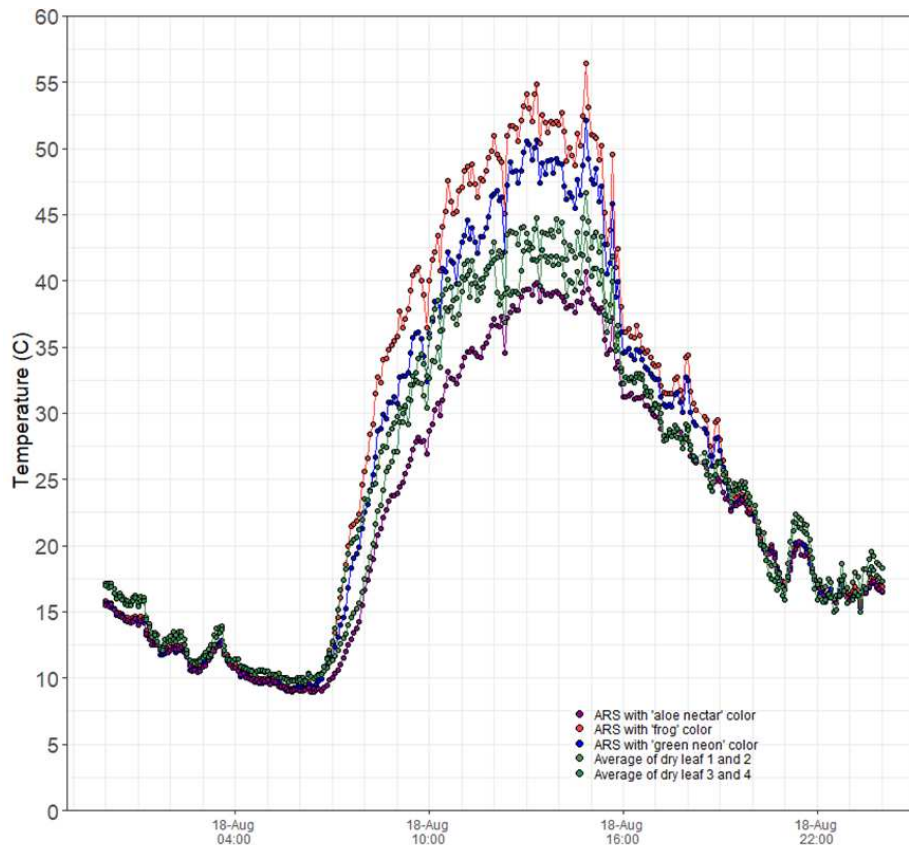


Figure C4. Example of the dry ARS temperature variation for three different paint colors (“aloe nectar”, “frog”, “green neon”) and the average temperature of four corn leaves covered with Vaseline representing maize dry leaves.

Determination of actual crop water stress in the field

Studies have verified the relationship between soil water content and transpiration rate (Sadras and Milroy, 1996) and characterized as a straight function below a threshold. Soil water availability exerts control over transpiration rate through the decrease of canopy conductance (She et al., 2013). The soil water content at which transpiration begins to decrease varies with crop species but can also between genotypes of the same specie (Sadras and Milroy, 1996; Verhoef and Egea, 2014; Gholipoor et al.,2012). Studies for maize by Gholipoor et al., (2012), showed that for different maize genotypes, the response of normalized transpiration to soil drying is defined by a

plateau at a threshold. Below the threshold, relative transpiration (RT) decreased with decreases in fraction of transpirable soil water (FTSW); however, this relation can be curvilinear (Verhoef and Egea, 2014). This is of special attention in breeding programs, given high FTSW threshold values would be able to restrict transpiration at higher soil water contents and would conserve more water for later usage in the growing season in these crop genotypes (Gholipour et al., 2012). This would mean that the threshold of a crop water stress index can vary with crop variety. However, the relation with yield reduction is a characteristic of high interest for irrigation management.

In addition, thresholds are not static and could also vary according to the evaporative demand, phenology stage, acclimatization (relative to the number of wet-dry cycles of the crop) and soil type (Sadras and Milroy, 1996). The FTSW threshold for a decline in transpiration may change with crop genotype but also with physiological traits, ie. due to the influence of aquaporins (transporting water across cell membranes) on the relative transpiration threshold, as their activity may be temperature dependent (Gholipour et al., 2012). It was also found that water stress could increase rapidly for smaller soil water depletions after a threshold. This is because the soil water potential and volumetric water content have a non-linear relationship (Chavez, 2015).

Data shows that transpiration starts decreasing when relative extractable water is below 0.56-0.58 to 0.6 (Figure 5), on August 30th. The lower relative transpiration between values of relative extractable water of 0.55 and 0.6 is assumed to be related to stomatal closure due to a very high atmospheric demand that day (Table 1). Results agree with Gholipour et al. (2013) who found that for certain hybrids, thresholds range from 0.56 to 0.6. The approach used in this study relies on the estimate of an average depth that defines root water uptake for the corn, where most of the water uptake occurs. However, rooting depth varies with soil type and may also show spatial

variability, besides the variables mentioned above; therefore, there is a potential variation in the estimation of the threshold for the relative extractable water (Sadras and Milroy, 1996).

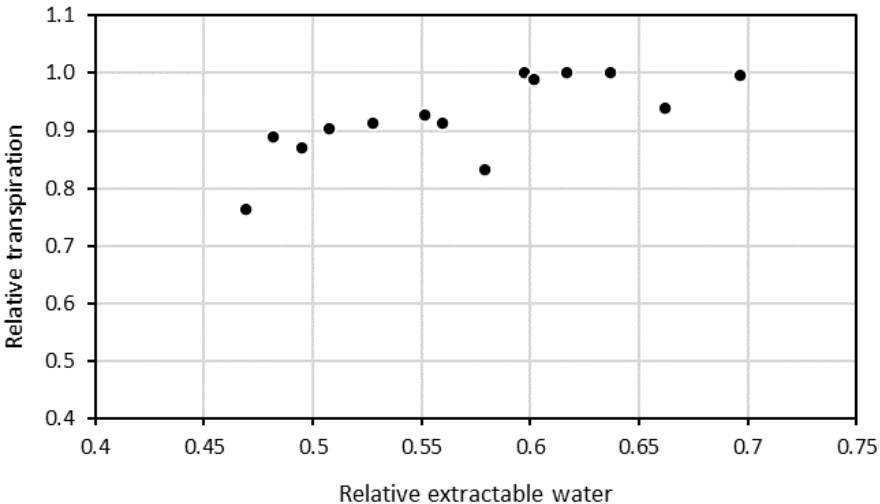


Figure C5. Relative transpiration as a function of relative extractable water.

Equations

Equations used in this study are described below.

Canopy conductance equations

- 1) Canopy conductance expressed from a dry leaf reference temperature (Jones et al., 2018), m/s:

$$g_w = \frac{g_{HR}(T_{Dry\ reference} - T_{canopy})\gamma}{\Delta(T_{canopy} - T_{air}) + VPD}$$

Being, $T_{Dry\ reference}$ the temperature from the dry reference dome, T_{canopy} the temperature from the infrared sensors pointing at the maize canopy and T_{air} the air temperature in Kelvin. VPD is the vapor pressure deficit in Pa, Δ is delta, rate of change of saturation vapor pressure with temperature, and γ psychrometric constant (Pa/K), calculations from ASCE (2005).

- 2) Canopy conductance derived from the aerodynamic equation, m/s:

$$r_v = \left[\frac{\rho_a C_a}{\gamma} \right] (e_{s\ Plant\ temperature} - e_a) \frac{1}{LE_{Sap\ Flow}} \quad [10]$$

$$r_c = r_v - r_{ah} \quad [11]$$

Being ρ_a the air density (Kg/m^3) and C_p (J/Kg.K) the specific heat of air, from Ham (2005) eq. 8 and 11.

Aerodynamic resistance, s/m, or conductance, m/s:

Assuming neutral stability of the atmosphere

$$r_{ah} = \frac{1}{k^2 u} \ln \left[\frac{(z-d)}{z_{om}} \right] \ln \left[\frac{(z-d)}{z_{oh}} \right] \quad [12]$$

Jones et al. (2018); Monteith and Unsworth (2013):

$$g_{ah} = \frac{k^2 u}{\left(\ln \left[\frac{(z-d)}{z_{om}} \right] \right)^2} \quad [13]$$

$h =$ crop height (m)

Zero plane displacement height, d:

$$d = 2/3 h$$

Roughness length for momentum, Z_{om} , m:

$$Z_{om} = 0.123 h$$

Roughness length for heat, Z_{oh} , m:

$$Z_{oh} = 0.1 Z_{om}$$

Von Karman's constant, k :

$$k = 0.41$$

Measurement height of sensors, z , m.

u is wind speed in m/s.

Parallel conductance to heat (g_{ah}) and radiative transfer (g_r), g_{HR} , (Jones, 2004, Jones 2018), m/s:

$$g_{HR} = g_r + g_{ah}$$

Conductance to radiative transfer, g_r , m/s:

$$g_r = \frac{4\varepsilon\sigma T_{air}^3}{\rho_a C_a} \quad [14]$$

Conductance to heat, g_{ah} , m/s:

$$g_{ah} = \frac{1}{r_{ah}} \quad [15]$$

emissivity of plant canopies, ε , (page 112, Table 1, Jones 2004):

$$\varepsilon_v = 0.98$$

Stefan-Boltzmann constant, σ , $\text{Wm}^{-2} \text{K}^{-4}$:

$$\sigma = 5.67 \times 10^{-8}$$

Infrared radiometer temperature corrections:

$$clf = 1 - s \quad [16]$$

$$s = \frac{R_s}{R_{so}} \quad [17]$$

Being, R_s solar irradiance and R_{so} clear-sky solar radiation from ASCE (2005).

Incoming shortwave radiation, R_s , is measured.

Effective emissivity for clear sky (Brutsaert, 1975), ϵ_{clear} :

$$\epsilon_{clear} = 1.24 \left(\frac{10e_a}{T_{air}} \right)^{1/7} \quad [18]$$

Sky temperature, T_{sky} , Evangelisti et al. (2019), K:

$$T_{sky}^4 = \epsilon_{sky} T_{air}^4 \quad [19]$$

ϵ_{sky} is modeled from Brutsaert (1975), Crawford and Duchon (1999) and Berni et al. (2009):

$$\epsilon_{sky} = \llbracket clf + (1 - clf)\epsilon_{clear} \rrbracket \quad [20]$$

Surface emissivity, Brunsell and Gillies (2002):

$$\epsilon_{surface} = Fr \epsilon_v + (1 - Fr)\epsilon_s \quad [21]$$

Soil emissivity, ϵ_s :

$$\epsilon_s = 0.93$$

Fr, is modeled for continuous data from ground surface reflectance measures with a multispectral radiometer MSR5 (Cropscan Inc.; Rochester, USA), using fractional ground cover, fc, from Johnson and Trout (2012) for ground cover estimation:

$$Fc = 1.26 NDVI - 0.18 \quad [22]$$

Being NDVI, the normalized difference vegetation index, using near infrared (NIR) and red surface reflectance wavelengths.

$$NDVI = \frac{NIR - Red}{NIR + Red} \quad [23]$$

IRT temperature corrected is the actual target surface temperature, T_{target} , K:

$$T_{target} = \left[\frac{T_{IRT}^4 - (1 - \varepsilon_{surface})T_{sky}^4}{\varepsilon_{surface}} \right]^{0.25} \quad [24]$$

Temperature from the IRT, T_{IRT} is the temperature corrected with the calibrator in Kelvin.

Transpiration rate (Jones et al., 2018), E_{dry} , J/m²s:

$$E_{dry} = \alpha g_{HR} \rho_a C_a (T_{Dry\ reference} - T_{canopy}) \quad [25]$$

Being $\alpha = 0.5$, a scaling factor to ETo, correcting for errors in $E_{Dry\ reference}$ from sensor calibration errors including incorrect spectral absorptance of the dome (Jones et al., 2018).

In this experiment:

$$\alpha = 1$$